Ref. Ares(2014)4050202 - 03/12/2014

European Commission
Information Society and Media

SEVENTH FRAMEWORK PROGRAMME

Network of Excellence

NEWCOM#

Network of Excellence in Wireless Communications#

FP7 Contract Number: 318306

WP1.2 – Opportunistic and cooperative communications

D12.2
Intermediate Results of N# JRAs on Opportunistic and Cooperative Communications

Contractual Delivery Date:	October 31, 2014
Actual Delivery Date:	November 21, 2014
Responsible Beneficiary:	CNIT
Contributing Beneficiaries:	CNIT, AAU, CNRS, CTTC, IASA, Technion, UCL, UOULU, VUT
Estimated Person Months:	25
Dissemination Level:	Public
Nature:	Report
Version:	1.0

PROPRIETARY RIGHTS STATEMENT
This document contains information, which is proprietary to the NEWCOM# Consortium.

This page is left blank intentionally

PROPRIETARY RIGHTS STATEMENT
This document contains information, which is proprietary to the NEWCOM# Consortium.

Document Information

Document ID:	**D12.2**
Version Date:	November 13, 2014
Total Number of Pages:	99
Abstract:	The report presents the Intermediate Results of N# JRAs on Opportunistic and Cooperative Communications and highlights the fundamental issues that have been investigated by the WP1.2. Furthermore, the report illustrates the Joint Research Activities (JRAs) already identified during the first year of the project which are currently ongoing and will be performed within WP1.2. For each activity there is a description, an illustration of the adherence and relevance with the identified fundamental open issues, a short presentation of the preliminary results, and a roadmap for the joint research work in the next years. Appendices for each JRA give technical details on the scientific activity in each JRA.
Keywords:	Opportunistic networks, cooperative communications, mobile clouds, cooperative sensing, multi-user communications.

Authors

IMPORTANT: The information in the following two tables will be directly used for the MPA (Monitoring Partner Activity) procedure. Upon finalisation of the deliverable, please, ensure it is accurate. Use multiple pages if needed. Besides, please, adhere to the following rules:

- Beneficiary/Organisation: For multi-party beneficiaries (CNIT) and beneficiaries with Third Parties (CNRS and CTTC), please, indicate beneficiary *and* organisation (e.g., CNIT/Pisa, CNRS/Supelec).
- Role: Please, specify: Overall Editor / Section Editor / Contributor.

Full Name	Beneficiary / Organisation	e-mail	Role
Sergio Palazzo	CNIT/UniCT	sergio.palazzo@cnit.it	Overall editor/contributor and WP Leader
Ivan Stupia	UCL	ivan.stupia@uclouvain.be	Section Editor (2.1 and 3.1) and Task 1.2.1 leader
Laura Galluccio	CNIT/ UniCT	laura.galluccio@cnit.it	Section Editor (2.2 and 3.2) and Overall editor/contributor
Aris Moustakas	IASA	arislm@phys.uoa.gr	Section Editor (2.3 and 3.3) and Task 1.2.3 leader
Riccardo Andreotti	CNIT/ UniPI	riccardo.andreotti@cnit.it	Contributor
George Arvanitakis	EURECOM	george.arvanitakis@eurecom.fr	Contributor

Francesca Bassi	CNRS/UniPS	francesca.bassi@lss.supelec.fr	Contributor
M. Benammar	CNRS/ SUPELEC	meryem.benammar@supelec.fr	Contributor
Mihai Badiu	AAU	in_mba@es.aau.dk	Contributor
Elena Veronica Belmega	CNRS	belmega@ensea.fr	Contributor
Chiara Buratti	CNIT/ UniBO	chiara.buratti@cnit.it	Contributor
Burak Cakmak	AAU	buc@es.aau.dk	Contributor
Lin Chen	CNRS	lin.chen@lri.fr	Contributor
Krzysztof Cichon	PUT	krzysztof.z.cichon@doctorate.put.poznan.pl	Contributor
Ioannis Dagres	IASA	jdagres@phys.uoa.gr	Contributor
Davide Dardari	CNIT/ UniBO	davide.dardari@unibo.it	Contributor
Paolo Del Fiorentino	CNIT/ UniPI	paolo.delfiorentino@cnit.it	Contributor
Salvatore D'Oro	CNIT/ UniCT	salvatore.doro@cnit.it	Contributor
Mohieddine El Soussi	UCL	mohieddine.elsoussi@uclouvain.be	Contributor
Spyros Evaggelatos	IASA	s.evaggelatos@di.uoa.gr	Contributor
Bernard Fleury	AAU	bfl@es.aau.dk	Contributor
Sophie Fosson	CNIT/ PoliTo	sophie.fosson@polito.it	Contributor
Filippo Giannetti	CNIT/ UniPI	filippo.giannetti@cnit.it	Contributor
Savo Glisic	UOULU	savo@ee.oulu.fi	Contributor
Maxime Guillaud	VUT	maxime.guillaud@tuwien.ac.at	Contributor
Carles Anton-Haro	CTTC	carles.anton@cttc.es	Contributor
Michel Kieffer	CNRS-UniPS	michel.kieffer@lss.supelec.fr	Contributor
Adrian Kliks	PUT	akliks@et.put.poznan.pl	Contributor
Wenjie Li	CNRS/UniPS	wenjie.li@lss.supelec.fr	Contributor
Beatriz Lorenzo	UOULU/VIGO	lorenzo@ee.oulu.fi	Contributor
Vincenzo Lottici	CNIT/ UniPI	vincenzo.lottici@cnit.it	Contributor
Enrico Magli	CNIT/ PoliTo	enrico.magli@polito.it	Contributor
Fabio Martignon	CNRS	fabio.martignon@lri.fr	Contributor
Javier Matamoros	CTTC	javier.matamoros@cttc.cat	Contributor
Giacomo Morabito	CNIT/ UniCT	giacomo.morabito@cnit.it	Contributor
Panayotis Mertikopoulos	CNRS	panayotis.mertikopoulos@imag.fr	Contributor
Florian Meyer	VUT	florian.meyer@tuwien.ac.at	Contributor
Stefan Mijovic	CNIT/ UniBO	stefan.mijovic@unibo.it	Contributor
Amor Nafkha	CNRS	amor.nafkha@supelec.fr	Contributor
Malek Naoues	CNRS/ SUPELEC	malek.naoues@cea.fr	Contributor
Gianni Pasolini	CNIT/UniBO	gianni.pasolini@unibo.it	Contributor
P. Piantanida	CNRS/ SUPELEC	pablo.piantanida@supelec.fr	Contributor
Erwin Riegler	VUT	erwin.riegler@tuwien.ac.at	Contributor
S. Shamai	Technion	sshlomo@ee.technion.ac.il	Contributor
Luc Vandendorpe	UCL	luc.vandendorpe@uclouvain.be	Contributor
Abdellatif Zaidi	CNRS	abdellatf.zaidi@ensta.org	Contributor
Vincenzo Zambianchi	CNIT/UniBO	vincenzo.zambianchi@unibo.it	Contributor
Alberto Zanella	CNIT/UniBO	alberto.zanella@cnit.it	Contributor

Reviewers

Full Name	Beneficiary / Organisation	e-mail	Date
Pierre Duhamel	CNRS	pierre.duhamel@lss.supelec.fr	23/10/ 2014
Marco Luise	CNIT/UniPI	marco.luise@cnit.it	13/11/ 2014

Version history

Issue	Date of Issue	Comments
0.1	15/07/ 2014	Table of comments, guidelines and assignments
0.2	16/09/ 2014	First complete draft version
0.3	24/09/ 2014	Updated version - second round of contributions
0.4	14/10/ 2014	Overall editing and updates
0.5	23/10/ 2014	Final version for Newcom# internal review
1.0	13/11/ 2014	Final version ready for delivery

Executive Summary

WP1.2 deals with the investigation of opportunistic and cooperative communications. It has been proved that cooperative communications provide considerable improvement in network performance by increasing the achievable capacity and allowing multiplexing among nodes composing the network. Therefore, if properly exploited, cooperation in wireless networks can be profitable and useful in several application scenarios.
As an example, cooperative communications are well-suited for opportunistic scenarios, which are those where mobile nodes are not always connected to each other but exploit the limited proximity time when opportunities for exchanging information arise to exchange their data.
In order to properly exploit cooperation among nodes, suited coding strategies and interference management techniques have to be considered.
As described in the project's Description of Work, the WP is divided into three Tasks, each with specific scope and objectives: Task 1.2.1 "Cooperative multi-user communication"; Task 1.2.2 "Optimal design of opportunistic networks and mobile clouds"; Task 1.2.3 "Cooperative sensing".
The deliverable presents the intermediate results in the thematic areas addressed in WP1.2 and highlights the issues that are currently under investigation.
For each Task, specific JRAs are addressed. In particular a short description clarifies the targets and the adherence and relevance with the identified fundamental open issues; technical details are reported in the annexes.

Table of Contents

1. Introduction 10
1.1 Glossary 10
1.2 List of Joint Research Activities (JRAs) 14
1.3 Main WP Achievements 14
2. Description of Activity and Collection of Results 17
2.1 JRA 1.2.1-1 An Information-Theoretic Pespective of Cooperation in Multi-User Communications 17
2.1.1 Description 17
2.1.2 Relevance with the identified fundamental open issues 17
2.1.3 Initial Results 17
2.1.4 Achievements and planned activities 17
2.2 JRA 1.2.1-2 Network coding for MARC 18
2.2.1 Description 18
2.2.2 Relevance with the identified fundamental open issues 18
2.2.3 Initial results 18
2.2.4 Achievements and planned activities 19
2.2.5 Publications 19
2.3 JRA 1.2.1-3 Message-passing methods for distributed wireless network optimization 20
2.3.1 Description 20
2.3.2 Relevance with the identified fundamental open issues 20
2.3.3 Initial Results 20
2.3.4 Achievements and planned activities 20
2.3.5 Publications 21
2.4 JRA 1.2.1-4 Distributed learning schemes for signal optimization in large wireless networks 22
2.4.1 Description 22
2.4.2 Relevance with the identified fundamental open issues 22
2.4.3 Initial results 22
2.4.4 Achievements and planned activities 22
2.4.5 Publications 23
2.5 JRA 1.2.1-5 Clusters organization for multi-hop cooperative communications 25
2.5.1 Description 25
2.5.2 Relevance with the identified fundamental open issues 25
2.5.3 Initial results 25
2.5.4 Achievements and planned activities 25
2.5.5 Publications 26
2.6 JRA1.2.2-1: Opportunistic relaying and forwarding 27
2.6.1 Description 27
2.6.2 Relevance with the identified fundamental open issues 27
2.6.3 Initial Results 28
2.6.4 Achievements and planned activities 28
2.6.5 Publications 28
2.7 JRA1.2.2-2: Game theoretic approach to timing channel communication 29
2.7.1 Description 29
2.7.2 Relevance with the identified fundamental open issues 29
2.7.3 Initial results 29

2.7.4 Achievements and and planned activities 29
2.7.5 Publications 30
2.8 JRA1.2.3-1: Multiple source detection, localization, and transmit power estimation in lognormal fading environment 31
2.8.1 Description 31
2.8.2 Relevance with the identified fundamental open issues 31
2.8.3 Initial results 32
2.8.4 Achievements and planned activities 32
2.9 JRA1.2.3-2: Cooperative Simultaneous Localization and Tracking 33
2.9.1 Description 33
2.9.2 Relevance with the identified fundamental open issues; 33
2.9.3 Initial results 33
2.9.4 Achievements and planned activities; 33
2.9.5 Publications 33
2.10 JRA1.2.3-3: Source detection in the presence of interference and noise 34
2.10.1 Description 34
2.10.2 Relevance with the identified fundamental open issues 34
2.10.3 Initial results 34
2.10.4 Achievements and planned activities 34
2.10.5 Publications 35
2.11 JRA1.2.3-4: Hybrid Spectrum Sensing Architecture for Cognitive Radio: Overcoming Noise Uncertainty 36
2.11.1 Description 36
2.11.2 Relevance with the identified fundamental open issues 36
2.11.3 Initial results 36
2.11.4 Achievements and Planned activities 36
2.11.5 Publications 36
2.12 JRA 1.2.3-5 on energy-efficient data collection and estimation in wireless sensor networks 38
2.12.1 Description 38
2.12.2 Relevance with the identified fundamental open issues 38
2.12.3 Initial Results 38
2.12.4 Achievements and planned activities 39
2.12.5 Publications 39

3. Conclusions and Prospects 41

4. Annexes: Technical Achievements: Detailed Description of JRA Results. 42

4.1 Annex A - JRA 1.2.1-2 Network coding for MARC 42
4.1.1 System Model 42
4.1.2 Compute-and-Forward Strategy 43
4.1.3 Numerical Results 46
4.1.4 References 48
4.2 Annex B - JRA 1.2.1-3 Message-passing methods for distributed wireless network optimization 49
4.3 Annex C - JRA 1.2.1-4 Distributed learning schemes for signal optimization in large wireless networks 49
4.3.1 Online optimization in MIMO-OFDM cognitive radio 49
4.3.2 Adaptive transmit policies for cost-efficient power allocation 58
4.4 Annex D - JRA 1.2.1-5 Clusters organization for multi-hop cooperative communications 65
4.4.1 Reference Scenario 65
4.4.2 Game Theoretical Formulation of the VAAs Formation Problem 67

4.4.3 Communication Protocol 70
4.4.4 Cluster Formation 70
4.4.5 VAA Formation 70
4.4.6 Cooperative Beamforming 71
4.4.7 Numerical results 71
4.4.8 References 72
4.5 Annex E - JRA 1.2.2-1 Opportunistic relaying and forwarding 73
4.5.1 Introduction 73
4.5.2 System model 73
4.5.3 Polymorphic Epidemic Routing 74
4.5.4 Recovery schemes 76
4.5.5 Performance 79
4.5.6 References 85
4.6 Annex F - JRA 1.2.2-2 Game theoretic approach to timing channel communication 86
4.6.1 Introduction 86
4.6.2 Proposed Game Model 86
4.6.3 Nash Equilibrium 87
4.6.4 References 89
4.7 Annex G - JRA 1.2.3-1 Multiple source detection, localization, and transmit power estimation in lognormal fading environment 89
4.7.1 Introduction 89
4.7.2 Propagation Model 90
4.7.3 Typical RSS Model in lognormal fading 91
4.7.4 Cramer-Rao Lower Bound 92
4.7.5 Performance Assesment 93
4.7.6 References 97
4.8 Annex H - JRA 1.2.3-3 Source detection in the presence of interference and noise 98
4.9 Annex I - JRA 1.2.3-4 Hybrid Spectrum Sensing Architecture for Cognitive Radio: Overcoming Noise Uncertainty 98
4.10 Annex I - JRA 1.2.3-5 on energy-efficient data collection and estimation in wireless sensor networks 98

1.Introduction

1.1 Glossary

3GPP	Third Generation Partnership Project
ACK	Acknowledge
AF	Amplify-and-Forward
AIC	Akaike Information Criterion
AMP	Approximate Message Passing
AOA	Angle of Arrival
AWGN	*Additive white Gaussian noise*
BER	Bit Error Rate
BP	Belief Propagation
BP	Basis Pursuit
BPDN	Basis Pursuit Denoising
CB	Cooperative Beamforming
CDF	Cumulative Distribution Function
CDMA	*Code Division Multiple Access*
CEM	Competitive Expectation Maximization
CF	Compress-and-Forward
CLA	Convergence Layer Adapter
CLRB	Cramér–Rao Lower Bound
CoD	Compute at the Destination
CoF	Compute-and-Forward
CoSLAT	Cooperative Simultaneous Localization And Tracking
CR	Cognitive Radio
CRB	Cramér–Rao Bound
CS	Compressed Censing
CSI	Channel State Information
CSIT	Channel State Information at the Transmitter
CSMA/CA	Carrier Sense Multiple Access with Collision Avoidance
DCM	Destination Cooperative Multicast

DNCM	Destination Non-Cooperative Multicast
DS	Dantzig Selector
DS-CDMA	Direct-Sequence Code Division Multiple Access
DSL	Digital Subscriber Line
DTN	Delay Tolerant Network
ECVF	Energy Consumption and VAA Formation
ED	Energy Detection
EDGE	Enhanced Data rates for GSM Evolution
EE	Energy Efficiency
EM	Expectation Maximization
EMDDA	Expected Multi-Destination Delay for Anycast
FIFO	First In First Out
FPGA	*Field Programmable Gate Array*
GMM	Gaussian Mixture Models
GP	Geometric Programming
GPRS	*General Packet Radio Service*
GSM	Global System for Mobile Communications
HSD	Hybrid Spectrum Detector
HTTP	HyperText Transfer Protocol
IA	Interference Alignment
IoT	Internet of Things
IPLF	Information Production and Link Formation
JRA	Joint Research Activity
KKT	Karush-Kuhn-Tucker
LASSO	Least-Absolute Shrinkage And Selection Operator
LDPC	Low-Density Parity-Check
LoP	Line of Position
LTE	*Long Term Evolution*
LTP	Licklider Transmission Protocol
LTP-T	Licklider Transmission Protocol Transport

MAC	Multiple Access Control
MANET	Mobile Ad-hoc *NETwork*
MARC	Multiple Access Relay Channel
MC	Mobile Cloud
MDL	Rissanen's Minimum Description Length
MF	Mean Field
MIMO	*Multiple Input and Multiple Output*
MIQP	Mixed Integer Quadratic Programming
ML	Maximum Likelihood
ML	Maximum Likelihood
MLE	Maximum-Likelihood Estimators
MRS	Multiple-Radio-Source
MVU	Maximum Variance Unfolding
MWG	McAfee Web Gateway
NE	Nash Equilibrium
ODE	Ordinary Differential Equations
OFDM	*Orthogonal Frequency-Division Multiplexing*
PA	Power Allocation
PC	Power Control
PDF	Probability Distribution Function
PER	Polymorphic Epidemic Routing
PF	Particle Filter
PKI	Public Key Infastructure
PMAC	Parallel Multiple Access Channel
POCS	Projection on Convex Sets
PSD	Power Spectral Density
PU	Primary User
QoS	Quality of Service
RA	Resource Allocation
RDA	Redundant Dictionary Arrangement

RF	Radio Frequency
RSS	Received Signal Strength
SAGE	Space Alternating Generalized EM
SDP	Semi-Definite Programming
SED	Sequential Energy Detector
SINR	Signal to Interference plus Noise Ratio
SISO	Single-Input Single-Output
SLAT	Simultaneous Localization And Tracking
SMTP	*Simple Mail Transfer Protocol*
SNR	Signal to Noise Ratio
SoA	Service oriented Architecture
SPBP	Sigma Point Belief Propagation
STBC	Space Time Block Coding
SU	Secondary User
TCP	Transmission Control Protocol
TCPCL	Transmission Control Protocol Convergence Layer
TDOA	Time Difference of *Arrival*
TOA	Time of Arrival
UDP	*User Datagram Protocol*
UMTS	*Universal Mobile Telecommunications System*
USRP	Universal Software Radio Platforms
V-MIMO	Virtual Multiple-Input and multiple-Output
VAA	Virtual Antenna Array
WCDMA	*Wideband Code Division Multiple Access*
WiMAX	Worldwide Interoperability for Microwave Access
WLAN	Wireless Local Area Network
WLS	Weighted Least-Squares
WSN	Wireless Sensor Network
WWWOFFLE	World Wide Web Offline Explorer

1.2 List of Joint Research Activities (JRAs)

Active JRAs in Task 1.2.1:

- JRA 1.2.1-1: An Information-Theoretic Pespective of Cooperation in Multi-User Communications
- JRA 1.2.1-2: Network coding for MARC
- JRA 1.2.1-3: Message-passing methods for distributed wireless network optimization
- JRA 1.2.1-4: Distributed learning schemes for signal optimization in large wireless networks
- JRA 1.2.1-5: Clusters organization for multi-hop cooperative communications

Active JRAs in Task 1.2.2:

- JRA1.2.2-1: Opportunistic relaying and forwarding
- JRA1.2.2-2: Game theoretic approach to timing channel communication

Active JRAs in Task 1.2.3:

- JRA1.2.3-1: Multiple source detection, localization, and transmit power estimation in lognormal fading environment
- JRA1.2.3-2: Cooperative Simultaneous Localization and Tracking
- JRA1.2.3-3: Source detection in the presence of interference and noise
- JRA1.2.3-4: Hybrid Spectrum Sensing Architecture for Cognitive Radio: Overcoming Noise Uncertainty

1.3 Main WP Achievements

During the reporting period the WP1.2 activities have profitably advanced. In particular, the research activities carried out by partners in JRAs led to the publication of numerous papers in conferences and journals. More specifically, the following papers have been already published or accepted for publication.

International Journal Publications:

[1] M. El Soussi and A. Zaidi and L. Vandendorpe, "Compute-and-Forward on a Multiaccess Relay Channel: Coding and Symmetric-Rate Optimization," IEEE Trans. on Wireless Communications, Vol. 13, No. 4, 2014, pp. 1932-1947.

[2] P. Mertikopoulos, E. V. Belmega, “Transmit without regrets: Online optimization in MIMO–OFDM cognitive radio systems,” IEEE Journal on Selected Areas in Communications, vol. 32, no. 11, November 2014.

[3] F. Meyer, O. Hlinka, F. Hlawatsch, Sigma Point Belief Propagation, IEEE Signal Processing Letters, 21(2), pages 145 - 149, 2014.

International Conference Publications:

[1] M.-A. Badiu, M. Guillaud, and B. H. Fleury, “Interference alignment using variational mean field annealing,” invited paper at the *Workshop on Physics-Inspired Paradigms in Wireless Communications and Networks (PHYSCOMNET)*, in *Proc. of the 12th International Symposium on Modeling and Optimization in Mobile, Ad Hoc, and Wireless Networks (WiOpt)*, Hammamet, Tunisia, 12-16 May 2014, pp. 585–590.

[2] M. Guillaud, M. Rezaee and G. Matz, “Interference Alignment via Message-Passing,” proc. *IEEE International Conference on Communications (ICC)*, Sydney, Australia, June 10-14, 2014.
[3] P. Coucheney and B. Gaujal, “Distributed optimization in multi-user MIMO systems with imperfect and delayed Information”, in ISIT ’14: Proceedings of the 2014 IEEE International Symposium on Information Theory, 2014.
[4] S. D’Oro, A. L. Moustakas, and S. Palazzo, “Adaptive transmit policies for cost-efficient power allocation in multi-carrier systems”, invited paper in RAWNET Workshop at WiOpt ‘14: Proceedings of the 12th International Symposium and Workshops on Modeling and Optimization in Mobile, Ad Hoc and Wireless Networks, 2014.
[5] Andreotti R., Stupia I., Mijovic S., Buratti C., Zanella A., Giannetti F., “VAA Formation Game for Cooperative Wireless Sensor Networks”, EuCNC 2014, Bologna, Italy.
[6] B. Lorenzo-Veiga, S. Glisic, L. Galluccio, Y. Fang. Adaptive Infection Recovery Schemes for Multicast Delay Tolerant Networks. Proc. of IEEE Globecom 2013. Atlanta, GA. December 2013.
[7] F. Meyer, B. Etzlinger, F. Hlawatsch, A. Springer, ‘A Distributed Particle-based Belief Propagation Algorithm for Cooperative Simultaneous Localization and Synchronization, in Proc. Asilomar 2013, Pacific Groove, CA, November, 2013.
[8] B. Etzlinger, F. Meyer, A. Springer, F. Hlawatsch, H. Wymeersch, Cooperative Simultaneous Localization and Synchronization: A Distributed Hybrid Message Passing Algorithm, in Proc. Asilomar 2013, Pacific Groove, CA, November, 2013.
[9] Spyridon Evangelatos and Aris L. Moustakas, “Statistical Mechanics Approach for the Detection of Multiple Wireless Sources via a Sensor Network”, Physcomnet, Tunisia, 2014.
[10] G. Bacci, E. V. Belmega, and L. Sanguinetti, “Energy-aware competitive link adaptation in small-cell networks”, invited paper in RAWNET Workshop at WiOpt ‘14: the 12th International Symposium and Workshops on Modeling and Optimization in Mobile, Ad Hoc and Wireless Networks, 2014.
[11] P. Mertikopoulos, E. V. Belmega, “Adaptive spectrum management in MIMO-OFDM cognitive radio: An exponential learning approach”, in ValueTools ’13: Proceedings of the 7th Int’l Conference on Performance Evaluation Methodologies and Tools, 2013.
[12] A. Nafkha, M. Naoues, K. Cichon, A. Kliks, "Experimental spectrum sensing measurements using USRP Software Radio platform and GNU-radio," Cognitive Radio Oriented Wireless Networks and Communications (CROWNCOM), 2014 9th International Conference on , vol., no., pp.429,434, 2-4 June 2014.
[13] S. M. Fosson, J. Matamoros, C. Antón-Haro, E. Magli, “Distributed support detection of jointly sparse signals." Acoustics, Speech and Signal Processing (ICASSP), 2014 IEEE International Conference on. IEEE, 2014.

Others:
[1] D. N. Urup, Distributed Localization in Dynamic Cooperative Wireless Sensor Networks using the Mean Field Approximation, Master Thesis, Aalborg University, 2014.

The JRAs carried out in this WP are really heterogeneous and cope with different issues related to opportunistic and cooperative communications.
In particular the most promising areas of investigation include distributed interference management, network organization and use of network coding, design of relaying and forwarding schemes for opportunistic scenarios, multisource localization and tracking in presence of interference. Many of these JRA activities are tightly related to the activities of the EUWIN platform. In particular, relaying and forwarding schemes to be tested in opportunistic scenarios could be implemented in the EUWIN platform and comparison between theoretical and experimental results will be provided in the next deliverables.

A relevant result of the activities carried out in this WP within the N# project is the high number of joint research activities which have already achieved tangible results in terms of Newcom# special sessions, special issues and invited presentations.

2. Description of Activity and Collection of Results

2.1 JRA 1.2.1-1 An Information-Theoretic Pespective of Cooperation in Multi-User Communications

Participating Researchers: M. Benammar (SUPELEC-CNRS), P. Piantanida (SUPELEC-CNRS) and S. Shamai (Technion)

2.1.1 Description

This JRA is active, although it currently has no new results to provide for the reporting period considered in this deliverable. The JRA leader has declared to expect a lot of significant results on a new problem they have recently faced, which will be included in the next incoming reports.

2.1.2 Relevance with the identified fundamental open issues

The Cognitive Multicast Interference Channel (IC) is similar to an interference channel with two sources and multiple destinations with the additional consideration that one of the sources has full non causal knowledge of both messages to be transmitted. The cognitive source can model the secondary transmitter, that upon sensing the primary transmitter's message, communicates the secondary message to the secondary user. As such, the secondary source should not create too much interference to the primaru user while transmitting the secondary message, so as not to cause impediment to the primary communication. However, it can also cooperate with the primary source and thus enhance the performance of the primary communication. Such a trade-off is well captured by the information theoretic analysis of the setting which allows to derive the optimal rate region and transmit strategies.

2.1.3 Initial Results

In this JRA, we investigate the capacity region of the Cognitive N-Multicast IC, where many primary users are interested in the same message and where there is only one secondary transmitter. An inner bound on the capacity region of this setting is derived, which combines the optimal coding techniques of the Broadcast Channel with rate-splitting for the interference channel. This inner bound recovers Marton's inner bound in the absence of the primary user.

2.1.4 Achievements and planned activities

We evaluate this rate region in both cases of very strong interference and very weak interference, showing that the respective rate regions are both converse and thus achieve the capacity region. Later, we will fully characterize the capacity region of the corresponding Gaussian cases resorting to standard upper bounding techniques and Gaussian arguments.

Results will be produced and reported into the next reporting period (Y3).

2.2 JRA 1.2.1-2 Network coding for MARC

Participating Researchers: M. El Soussi (UCL), A. Zaidi (CNRS- Université Paris-Est Marne-La-Vallée), and L. Vandendorpe (UCL)

2.2.1 Description

This JRA considers a system in which multiple users communicate with a destination with the help of multiple half-duplex relays. Based on the compute-and-forward scheme, each relay, instead of decoding the users' messages, decodes an integer-valued linear combination that relates the transmitted messages. Then, it forwards the linear combination towards the destination. In this work, the relays do not coordinate among themselves in computing the linear combinations. Thus, given these linear combinations, the destination may or may not be able to recover the transmitted messages since the linear combinations are not always full rank. Therefore, this JRA proposes an algorithm where we optimize the precoding factor at the users such that the probability that the equations are full rank is increased and that the transmission rate is maximized.

2.2.2 Relevance with the identified fundamental open issues

In this work, participating partners extend their previous work (described in the previous deliverable) to the case of multi-user and multi-relay. In that previous work, they studied the two users multiple access relay channel with CoF strategy where they maximize the transmission rate by properly allocating the precoding factors (powers) at the users and computing the integer coefficients at the relays. In the previous work, researchers propose a method to compute the integer coefficient vectors of the linear combinations where the relays jointly optimize the integer vectors in such a way that the transmission rate is maximized and the matrix formed by these vectors is full rank. This method, however, is not practical for large networks since additional signaling overhead is needed among the relays.
In this setting, each relay independently (i.e. no coordination among the relays) computes a linear combination and then forwards it to the destination. Hence, there is a possibility that the received linear combinations at the destination are not full rank and thus the destination is not able to decode the transmitted messages. It is shown that, by considering precoding allocation at the users, the probability of rank failure at the destination decreases since the precoding factor alters the channels between the users and the relays and hence alters the integer coefficient vectors. Thus, the objective is to allocate the powers at the users side in such a way that the received linear combinations at the destination are full rank and that the transmission rate is maximized.

2.2.3 Initial results

In this JRA, the symmetric outage rate is used to measure the performance of the coding strategy. It is shown that the proposed method achieves a symmetric outage rate slightly less than what is obtained using the method in a previous work. However, note that in this previous work the integer coefficient vectors are jointly computed among the relays. Each relay finds a candidate set that contains several integer vectors. From those candidate sets, the relays jointly select from each set an integer vector to construct a full rank matrix that maximizes the transmission rate. In order to jointly select the integer coefficient vectors, the relays need either to signal their candidate sets to each other or to transmit them to a central controller which would perform the selection and send the result back to the relays. This is clearly not practical for a large number of users and relays and makes the proposed method more practical and efficient. Moreover, the complexity to select the independent integer vectors from the candidate sets is of order M^T where M is the number of relays and T is the number of integer vectors in each set (or the number of decoded linear combinations at each relay).

2.2.4 Achievements and planned activities

In the new proposed method, the complexity to select the independent integer vectors from the candidate sets is zero since each relay independently computes an integer vector. Also, it is shown that the proposed algorithm outperforms other algorithms proposed in the literature and that CoF strategy, in this regime, has better performance than standard DF (Decode-and-Forward) and CF (Compress-and-Forward).
Also, it is shown that the probability that the linear combinations are not full rank is quite small using the proposed method compared with other methods. Hence, precoding allocation can help to increase the transmission rate, to decrease the probability of rank failure, and to reduce the complexity at the relays.
So far, it has been assumed that the channels are flat fading and perfectly known at the transmitters and that the relays can perfectly decode the linear combinations. In future works, the problem of selective channels, the problem of imperfect channels information, and the problem where the relays decodes the linear combinations with an error will be addressed.

2.2.5 Publications

[1] M. El Soussi and A. Zaidi and L. Vandendorpe, "Compute-and-Forward on a Multiaccess Relay Channel: Coding and Symmetric-Rate Optimization," IEEE Trans. on Wireless Communications, Vol. 13, No. 4, 2014, pp. 1932-1947.

2.3 JRA 1.2.1-3 Message-passing methods for distributed wireless network optimization

Participating researchers: Mihai-Alin Badiu (AAU), Maxime Guillaud (VUT), Bernard Fleury (AAU)

2.3.1 Description

The overall goal of this JRA is to design distributed interference management schemes requiring only local information exchange at any given point of the network, while retaining the performance of centralized schemes.
So far, the focus is on the interference alignment (IA) strategy, as it is a promising technique for achieving the full degrees-of-freedom of the interference channel. The objective is to develop algorithms that find solutions to the IA problem in the MIMO interference channel. The algorithms should admit distributed implementation -- this property is highly desirable in networks with large number of nodes. Since message-passing techniques provide a systematic methodology for designing algorithms that perform distributed computations, the applicability of algorithms such as sum-product (belief propagation), min-sum or variational message-passing is explored.

2.3.2 Relevance with the identified fundamental open issues

Even though the IA problem consists in finding precoders which satisfy a set of relatively simple conditions, closed-form solutions for the precoders are lacking (except for some simple system setups). This has determined researchers to use numerical algorithms, e.g., based on alternating optimization.
An added benefit of the use of message-passing is that this class of algorithms is particularly suitable to a distributed implementation. This is because the message formulation (and the associated bipartite graph) clearly captures the dependency between the optimization variables and the data. Furthermore, it also enables an explicit analysis of the dependency on locally available data; interestingly, the algorithms obtained so far only require local data (channel state information) for the computation of the messages.
Another issue is selecting an appropriate cost function to be optimized: the cost function should be relevant (related) to the ultimate performance one want to maximize and, at the same time, should permit tractable message-passing computations.
Although message-passing has been applied before for designing precoders that maximize the sum-rate, the solution space was restricted to a finite discrete codebook of precoders. However, for the IA problem the precoders should have continuous values, meaning that the sought algorithms should operate over continuous variable space.

2.3.3 Initial Results

An iterative algorithm for solving the IA problem for the MIMO interference channel has been developed. The problem is formulated as an optimization problem whose cost function is the total weighted interference leakage. The deterministic annealing approach in conjunction with the mean field approximation (variational message-passing) to minimize the cost function has been considered. The computations of the resulting iterative algorithm can be distributed over the network. Existing algorithms, i.e. those by Gomadam et al. and Peters & Heath, can be instantiated as special cases of the proposed approach.

2.3.4 Achievements and planned activities

The proposed algorithm shows slightly faster convergence than the iterative leakage minimization (ILM) algorithm by Gomadam for some settings of the annealing scheme.

Furthermore, for a system configuration in which IA is not feasible, the approach proposed in this JRA also obtained significantly higher sum rates than ILM in asymmetric scenario.
Several directions in which the work can be continued have been identified. It is highly relevant to further improve convergence speed; for this purpose, studying other approximations than mean field (such as the Bethe approximation) could be an option. Another research direction is to explore other cost functions, which are more related to the data rate. Also, extending the method so that it can deal with channel uncertainty is definitely pertinent. In the studied problem, the number of interference-free dimensions desired at each receiver is given; a future activity is to devise an algorithm which, given the channel, jointly maximizes the number of interference-free dimensions and finds the corresponding precoders for IA. Finally, in a distributed implementation, the choice of the mapping between the nodes in the graph (whose topology is determined by the cost function), and the devices in the network, will impact the amount and the nature of the messages actually being exchanged between the devices; so far, the critical question of finding the optimal mapping remains largely open.

2.3.5 Publications

[1] M.-A. Badiu, M. Guillaud, and B. H. Fleury, “Interference alignment using variational mean field annealing,” invited paper at the *Workshop on Physics-Inspired Paradigms in Wireless Communications and Networks (PHYSCOMNET)*, in *Proc. of the 12th International Symposium on Modeling and Optimization in Mobile, Ad Hoc, and Wireless Networks (WiOpt)*, Hammamet, Tunisia, 12-16 May 2014, pp. 585–590.

[2] M. Guillaud, M. Rezaee and G. Matz, “Interference Alignment via Message-Passing,” proc. *IEEE International Conference on Communications (ICC)*, Sydney, Australia, June 10-14, 2014.

2.4 JRA 1.2.1-4 Distributed learning schemes for signal optimization in large wireless networks

Participating Researchers: P. Mertikopoulos (CNRS), E. V. Belmega (CNRS), S. D'Oro (CNIT/Catania), A. L. Moustakas (IASA), S. Palazzo (CNIT/Catania)

2.4.1 Description

During the current reporting period, CNIT expressed interest in JRA 1.2.1-4. After a series of research meetings (beginning with the N# Lisbon meeting in January 2014), the team was enlarged and new research directions were identified and pursued.
This JRA includes two sub-activities carried out by two research groups: Group 1 consists of CNRS and IASA. Group 2 consists of CNIT-CT, IASA and CNRS.
The research output of these activities is summarized in the publications section below (1 IEEE JSAC paper, 3 conference papers, while 2 additional journal papers are currently in preparation).
Efforts within the framework of JRA 1.2.1-4 focused on developing distributed learning algorithms for efficient and robust signal optimization in multiple-input, multiple-output (MIMO) uplink multiple access channels [1], and optimizing the throughput of opportunistic wireless users in MIMO-OFDM cognitive radio networks [2,3].
Given the importance of conserving battery power in wireless transmissions, we also developed an adaptive transmit policy for efficient power allocation in multi-carrier systems (joint work between CNRS, IASA and CNIT-CT) [4].

2.4.2 Relevance with the identified fundamental open issues

Individual transmit signal optimization is one of the core issues for the efficient operation of a wireless network, especially when the network in question is deployed at a very large scale that precludes centralized control. However, any attempt at optimizing the transmit policy of a wireless user must overcome several major challenges, such as imperfect channel state information, delayed (and potentially obsolete) measurements, lack of coordination between users, etc. To that end, the overarching objective of JRA 1.2.1-4 is to apply the tools and techniques of the theory of learning in order to achieve distributed optimization methods for efficient network operation - and thus to effectively achieve the users' cooperation.

2.4.3 Initial results

In this JRA several issues in cooperative wireless networks have been investigated. More in detail, researchers focused on the implication of MIMO and OFDM techniques on achievable network performance. Research activities started with the exploration of the problem of distributed learning in multiple access networks where interference management and power control are exploited to improve network performance. Initial results have shown that distributed learning techniques are promising tools to allow individual mobile users to cooperate and reach efficient operating point by exploiting local measurements. Obtained results have shown that high performance can be achieved even in the case of imperfect measurements.

2.4.4 Achievements and planned activities

In the context of transmit signal optimization in MIMO multiple access channels, the problem of signal covariance optimization under imperfect (and possibly delayed) channel state information has been analyzed. Starting from the continuous-time learning scheme of matrix

exponential learning, a distributed solution algorithm has been developed. This solution is obtained by introducing a damping term which ensures the method's stability under stochastic perturbations and delays (or asynchronicities) of arbitrary magnitude. As opposed to traditional water-filling methods, the convergence properties of the proposed algorithm (speed and accuracy) can be controlled by tuning the damping coefficient; accordingly, the algorithm converges arbitrarily close to an optimum signal covariance profile within a few iterations (even for large numbers of users and/or antennas per user), and this convergence remains robust in the presence of imperfect measurements and asynchronous user updates [1].

To allow for user mobility and less structured network paradigms, cognitive radio systems that evolve dynamically over time due to changing user and environmental conditions have also been investigated. To combine the advantages of orthogonal frequency division multiplexing (OFDM) and multiple-input, multiple-output (MIMO) technologies, a full MIMO–OFDM cognitive radio network where wireless users with multiple antennas communicate over several non-interfering frequency bands has been considered. As the network's primary users (PUs) come and go in the system, the communication environment changes constantly (and, in many cases, randomly). Accordingly, the network's unlicensed, secondary users (SUs) must adapt their transmit profiles "on the fly" in order to maximize their data rate in a rapidly evolving environment over which they have no control. In this dynamic setting, research activities have been focused on dynamic transmit policies that lead to *no regret*, i.e. that perform at least as well as (and typically outperform) even the best fixed transmit profile in hindsight. Drawing on powerful mirror descent techniques, a no-regret transmit policy for the system's SUs which relies only on local channel state information (CSI) has been derived. Using this method, the system's opportunistic users are able to track their individually evolving optimum transmit profiles remarkably well, even under rapidly (and randomly) changing conditions. Importantly, the proposed policy leads to no regret even if the SUs' channel measurements are subject to arbitrarily large observation errors (the imperfect CSI case), thus ensuring the method's robustness in the presence of uncertainties [2,3].

Finally, to account for cost/energy-efficient power allocation, OFDM networks consisting of wireless users who seek to maximize their transmission rate subject to pricing or power limitations have been studied. By formulating the problem as a non-cooperative game, it has been shown that the system admits a unique equilibrium. Moreover, we have proposed [4] a distributed exponential learning scheme which allows users to converge to the game's equilibrium exponentially fast, using only local channel state information (CSI) and signal to interference-plus-noise ratio (SINR) measurements.

In the next phase of N#, researchers plan to focus their efforts on extending the joint work above to networks consisting of mobile, opportunistic users. Two papers are already in preparation and will be submitted to IEEE journals within the span of the next few months. In addition, a semester-long research visit of P. Mertikopoulos (CNRS) to IASA is planned to take place in the spring semester of 2014 in order to advance the development of distributed cooperative learning methods for coalition formation in cognitive radio networks.

2.4.5 Publications

[1] P. Coucheney, B. Gaujal, and P. Mertikopoulos "*Distributed optimization in multi-user MIMO systems with imperfect and delayed Information*", in ISIT '14: Proceedings of the 2014 IEEE International Symposium on Information Theory, 2014.

[2] P. Mertikopoulos and E. V. Belmega, "*Adaptive spectrum management in MIMO-OFDM cognitive radio: An exponential learning approach*", in ValueTools '13: Proceedings of the 7th Int'l Conference on Performance Evaluation Methodologies and Tools, 2013.

[3] P. Mertikopoulos and E. V. Belmega, "*Transmit without regrets: Online optimization in MIMO–OFDM cognitive radio systems*," IEEE Journal on Selected Areas in Communications, vol. 32, no. 11, November 2014.

[4] S. D'Oro, P. Mertikopoulos, A. L. Moustakas, and S. Palazzo, "*Adaptive transmit policies for cost-efficient power allocation in multi-carrier systems*", invited paper in WiOpt '14: Proceedings of the 12th International Symposium and Workshops on Modeling and Optimization in Mobile, Ad Hoc and Wireless Networks, 2014.

2.5 JRA 1.2.1-5 Clusters organization for multi-hop cooperative communications

Participating Researchers: Riccardo Andreotti (CNIT-Pisa), Paolo del Fiorentino (CNIT-Pisa), Filippo Giannetti (CNIT-Pisa), Vincenzo Lottici (CNIT-Pisa), Ivan Stupia (UCL), Chiara Buratti (CNIT-Bologna), Stefan Mijovic (CNIT-Bologna), Alberto Zanella (CNIT-Bologna).

2.5.1 Description

This JRA considers a Wireless Sensor Network (WSN), where nodes form Virtual Antenna Arrays (VAAs) use cooperative beamforming to transmit toward a sink. On one hand cooperation greatly increases link capacity, but on the other, it introduces a certain overhead. This tradeoff is analyzed by properly formulating the VAA formation problem as a noncooperative game with complete information, where sensor nodes aim at forming VAAs to maximize their own successful transmission rate, while keeping under control the energy consumed for the signaling within VAAs. Based on this analysis, we then introduce a communication protocol for VAA formation.

2.5.2 Relevance with the identified fundamental open issues

Traditional cooperating techniques poses several technical challenges in a sparse node scenario, where nodes should decide whether or not to accept new nodes in their coalition, mainly because of the large amount of signaling packets required to establish the cooperation. Therefore we propose to model and study such iterations resorting to the tool of noncooperative game theory. The latter formulation does not mean that one cannot produce an outcome that can be socially useful, but rather that the global behavior emerges through a sequence of individual choices that may modify the outcomes of the others players, i.e., cooperating nodes, in a positive manner.

2.5.3 Initial results

The activity started from the analysis carried out during year 1, where the VAA formation problem was modeled as that of information sharing in a social network (SN). In detail, the sensors' transmit power is treated as the contents that can be shared among users in an SN, while the relationships established to share those contents model the VAAs structure. Resorting to the Dixit-Stieglitz preference model to evaluate the benefit function of every node, at the equilibrium (i.e., the solution of the game leads) we get a useful structure, where there are only two kinds of nodes, those with low transmit power and those with high transmit power. The former can form a coalition only with the latter, which is suitable for a VAA structure where the sensor nodes with high energy availability can help the sensors with a poor battery status.

2.5.4 Achievements and planned activities

Relying on the design guidelines obtained with the game theoretical analysis, the various steps of the communication protocol required to get the cooperative beamforming transmission have been derived and analyzed, namely the cluster formation, the VAA formation and the cooperative beamforming. Numerical results show the benefits of cooperation among nodes compared to the case where no cooperation is present. In particular, by properly setting a parameter of the Dixit-Stieglitz model the, trade-off between the performance improvement due to the cooperation and the increment of energy consumption due to required overhead can be tuned depending on the design guidelines. Results showed also the impact of considering a realistic communication protocol,

accounting for packets losses, compared to the ideal case achieved through the game. By properly setting the parameters of the protocol, game solution can be reached.
A proprietary simulator has been designed for the purpose of performance evaluation. It is written in C++ and it simulates the scenario with the described communication protocol.

2.5.5 Publications

[1] Andreotti R., Stupia I., Mijovic S., Buratti C., Zanella A., Giannetti F., "VAA Formation Game for Cooperative Wireless Sensor Networks", EuCNC 2014, Bologna, Italy.

2.6 JRA1.2.2-1: Opportunistic relaying and forwarding

Participating Researchers: Laura Galluccio (CNIT-CT), Savo Glisic (UOULU), Beatriz Lorenzo Veiga (University of Vigo, Associate Partner Type II, formerly UOULU)

2.6.1 Description

Delay tolerant networks consist of nodes moving around and occasionally happening to come into each other's proximity. During the limited proximity time nodes can exchange data; this very slow data dissemination process is usually assumed to happen according to a replication-based methodology.
In case of multicast DTN application scenarios, due to the long propagation delay and the consequent large overhead associated to the replication approach, data delivery may become a critical issue. In order to reduce the dissemination overhead, these mechanisms are typically combined with infection recovery procedures that remove packet copies from the network as soon as the first node of the multicast group is reached. This however could be performed too early, thus stopping the dissemination process before all destinations have been reached.
This JRA considers a new dimension in multicast data dissemination, namely social-driven data dissemination. In this process, the dissemination procedure is not trivially epidemic, therefore exploiting the intrinsic sociality of users and their interests to reduce the delivery overhead and speeding up the dissemination in multicast scenarios. More specifically a dissemination procedure where users are not individual members of the network but can be aggregated into groups which share interests and disseminate packets according to some group policy is considered. Researchers want to investigate on the impact of such grouping into the dissemination procedure. Moreover they also combine this mechanism with an adaptive infection recovery procedure aimed at controlling and progressively reducing the number of copies of a packet circulating into the network. The analysis shows that sociality of users can speed up the delivery process and is a critical feature for controlling the adaptive recovery.

This JRA includes two sub-activities carried out by two research groups: Group 1 consists of CNIT-CT and CNIT-BO and is involved in a theoretical joint research activity converging into the experimental activities which will be carried out in WP2.2 "Networking technologies for the Internet of Things (IoT) with mobile clouds". In particular, the feedback obtained by theoretical studies on opportunistic networking will be used by CNIT-CT researchers working in Track 2 to appropriately design algorithms to be tested in the EuWIN platform. Currently the first subJRA involving CNIT-CT and CNIT-BO does not have new results to provide for the time period considered in this deliverable.
Group 2 consists of CNIT-CT and UOULU and is involved in a theoretical joint research activity activity.

2.6.2 Relevance with the identified fundamental open issues

The relevance of this activity with respect to project goals is to be searched in the consideration of the impact of sociality on dissemination mechanisms in opportunistic networks where multicast applications are supported. In particular, the combination of network coding for throughput improvement and sociality increases the chances that data are successfully and reliably forwarded in disconnected opportunistic scenarios.

2.6.3 Initial Results

Delay Tolerant Networks have attracted the interest of researchers for the challenging features related to communication support in time varying wireless channels with mobile users and unpredictable variations in channel conditions.
In these scenarios, support of multicast paradigms is even harder because of the long delay related to sporadic users contacts.
The traditional paradigms for multicast information delivery in DTNs usually employ an epidemic- like approach to guarantee data delivery at the cost of an excessive overhead and energy consumption. Accordingly recovery strategies have been proposed which limit this overhead at the cost of risking to early interrupt data dissemination.

2.6.4 Achievements and planned activities

During this second year, we have focused on the support of multicasting in DTNs using adaptive recovery strategies which take into account sociality of users. More specifically we have modeled sociality of groups through an interest-casting approach and shown that use of sociality can help to overcome the limitations of either an epidemic packet storm or a non efficient packet delivery in multicast environments. Our analysis can represent a starting point for the efficient design of adaptive recovery schemes in multicast DTNs.
As a future work, we would like to collect statistics on inter-contact time distributions and use them in our theoretical framework. We would like also to implement a simplified testbed of such an opportunistic network and compare experimental results with the theoretical ones

2.6.5 Publications

[1] B. Lorenzo-Veiga, S. Glisic, L. Galluccio, Y. Fang. Adaptive Infection Recovery Schemes for Multicast Delay Tolerant Networks. Proc. of IEEE Globecom 2013. Atlanta, GA. December 2013.

2.7 JRA1.2.2-2: Game theoretic approach to timing channel communication

Participating Researchers: Salvatore D'Oro, Laura Galluccio, Giacomo Morabito and Sergio Palazzo (CNIT-CT), Fabio Martignon and Lin Chen (CNRS-UPS)

2.7.1 Description

During last year, research activities carried out within this JRA have been focused on the extension of a previous work on game theoretic analysis of jammed timing channels. More in detail, researchers aimed at proposing a more realistic scenario where the considered utility functions reflect the real concerns of each player. Furthermore, the considered transmission scheme has been modified so that the proposed study also applies to a wide range of possible wireless applications and scenarios where security and energy consumption are critical issues.
Researchers have focused on the study of the Nash Equilibrium (NE) in order to prove its uniqueness and demonstrate how each player can individually reach such an equilibrium in a distributed fashion.
In this JRA a hierarchical game where the target node anticipates the strategy of the jammer has been also considered. In fact, we expect that such hierarchy helps both players in improving their own utility.
In order to take into account the imperfectness of the information on some system parameters, the impact of imperfect knowledge on the outcome of the game has also been investigated. As imperfectness could strongly affects the outcome of the game, researchers are searching for any analytical/heuristic rules that allow the target node in achieving a high payoff even in the imperfect knowledge case.

2.7.2 Relevance with the identified fundamental open issues

Even though there are plenty of game theoretical studies on jammed scenarios dealing with security issues at the physical layer of the ISO/OSI stack, there are only few studies on jammed timing channels in wireless networks.
The main objective of this JRA is to relax several assumptions in the already existing literature to provide a new game theoretical analysis that produces useful and novel insights.
So far, obtained results showed that timing channels are a promising technique to avoid jamming attacks in wireless networks as it is possible to transmit information even when a jamming attack is ongoing, and it is possible to reduce the energy consumption of the transmission as it exploits coded silence periods to convey the transmitted data.

2.7.3 Initial results

In the considered model the trade-off between the achievable capacity and the energy consumption which is a critical issue in wireless networks has been considered.
Simulation results have shown that timing channels are feasible and robust to jamming attacks in several wireless network applications.
Furthermore, it has been found that the energy constraints strongly impact the achieved utility and, as a consequence, reduce the strategy space of each player participating in the game.

2.7.4 Achievements and and planned activities

Surprisingly, some preliminary results show that, in some cases, introducing hierarchy in the jamming game is useful for both players and not only for the leader. In fact, in a hierarchical structured game, such as the Stackelberg game, where the target node acts as the leader and the jammer as the follower, it is expected that the Stackelberg game strictly outperforms the ordinary Nash game. Therefore, the output of the Stakelberg game is a win-win solution for both the target node and the jammer.

The paper “Defeating jamming with the power of silence: a game-theoretic analysis”, S. D’Oro, L. Galluccio, G. Morabito, S. Palazzo, L. Chen, F. Martignon, with acknowledgement to the NEWCOM# project, contains all analytical and simulation results from this JRA, has been recently accepted for publication on the IEEE Transactions on Wireless Communications.
In order to consider more complex scenarios, next research activities within this JRA will be focused on the extension of the analytical framework to the multi-player scenario.

2.7.5 Publications

[1] S. D’Oro, L. Galluccio, G. Morabito, S. Palazzo, L. Chen, F. Martignon, “Defeating jamming with the power of silence: a game-theoretic analysis” to appear on IEEE Transactions on Wireless Communications.

2.8 JRA1.2.3-1: Multiple source detection, localization, and transmit power estimation in lognormal fading environment

Participating Researchers: Ioannis Dagres (IASA) – George Arvanitakis (Eurecom) - Adrian Kliks (PUT)

2.8.1 Description

This year research activities focus on analyzing the performance of RSS based localization, for first time in a correlated log-normal environment. The main goal was to answer the following questions: a) what is the needed density of a (real-time) measurement network for a target localization performance? b) what is the density reduction requirement when utilizing past measurements? A rather simple analytic model for the propagation environment will be assumed in order to assess the performance gain of utilizing past measurements. Finally, the last and most important question is: how close are those conclusions to the true performance encountered in practice?
This is a difficult question, since any experimental setup represents just one realization of the random performance of a specific situation. As long as the theoretical model is close to the real one, you expect at least the general conclusions to be in agreement with experimental results. There exists though, a lot of work in the litterature which shows a qualitative agreement on the potential gains [1] when exploiting spatial correlation. In order to have also a quantitative one, a large number of experimental campaigns is needed. This JRA also provides a considerable contribution to this collective effort by one more experimental campaign in an indoor environment using the OpenAirInterface (OAI) platform. Based on the collected measurements, various options for modeling the spatial correlation were assessed.

The goal of this JRA is the extension of the work started in [1], targeting three aspects a) Algorithmic design b) Propagation model and spatial correlation c) Prior information. The experimental aspect of this work is directly related to JRAF Design and experimental validation of algorithms for active and passive indoor positioning (2.1.3) and JRA 2.3.3.1 Localization with Distributed Antennas.

2.8.1.1 References

[1] I. Dagres, A. Polydoros, D. Denkovski, M. Angjelicinoski, V. Atanasovski, and L. Gavrilovska, “Algorithms and bounds for energy-based multi-source localization in log-normal fading,” in Globecom Workshops (GC Wkshps), 2012 IEEE, 2012, pp. 410–415.
[2] B. Zhang, C. Zhang, and X. Yi, “Competitive EM algorithm for finite mixture models,” Pattern Recognit., vol. 37, no. 1, pp. 131–144, Jan. 2004.

2.8.2 Relevance with the identified fundamental open issues

All prior work on multi-source localization assumed no spatial correlation. Assuming availability of a database with localized Received Signal Strength (RSS) measurements, the performance of RSS based localization in correlated log-normal propagation environment is analyzed by proper use of the Crammer Rao Lower Bound. Researchers are interested in assessing the localization performance as a function of the density of the real time sensor network and the density of the stored (past) measurements. Based on those results, valuable conclusions are given for the deployment of practical sensor localization networks using RSS. Results of real experiment in indoor environment are presented that demonstrates the potential gains of such an approach and also provides practical considerations.

2.8.3 Initial results

Using the CRLB and proper semi-analysis it has been shown that large performance gains are expected when the spatial correlation is exploited by the use of a database of past measurements. The utilization of past measurements has been used very often in the literature, but a semi-analytic approach that reveals the scaling of the needed sensor network is introduced for the first time. The corresponding experimental part is described in the deliverable of the relevant Track.

2.8.4 Achievements and planned activities

As far as the algorithmic development is concerned, the work on the analysis and performance assessment of a novel Competitive Expectation Maximization (C-EM) algorithm (proposed in [2]) for multisource localization has been finalized. The design of measurement campaigns for testing the proposed algorithm is under preparation.

Regarding the work on spatial correlation and prior knowledge, we have derived performance bounds when spatial correlation exists and access to a database of past measurements is granted. The experimental part of this work was conducted by the use of the OpenAir interface platform. A conference paper is under preparation.

The extension of this work for multiple sources is under preparation. A journal paper that contains the collective results of all efforts within this activity is also under preparation.

2.9 JRA1.2.3-2: Cooperative Simultaneous Localization and Tracking

Participating Researchers: Florian Meyer (TUV), Burak Cakmak and Bernard Henri Fleury (AAU).

2.9.1 Description

Two competing message-passing algorithms are presently used in distributed localization in cooperative networks: belief propagation and mean-field approximation. Each method has its virtues and shortcomings. This JRA will exploit a recently developed theoretical framework to compare these approaches and possibly combine them.
The JRA will also address complexity issues of existing particle-based localization algorithms based on message passing. This will be done by finding efficient approximate representations for messages and beliefs with the goal of making the algorithms feasible for large-scale localization scenarios with mobile nodes.
Finally, researchers aim to develop distributed algorithms that jointly estimate the locations and clock parameters of the network nodes in a fully decentralized fashion.

2.9.2 Relevance with the identified fundamental open issues;

It is unclear in which localization scenario belief propagation message passing performs better than variational message passing or if performance achievements can be obtained by a combined MF/BP approach. Exisiting particle-based BP algorithms are too complex for any practical application. Localization and synchonization are two important tasks in cooperative networks. Often, both localization and synchonization algorithms are based on timing measurements between neighboring nodes in the network. However, typically both problems are usually addressed separately.

2.9.3 Initial results

Three contributions have been obtained :

1- A low-complexity localization algorithm based on MF message passing and gradient descent was developed.

2- A low-complexity localization algorithm based on BP message passing and sigma points was developed.

3- Two algorithms based on belief propagation message passing for simultaneous localization and synchronization among nodes in distributed networks have been presented.

2.9.4 Achievements and planned activities;

A journal paper in which the developed low complex localization algorithms are presented and compared in a large-scale dynamic setting is going to be prepared.

2.9.5 Publications

[1] D. N. Urup, Distributed Localization in Dynamic Cooperative Wireless Sensor Networks using the Mean Field Approximation, Master Thesis, Aalborg University, 2014.
[2] F. Meyer, O. Hlinka, F. Hlawatsch, Sigma Point Belief Propagation, IEEE Signal Processing Letters, 21(2), pages 145 - 149, 2014.
[3] F. Meyer, B. Etzlinger, F. Hlawatsch, A. Springer, ‘A Distributed Particle-based Belief Propagation Algorithm for Cooperative Simultaneous Localization and Synchronization, in Proc. Asilomar 2013, Pacific Groove, CA, November, 2013.

[4] B. Etzlinger, F. Meyer, A. Springer, F. Hlawatsch, H. Wymeersch, Cooperative Simultaneous Localization and Synchronization: A Distributed Hybrid Message Passing Algorithm, in Proc. Asilomar 2013, Pacific Groove, CA, November, 2013.

2.10 JRA1.2.3-3: Source detection in the presence of interference and noise

Participating researchers: Aris Moustakas, Spyridon Evangelatos (IASA) – Erwin Riegler (TUV)

2.10.1 Description

The purpose of this JRA is to provide a method to obtain fundamental limits for the detectability of multiple primary sources from a sensor network in the presence of interference and noise. The basic tools are borrowed from statistical physics and the theory of spin glasses.
Researchers have applied a two-pronged approach to the problem. In the first, it is assumed that the connectivity matrix is sparse with a finite number of connections for each source and sensor. This problem can be solved using the theory of dilute spin glasses. The pros of this analysis are the fact that it is more realistic while the cons are the complexity of the solution. In contrast the second approach is to assume a full connectivity limit. In this case, the matrix can more accurately include details of the channel, such as fading, which can be dealt with much easier. In contrast, of course the full matrix approximation is expected not to be too accurate in the 2-dimensional setting.
The above approach can provide closed form expressions that are valid for arbitrary random networks. These can then be used to compare with results in JRA1.2.3-1 and JRA1.2.3-2.

2.10.2 Relevance with the identified fundamental open issues

The focus here is to provide analytical expressions for the detection error rate that are valid for large systems and can be used for system dimensioning. This methodology is tailored for large scale systems.

2.10.3 Initial results

In this year most of the analysis in the case of sparse systems for the discrete case of on-off detection has been concluded. Researchers have shown good agreement with experimental values of various sized networks. A method to create a random bipartite graphe with connectivities that follow the Poisson distribution which is derived from the probability that a given sensor-source pair is connected with SINR greater than a given threshold has been provided. Researchers also provided an algorithm of messaging between sensors, which is based on their proximity on the graph.
The above methodology for the sparse network case with continuous powers has been generalized. Researchers are currently evaluating the message passing algorithm and the corresponding population dynamics approach.
In the context of the full matrix approximation, it has been shown that the replica symmetric equations hold for arbitrary random gain matrices.

2.10.4 Achievements and planned activities

The sparse network methodology seems to be working exceedingly well and researchers would like to augment it and also compare it with other more greedy approaches such as the OMP method.

2.10.5 Publications

[1] Spyridon Evangelatos and Aris L. Moustakas, “Statistical Mechanics Approach for the Detection of Multiple Wireless Sources via a Sensor Network”, Physcomnet, Tunisia, 2014.

2.11 JRA1.2.3-4: Hybrid Spectrum Sensing Architecture for Cognitive Radio: Overcoming Noise Uncertainty

Partners: Amor Nafkha (SUPELEC/CNRS), Malek Naoues (SUPELEC/CNRS), Adrian Kliks and Krzysztof Cichon (PUT)

2.11.1 Description

This JRA addresses the problem of SNR-wall in non-cooperative systems where the spectrum sensor suffers from a minimum SNR below which it is impossible to reliably detect the primary user's signal. The main objective through this JRA is to develop and implement two low-complexity spectrum sensing schemes in order to overcome the problem of the noise uncertainty. Two methods are applied in this activity; the first one is based on a combination of energy detector (ED) and cyclostationnary feature detector (CFD), the other one makes use of a double threshold sequential energy detector (SED).
The SED processes similarly as the traditional ED but its application can reduce the sensing time. The main idea here is based on the assumption that for a strong primary user signal (resp. no primary user signal), the number of used samples that should be collected to make a decision can be drastically reduced. The combination between the ED and the CFD detectors adopts the following principle: two fixed thresholds are considered for sensing decision, if the value of the test is between the considered thresholds, the CFD detector is applied.

2.11.2 Relevance with the identified fundamental open issues

The fundamental problem addressed in this activity is to implement, using GnuRadio with USRP platforms and/or FPGA, an adaptive and low-complex spectrum sensing scheme for cognitive radio systems to overcome noise uncertainty. Motivated by the fact that ED is the simplest sensing technique and can easily be implemented, we concentrate on this case. To cope with the problem of sensing time, which must be reduced as much as possible, the first part of this JRA considered a fixed double threshold scheme for the energy detector. The above part was implemented on software defined radio prototype by utilizing USRP N210 as hardware and GnuRadio as software platforms.

2.11.3 Initial results

The JRA's *initial results were or will be published in:*

1. IEEE Crowncom 2014 conference paper (invited paper).
2. IEEE Wicon 2014 conference paper (submitted)
3. Eurasip JWCN 2014 Journal paper: SI on Experimental Evaluation in Wireless communications (in progress)

2.11.4 Achievements and Planned activities

The main activities will be organized through the following steps:

1. Build a hardware demonstrator for adaptive double threshold spectrum sensing based on the USRP platforms.
2. Build a hardware demonstrator for spectrum sensing using FPGA platforms.

2.11.5 Publications

[1] A. Nafkha, M. Naoues, K. Cichon, A. Kliks, "Experimental spectrum sensing measurements using USRP Software Radio platform and GNU-radio," Cognitive Radio Oriented Wireless Networks and Communications (CROWNCOM), 2014 9th International Conference on , vol., no., pp.429,434, 2-4 June 2014.

2.12 JRA 1.2.3-5 on energy-efficient data collection and estimation in wireless sensor networks

Participating Researchers : Michel Kieffer, Francesca Bassi, Wenjie Li (CNRS-UniPS), Davide Dardari, Vincenzo Zambianchi, Gianni Pasolini (CNIT-UniBo), Sophie Fosson, Enrico Magli (CNIT-PoliTo), Javier Matamoros, Carles Anton-Haro (CTTC).

2.12.1 Description

This JRA is a cross work package research that belongs to WP 1.2 and WP 1.3. Therefore, for the sake of completeness, some of the information will be duplicated in their respective deliverables.

The activity of the reporting period has revolved around several research visits between the partner institutions.

Research visit: Sophie Fosson (CNIT-PoliTo) to CTTC
Dates: June 14th, 2013 – July 14th, 2014.
Title: Distributed sparse signal estimation: new models and solutions.
Funding: funded by the Newcom# Mobility Grant program.

Research visit: Vincenzo Zambianchi (CNIT-UniBo) to CNRS-UPS
Dates: November 7th, 2013 – May 7th, 2014.
Title: Distributed field estimation via consensus techniques.
Funding: partially funded by the Newcom# Mobility Grant program.

Research visit: Wenjie Li (CNRS-UPS) to CNIT-UniBo
Dates: May, 10th – July, 27th 2014 and Septembre 11th – October 31st, 2014
Title: Distributed outlier detection in wireless sensor networks
Funding: funded by the Newcom# Mobility Grant program.

2.12.2 Relevance with the identified fundamental open issues

During the reporting period the joint activity of S. Fosson, E. Magli (CNIT-PoliTo), and J. Matamoros, C. Antón-Haro has been devoted to the problem of the distributed detection of signals with sparse and common support from the netwok measurements. This is in adherence with the identified open issue 6 (possibility to distribute compressive sensing techniques to enable signal acquisition in wireless sensor networks).
The joint activity of V. Zambianchi, D. Dardari, G. Pasolini (CNIT-UniBo), and M. Kieffer, F. Bassi (CNRS-UPS) has been devoted to the study of the efficiency of consensus algorithms for information dissemination in the network, when the problem is the estimation of a parameter vector from the set of all measurements. This is in adherence with the identified open issue 3 (energetic efficiency of distributed data dissemination strategies).
The joint activity of W. Li, M. Kieffer, F. Bassi (CNRS-UPS), and D. Dardari, G. Pasolini (CNIT-UniBo), and has been devoted to the study of distributed outlier/fault detection in wireless sensor networks. This is in adherence with the identified open issue 7 (robusteness against sensor failure).

2.12.3 Initial Results

First, researchers have addressed the problem of distributed support detection of multiple sparse signals with common support. Specifically, a distributed setting by which signals are

acquired by the individual nodes of a network has been considered. In this scenario, a decentralized scheme has been proposed, referred to as Distributed iterative Thresholding (DiT), for in-network support detection. The approach is reminiscent of the iterative soft and hardthresholding methods. DiT has been proved to converge and the numerical results have revealed that DiT achieves consensus in the signal support in most cases.
Next, in the same distributed setting, researchers have considered the case where the observed signals are correlated. In particular, it has been assumed that the observed signals are composed of a common sparse component plus an innovation sparse component. First, a centralized solution based on the Alternating Direction Method of Multipliers (ADMM) has been developed. Then, a distributed version for in-network reconstruction called DADMM has been proposed. Finally, in order to reduce the amount of information exchanged that such distributed approach entails, a novel scheme requiring only binary message exchanges among neighboring nodes called DADMM-1 bit has also been proposed.
Numerical results have revealed that, after convergence, the proposed distributed algorithms perform virtually identical to the centralized ADMM. More importantly, the DADMM-1 bit only requires 3 times more iterations to converge than the DADMM.

2.12.4 Achievements and planned activities

The joint work of CTTC and CNIT-PoliTo on signal support detection is detailed in the Annex. It has been partly presented at the ICASSP 2014 conference, in Florence. The work on distributed ADMM algorithms for in-network reconstruction of sparse signals has been partly submitted to GlobalSIP'14. A journal paper is in preparation.

CNRS-UPS and CNIT-UniBo work on distributed algorithms for the characterization of non-asymptotic confidence region in sensor networks. A variant of the sign-perturbed-sum algorithm by Campi et al. has been proposed. Three data collection strategies adapted to the distributed SPS algorithm are compared theoretically and experimentally. These reults are detailed in the Annex. This work has been partly presented at the EuCNC 2014 conference in Bologna. A journal paper has been submitted.

CNRS-UPS and CNIT-UniBo work on outlier detection in wireless sensor networks. An iterative algorithm is proposed able to isolate more than 30% of sensors providing outliers. The equilibrium properties and dynamics of the algorithm are studied. T is detailed in the Annex. A journal and a conference paper are in preparation. The next step is to evaluate the proposed technique in the context of the DATASENS platform.

2.12.5 Publications

[1] Distributed support detection on jointly sparse signals, S. Fosson (CNIT/PoliTo), J. Matamoros (CTTC), C. Antón-Haro (CTTC), E. Magli (CNIT/PoliTo), IEEE International Conference on Acoustics, Speech and Signal Processing (ICASSP), Florence, Italy, May 2014, pp 6434 – 6438
[2] Distributed SPS Algorithms for Non-Asymptotic Confidence Region Evaluation, V. Zambianchi (CNIT-UniBo), M. Keffer (CNRS-UPS), F. Bassi (CNRS-UPS), G. Pasolini (CNIT-UniBo), D. Dardari (CNIT-UniBo), European Conference on Networks and Communications (EuCNC), Bologna, Italy, June 2014, pp 1 – 5.
[3] F. Bassi, A. Fraysse, E. Dupraz, M. Kieffer. Rate-distortion bounds for Wyner-Ziv coding with Gaussian scale mixture correlation noise, to appear in IEEE transactions on Information Theory, 2014.

Submitted

[1] W. Li, F. Bassi, M. Kieffer. Robust Bayesian compressed sensing over finite fields: asymptotic performance analysis, submitted to IEEE transactions on Information Theory, 2014.
[2] J. Matamoros, S. Fosson, E. Magli, C. Antón-Haro, Distributed ADMM for in-network reconstruction of sparse signals with innovations, submitted to IEEE Global Conference on Signal and Information Processing (GlobalSIP).
[3] V. Zambianchi, M. Kieffer, G. Pasolini, D. Dardari, F. Bassi, Efficient distributed confidence region characterization over wireless sensor networks, submitted in IEEE trans. on Wireless Communications, 2014.

3. Conclusions and Prospects

This deliverable provides a presentation of the ongoing Newcom# activities and JRAs in WP1.2. It is evident that a multiplicity of topics are addressed which cover the opportunistic and cooperative communications fields.

From the observation of the research topics addressed by partners, it emerges that promising areas of investigation include distributed interference management, and network organization when use of network coding is also explored. Also, the design of relaying and forwarding schemes for opportunistic scenarios which require the use of unconventional information encoding approaches, e.g. timing channel, to reduce energy consumption is analyzed. Finally, multisource localization and tracking are studied also in presence of interference and noise while taking into account the energy consumption associated to the procedure.
A remarkable outcome of the activities carried out in the first period of the project is the high number of joint research activities which have already achieved tangible results in terms of accepted papers appearing in conferences and journals, Newcom# special sessions, special issues and invited presentations.

The research activities carried out in these two years will go on while also being enriched with new perspectives given by the integration of partners skills.
Many of these JRA activities will also provide useful feedback to the EUWIN platform.
In particular relaying and forwarding schemes to be tested in opportunistic scenarios will be considered for possible implementation in the EUWIN platform and comparison between theoretical and experimental results will be provided in the next deliverables.
The results of the future activities will be again quantified in terms of number of papers accepted and published in high level international conferences and journals as well as in the organization of Newcom# special sessions and special issues. Finally presentations given by Newcom# partners will be a tool for dissemination of partners activities

4. Annexes: Technical Achievements: Detailed Description of JRA Results

4.1 Annex A - JRA 1.2.1-2 Network coding for MARC

4.1.1 System Model

We consider the communication system shown in Figure 1 where a set of M users U*m*, *m* = *1,..,M* , communicate with a destination with the help of *M* relays. Each user U*m* wants to transmit a message *Wum*, which belongs to a set of alphabets *Wum*, to the destination reliably in 2n uses of the channel. At the end of the transmission, the destination recovers the transmitted messages using its outputs. Let R*um* be the transmission rate of message *Wum*. We concentrate on the symmetric rate case, i.e., R*um* = Rsym = R. We divide the transmission time into two transmission periods with each of length n channel uses. Also, we assume that the users are unable to communicate directly with the destination and the relays operate in a half-duplex mode.

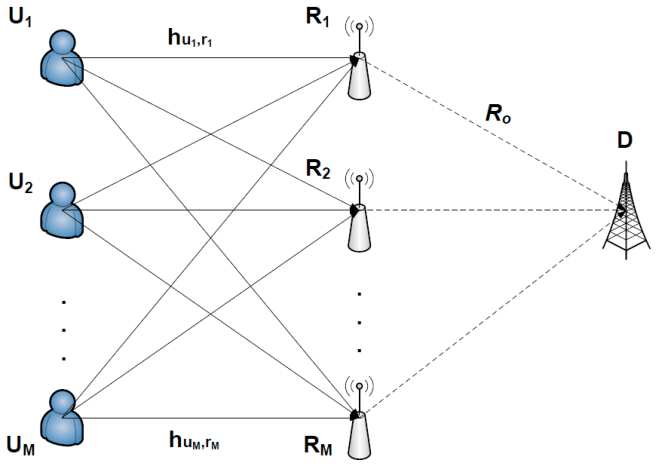

Figure 1 : Multi-user Multi-relay network

During the first transmission period, each user U*m* encodes its message *Wum* ∈ [NG2011; 2^{2nR}] into a codeword x*um* using nested lattice codes [NG2011] [EZV2014] and sends it over the channel. Let y*rm* be the signal received respectively at relay m during this period. This signal is given by

$$\mathbf{y}_{r_m} = \sum_{i=1}^{M} h_{u_i,r_m}\mathbf{x}_{u_i} + \mathbf{z}_{r_m} \qquad (4.2.1)$$

where h_{u_i,r_m} is the channel gain on the link between user Ui and relay *m*, and z*rm* is additive background noise at relay *m*.

During the second transmission period, each relay forwards the decoded linear combination to the destination through its own bit pipe with rate *Ro* bits per channel use.

Throughout this section, we assume that all channel gains are real-valued and fixed. We also assume that the users have full channel state informations (CSI) and that relay *m* only knows the channel vector $\mathbf{h}_{r_m} = [h_{u_1,r_m},\ldots,h_{u_M,r_m}]^T \in R^M$ to itself; and the noises at the relays are independent among each others, and independently and identically distributed (i.i.d)

Gaussian, with zero mean and variance *N*. Furthermore, we consider the following individual constraints on the transmitted power (per codeword),

where *Pum* ≥ 0 is a constraint imposed by the system; *P* ≥ 0 is given, and β_{u_m} is the precoding factor that can be chosen to adjust the actual transmitted power, and is such that $0 \leq |\beta_{u_m}| \leq \sqrt{P_{u_m}/P}$.
The following notations are used throughout the section. For convenience, we use the shorthand vector notation $\boldsymbol{\beta} = [\beta_{u_1}, \ldots, \beta_{u_M}]^T \in R^M$. We also use $\boldsymbol{\beta}^* \mathbf{h}_m$ to denote the Hadamard product of $\boldsymbol{\beta}$ and $\mathbf{h}_m$, ***In*** to denote n-by-n identity matrix and rank(***X***) to denote the rank of matrix ***X***. Finally, we assume that logarithms are taken to base 2; and, for x $\in R$, $\log^+(x) = \max\{\log(x); 0\}$.

4.1.2 Compute-and-Forward Strategy

The following proposition provides an achievable symmetric-rate for the multi-user multi-relay model that we study.

Proposition 1: For any set of channel matrix $\mathbf{H} = [\mathbf{h}_1, \ldots, \mathbf{h}_M]^T \in R^{nxM}$, the following symmetric-rate
is achievable for the model that we study [NG2011, Theorem 5][DS1977,Proposition 1]:

$$R_{\text{sym}}^{\text{CoF}} = \max_{\{\mathbf{a}_m\}_{m=1}^{M}, \boldsymbol{\beta}} \min\left\{\min_m R(\mathbf{a}_m, \mathbf{h}_m, \beta),\ R_o\right\}, \qquad (4.2.2)$$

where the maximization is over the precoding vector $\boldsymbol{\beta}$ such that $0 \leq |\beta_{u_m}| \leq \sqrt{P_{u_m}/P}$ and over the integer coefficients $\mathbf{a}_m \in Z^M$, *m=1,…,M*, such that rank(***A***)= M, $\mathbf{A} = [\mathbf{a}_1, \ldots, \mathbf{a}_M]^T \in Z^{MxM}$, and

$$R(\mathbf{a}_m, \mathbf{h}_m, \beta) = \log^+\left(\left(\|\mathbf{a}_m\|^2 - \frac{P((\beta \circ \mathbf{h}_m)^T \mathbf{a}_m)^2}{N + P\|\beta \circ \mathbf{h}_m\|^2}\right)^{-1}\right) \qquad (4.2.3)$$

In this strategy, each relay independently computes a linearcombination that relates the users' codewords and thenforwards it to the destination. The destination recovers the transmitted messages only if the received linear combinationsare full rank. In order to increase the probability that the received linear combinations are full rank and to maximize the transmission rate of Proposition 1, we develop at the users an iterative algorithm that finds the optimum precoding vector $\boldsymbol{\beta}$.

4.1.2.1 Symmetric Rate Optimization

The following section is devoted to finding optimal precoding and integer-coefficients that maximize the symmetric-rate of Proposition 1.

1) Problem Formulation: Consider the symmetric-rate $R_{\text{sym}}^{\text{CoF}}$ as given in Proposition 1. The optimization problem can be stated as:

$$(\text{OP}): \quad \max_{\{\mathbf{a}_m\}_{m=1}^{M}, \boldsymbol{\beta}} \min\left\{\min_m R(\mathbf{a}_m, \mathbf{h}_m, \beta),\ R_o\right\} \qquad (4.2.4a)$$

$$\text{s. t.} \quad -\sqrt{\frac{P_{u_m}}{P}} \leq \beta_{u_m} \leq \sqrt{\frac{P_{u_m}}{P}} \qquad (4.2.4b)$$

$$\text{rank}(\mathbf{A}) = M. \qquad (4.2.4c)$$

The optimization problem (OP) is a non-linear mixed integer optimization problem. Thus it is hard to find $\boldsymbol{\beta}$ and $\{\mathbf{a}_m\}_{m=1}^{M}$ jointly in a reasonable time [EZV2014]. Therefore, we propose an iterative optimization where we find appropriate precoding vector $\boldsymbol{\beta}$ and integer coefficients $\{\mathbf{a}_m\}_{m=1}^{M}$alternately. Let us denote by $R_{\text{sym}}^{\text{CoF}}[\iota]$ the value of the symmetric-rate at some iteration $\iota \geq 0$. We develop "Algorithm OP" to find the appropriate $\boldsymbol{\beta}$ and $\{\mathbf{a}_m\}_{m=1}^{M}$that maximize $R_{\text{sym}}^{\text{CoF}}$.

As described in "Algorithm OP", we find the appropriate $\boldsymbol{\beta}$ and $\boldsymbol{A}$, alternately. The iterative process in "Algorithm OP" terminates if either one of the following conditions holds: i) $\|\boldsymbol{\beta}^{(\iota)} - \boldsymbol{\beta}^{(\iota-1)}\|$ and $|R_{\text{sym}}^{\text{CoF}}[\iota] - R_{\text{sym}}^{\text{CoF}}[\iota-1]|$ are smaller than prescribed small strictly positive constants ϵ_1 and ϵ_2, respectively — in this case, the optimized value of the symmetric-rate is $R_{\text{sym}}^{\text{CoF}}[\iota]$ and is obtained using $\boldsymbol{\beta}^{*} = \boldsymbol{\beta}^{(\iota)}$ and $\boldsymbol{A}^{*} = \boldsymbol{A}^{(\iota)}$ ii) rank($\boldsymbol{A}^{(\iota)}$) < *M*— in this case, if $\iota = 1$ the optimized value of the symmetric-rate is obtained using $\boldsymbol{\beta}^{*} = 0$ and $\boldsymbol{A}^{*} = 0$ otherwise $\boldsymbol{\beta}^{*} = \boldsymbol{\beta}^{(\iota-1)}$ and $\boldsymbol{A}^{*} = \boldsymbol{A}^{(\iota-1)}$.

We should note that by considering different initial values $\boldsymbol{\beta}^{(0)}$ a higher transmission rate can be obtained and the probability to get full rank linear combinations can be increased.

Algorithm OP Iterative algorithm to compute $R_{\text{sym}}^{\text{CoF}}$

1: Initialization: set $\iota = 1$ and $\beta = \beta^{(0)}$, where $\beta^{(0)}$ is a given initial value
2: Set $\beta = \beta^{(\iota-1)}$ in (4.2.4), and solve the obtained problem as described below. Denote by $\mathbf{A}^{(\iota)}$ the found $\mathbf{A}$
3: **If** rank($\mathbf{A}^{(\iota)}$) = M
4: Set $\mathbf{A} = \mathbf{A}^{(\iota)}$ in (4.2.4), and solve the obtained problem using Algorithm OP-1 given below. Denote by $\beta^{(\iota)}$ the found β
5: Increment the iteration index as $\iota = \iota + 1$, and go back to Step 2
6: Terminate if $\|\beta^{(\iota)} - \beta^{(\iota-1)}\| \leq \epsilon_1$, $|R_{\text{sym}}^{\text{CoF}}[\iota] - R_{\text{sym}}^{\text{CoF}}[\iota-1]| \leq \epsilon_2$
7: **Else**
8: **If** $\iota = 1$
9: Terminate and set $\beta = \mathbf{0}$ and $\mathbf{A} = \mathbf{0}$
10: **Else**
11: Terminate and set $\beta = \beta^{(\iota-1)}$ and $\mathbf{A} = \mathbf{A}^{(\iota-1)}$
12: **End**
13: **End**

2) Integer Coefficients Optimization: In this section, we search for the integer coefficients $\{\mathbf{a}_m\}_{m=1}^{M}$ for a given $\boldsymbol{\beta}$. The optimization problem (OP) can be equivalently written as

$$\min_{\{\mathbf{a}_m\}_{m=1}^{M},\,\Delta_1} \quad \Delta_1 \tag{4.2.5a}$$

$$\text{s. t.} \quad \Delta_1 \geq \mathbf{a}_m^T \Omega_m \mathbf{a}_m \tag{4.2.5b}$$

$$\Delta_1 \geq 2^{-R_o} \tag{4.2.5c}$$

where $\Delta_1 \in R$ is simultaneously a slack variable and the objective function, and $\Omega_m = \frac{\nu(\boldsymbol{\beta}^H \mathbf{h}_m)(\boldsymbol{\beta}^H \mathbf{h}_m)^T}{N+\nu\|\boldsymbol{\beta}^H \mathbf{h}_m\|^2} \in R^{M\times M}$.

The optimization problem (4.2.5) is a mixed integer quadratic programming (MIQP) problem [EZV2014] [F1995] and can easily and efficiently be solved using branch and bound method [W1998].

3) Precoding Allocation: In this section, we optimize the precoding vector $\boldsymbol{\beta}$ for given $\{\mathbf{a}_m\}_{m=1}^{M}$. Again, we can rewrite the optimization problem (OP), for *m = 1,…, M*, as

$$\min_{\boldsymbol{\beta}, \Delta_2} \quad \Delta_2 \tag{4.2.6a}$$

$$\text{s. t.} \quad \Delta_2 \geq \|\mathbf{a}_m\|^2 - \frac{P((\boldsymbol{\beta} \circ \mathbf{h}_m)^T \mathbf{a}_m)^2}{N + P\|\boldsymbol{\beta} \circ \mathbf{h}_m\|^2} \tag{4.2.6b}$$

$$\Delta_2 \geq 2^{-R_o} \tag{4.2.6c}$$

$$-\sqrt{\frac{P_{u_m}}{P}} \leq \beta_{u_m} \leq \sqrt{\frac{P_{u_m}}{P}} \tag{4.2.6d}$$

where $\Delta_2 \in R$ is simultaneously a slack variable and the objective function. The optimization problem in (4.2.6) is non-linear and non-convex. This problem can be formulated as a complementary geometric program (CGP) [EZV2014] [CTPO2007] and can be solved easily and efficiently as described in [EZV2014]. To solve a CGP problem, we need to transform it into a geometric program (GP). This means that the variables in the optimization problem should be all positive, and the objective function and the constraints should be posynomials. We define $\boldsymbol{c} = [c_{u_1}, \ldots, c_{u_M}]^T \in R^M$, and $\boldsymbol{\delta} = [\delta_{u_1}, \ldots, \delta_{u_M}]^T \in R^M$, such that $c_{u_m} > \sqrt{P_{u_m}/P}$ and $\delta_{u_m} = \beta_{u_m} + c_{u_m}$ for *m=1,…,M*.

It can easily be seen that the elements of $\boldsymbol{\delta}$ are all strictly positive. Hence, the optimization problem (4.2.6) can be written in the following form,

$$\min_{\boldsymbol{\delta}, \Delta_2} \quad \Delta_2 \tag{4.2.7a}$$

$$\text{s. t.} \quad \frac{f_m(\boldsymbol{\delta}, \Delta_2)}{g_m(\boldsymbol{\delta}, \Delta_2)} \leq 1 \tag{4.2.7b}$$

$$\frac{2^{-R_o}}{\Delta_2} \leq 1 \tag{4.2.7c}$$

$$-\sqrt{\frac{P_{u_m}}{P}} + c_{u_m} \leq \delta_{u_m} \leq \sqrt{\frac{P_{u_m}}{P}} + c_{u_m}, \tag{4.2.7d}$$

where the constraints in (4.2.7b) correspond to the constraints in (4.2.6b), and $f_m(\boldsymbol{\delta}, \Delta_2)$ and $g_m(\boldsymbol{\delta}, \Delta_2)$ are posynomial functions. It is easy to see that the constraints in (4.2.7b) are not posynomial since a ratio of posynomial functions is not posynomial [CTPO2007]. Therefore, we use Lemma 1 of [EZV2014] to approximate the functions $g_m(\boldsymbol{\delta}, \Delta_2)$ with monomials $\hat{g}_m(\boldsymbol{\delta}, \Delta_2)$ around some initial value. We should note that the ratio between posynomial and monomial can be upper bounded by a posynomial [CTPO2007]. Thus, the optimization problem (4.2.7) is now a GP problem and can be solved easily using an interior point approach. To improve the accuracy of the approximation, the found solution of the GP problem is used as an initial value to transform again the CGP into a new GP problem. This process is repeated until convergence to a stationary point. The problem of finding $\boldsymbol{\delta}$ for given $\{a_m\}_{m=1}^M$ is described in “Algorithm OP-1”.

Algorithm OP-1 Precoding allocation for $R_{\text{sym}}^{\text{CoF}}$

1: Set $\delta^{(0)}$ to some initial value. Compute $\Delta_2^{(0)}$ using $\delta^{(0)}$ and set $\iota_2 = 1$
2: Approximate $g(\delta^{(\iota_2)}, \Delta_2^{(\iota_2)})$ with $\tilde{g}(\delta^{(\iota_2)}, \Delta_2^{(\iota_2)})$ around $\delta^{(\iota_2-1)}$ and $\Delta_2^{(\iota_2-1)}$ using Lemma 1 of [2]
3: Solve the resulting approximated GP problem using an interior point approach. Denote the found solutions as $\delta^{(\iota_2)}$ and $\Delta_2^{(\iota_2)}$
4: Increment the iteration index as $\iota_2 = \iota_2 + 1$ and go back to Step 2 using δ and Δ_2 of step 3
5: Terminate if $\|\delta^{(\iota_2)} - \delta^{(\iota_2-1)}\| \leq \epsilon_1$

4.1.3 Numerical Results

In this section, we provide some numerical examples where we measure the performance of the coding strategy using symmetric outage rate. We compare our coding strategy with the traditional strategies for *M* = 2. Also, we consider different algorithms and we compare them with the proposed algorithm "Algorithm OP". The symmetric outage rate is given by [NG2011],

$$R_{\text{Out}}^{\text{CoF}} = \sup\{R : p_{\text{out}}(R) \leq \mu\}$$

where $p_{\text{Out}}(R)$ is the outage probability and is given by

$$p_{\text{Out}}(R) = \Pr(R_{\text{Sym}}^{\text{CoF}} < R)$$

Throughout this section, we assume that the channel coefficients are modeled with independent
and randomly generated variables, each generated according to a zero-mean Gaussian distribution
with variance $\sigma_{a_{i,r_j}}^2$ for *i, j = 1,2*. Also, we set P_{a_1} = 20 dBW, P_{a_2} = 20 dBW, P = 20 dBW, and $\mu = 1/4$.

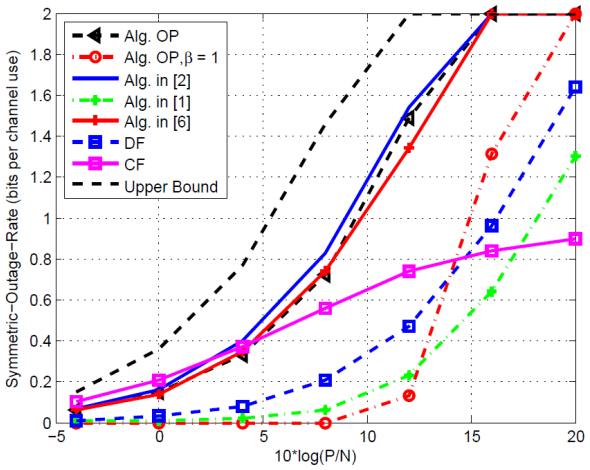

Figure 2 : Symmetric outage rates, *Ro* = 2 bits per channel use, $\sigma_{a_{i,r_j}}^2$=0dB for i,j=1,2.

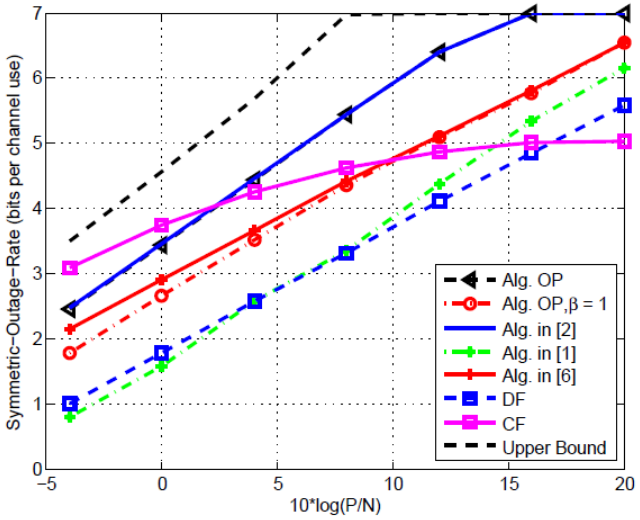

Figure 3 : Symmetric outage rates, *Ro* = 2 bits per channel use, σ^2_{i,T_j}=20dB for i,j=1,2.

Figures 2 and 3 show the symmetric outage rate obtained using the CoF approach under different optimization algorithms: i) using "Algorithm OP", i.e., R_{Out}^{CoF} (Alg. OP), ii) using the integer coefficients algorithm described above with β = 1, i.e., R_{Out}^{CoF} (Alg. OP, β = 1), iii) using the algorithm described in [EZV2014], i.e., R_{Out}^{CoF} (Alg. in [WC2012]), iv) using the integer coefficients algorithm described above but forcing relay *m* to compute an equation with $a_{m,m} \neq 0$, i.e., R_{Out}^{CoF} (Alg. in [W1998]) v) using the algorithm described in [WC2012] i.e., R_{Out}^{CoF} (Alg. in [WC2012]) as functions of 10 log(P/N). The figures also show the symmetric outage rates obtained using DF, CF and the upper bound as given in [NG2011].

For the example shown in Figure 2, we observe that "Algorithm OP" achieves a symmetric outage rate slightly less than what is obtained using the algorithm in [EZV2014]. Also, we observe that "Algorithm OP" has a performance similar to that in [WC2012] at low values of P/N, however it has higher performance at mid and high values of P/N. In [EZV2014] and [WC2012], the integer coefficient vectors are jointly computed among the relays. In these methods, each relay finds a candidate set that contains several integer vectors. From those candidate sets, the relays jointly select from each set an integer vector to construct a full rank matrix that maximizes the transmission rate. In order to jointly select the integer coefficient vectors, the relays need either to signal their candidate sets to each others or to transmit them to a central controller. This makes those methods not practical for a large number of users and relays and makes the proposed method more practical and efficient. Moreover, the complexity to select the independent integer vectors from the candidate sets is $O(M^T)$ where T is the number of integer vectors in each set. In contrast, in the proposed method, it is zero since each relay independently computes an integer vector. Also, we observe that "Algorithm OP" outperforms the other described algorithms and that CoF strategy, in this regime, has better performance than standard DF and CF as it has been shown in [NG2011].

Figure 3 depicts the same curves for other channel variances. In this case, we observe that both algorithms "Algorithm OP" and the one in [EZV2014] have the same performance. Also, we observe that "Algorithm OP" significantly outperforms the algorithm in [WC2012].

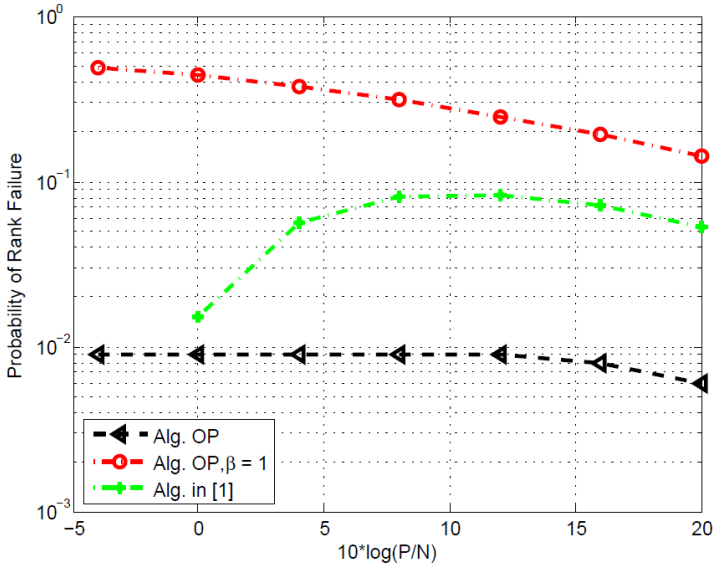

Figure 4 : Probability of rank failure, *Ro* = 2 bits per channel use, $\sigma^2_{h_{i,r_j}}$=0dB for i,j=1,2.

In Figure 4, we observe that the probability that the linear combinations are not full rank is quite small using "Algorithm OP" compared with the other algorithms. Hence, we notice that precoding allocation can help to increase the transmission rate, to decrease the probability of rank failure, and to reduce the complexity at the relays.

4.1.4 References

[NG2011] B. Nazer and M. Gastpar. Compute-and-forward: Harnessing interference through structured codes. *IEEE Trans. Inf.Theory*, 57:6463–6486, 2011.

[EZV2014] M. El Soussi, A. Zaidi, and L. Vandendorpe. Compute-and-forward on a multiaccess relay channel: Coding and Symmetric-Rate Optimization. *IEEE Trans. on Wireless Communications*, 13: 1932-1947, 2014.

[F1995] C. A. Floudas, Nonlinear and mixed integer optimization. Oxford University Press, 1995.

[W1998] L. A. Wolsey, Integer programming. John Wiley and Sons, 1998.

[CTPO2007] M. Chiang, C. W. Tan, D. P. Palomar, D. O'Neill, and D. Julian, "Power control by geometric programming," IEEE Trans. Wireless Communications, vol. 6, pp. 2640–2651, July 2007.

[WC2012] L. Wei and W. Chen, "Compute-and-forward network coding design over multi-source multi-relay channels," IEEE Trans. Wireless Communications, vol. 11, pp. 3348–3357, 2012.

4.2 Annex B - JRA 1.2.1-3 Message-passing methods for distributed wireless network optimization

For technical details see:

[1] http://ieeexplore.ieee.org/xpls/abs_all.jsp?arnumber=6850351&tag=1
[2] http://arxiv.org/abs/1310.2435

4.3 Annex C - JRA 1.2.1-4 Distributed learning schemes for signal optimization in large wireless networks

4.3.1 Online optimization in MIMO-OFDM cognitive radio

4.3.1.1 Introduction

The explosive spread of Internet-enabled mobile devices has turned the radio spectrum into a scarce resource which, if not managed properly, may soon be unable to accommodate the soaring demand for wireless broadband and the ever-growing volume of data traffic and cellphone calls. Exacerbating this issue, studies by the US FCC and the NTIA have shown that this vital commodity is effectively squandered through underutilization and inefficient use:
only 15% to 85% of the licensed radio spectrum is used on average, leaving ample spectral voids that could be exploited for opportunistic radio access [GAO04,FCC02].

In view of the above, the emerging paradigm of cognitive radio (CR) has attracted considerable interest as a promising counter to spectrum scarcity [MM99,ZS07,Hay05,GJMS09]. At its core, this paradigm is simply a two-level hierarchy between communicating users based on spectrum licensing. On the one hand, the network's primary users (PUs) have purchased spectrum rights but allow others to access it provided that their negotiated quality of service (QoS) guarantees are not violated; on the other hand, the network's secondary users (SUs) are free-riding on the licensed part of the spectrum, but they have no QoS guarantees and must conform to the constraints imposed by the PUs. In this way, by opening up the unfilled ``white spaces'' of the licensed spectrum to opportunistic radio access, the overall utilization of the wireless medium can be greatly increased without compromising the performance guarantees that the network's licensed users have already paid for.

Orthogonally to the above, the seminal prediction that multiple-input, multiple-output (MIMO) technologies can lead to substantial gains in information throughput [FG98,Tel99] opens up additional ways for overcoming spectrum scarcity. In particular, by employing multiple antennas, it is possible to exploit spatial degrees of freedom in the transmission and reception of radio signals, the only physical limit being the number of antennas that can be deployed on a portable device. As a result, the existing wireless medium can accommodate greater volumes of data traffic per Hertz without requiring the reallocation (and subsequent re-regulation) of additional frequency bands.

In this JRA, we combine these two approaches and focus on dynamic MIMO CR systems comprising several wireless users (primary and secondary alike) who communicate over multiple non-interfering channels. In this evolving (and unregulated) context, the intended

receiver of a message has to cope with unwarranted interference from a large number of transmitters, a factor which severely limits the capacity of the wireless system in question. As a result, given that the system's SUs cannot rely on contractual QoS guarantees to achieve their desired throughput levels, the maximization of their achievable transmission rates under the operational constraints imposed by the network's PUs becomes a critical issue.

On that account, and given that the theoretical performance limits of MIMO systems still elude us (even in basic network models such as the interference channel), a widespread approach is to treat the interference from other users as additive colored noise and to use the mutual information for Gaussian input and noise as a unilateral performance metric [Tel99]. However, since users cannot be assumed to have full information on the wireless system as it evolves over time (due to the arrival of new users, fluctuations in the PUs' demand, etc.), they must optimize their signal characteristics ``on the fly'', based only on locally available information. Hence, our aim in this JRA is to derive a dynamic transmit policy that allows the system's SUs to adapt to changes in the wireless medium and to track their individually optimum transmission profiles using only local (and possibly imperfect) channel state information (CSI).

This setting is fairly general and involves cognitive SUs with significant control over both spatial (MIMO) and spectral (OFDM) degrees of freedom. To the best of our knowledge, only special cases of this problem have been considered in a CR setting. For instance, [ZS11,SP10,WSP11] analyzed the case where there is only one channel and the environment is ***static*** (i.e. the system's SUs only react to each other and the PUs' spectrum utilization is fixed); in this context, [ZS11] characterized the best spatial covariance profile for the interacting SUs whereas [SP10,WSP11] described how to reach a Nash equilibrium in the resulting non-cooperative game. On the other hand, [NC05,AMTS11,Li09,GKJ10] proposed different learning schemes for optimal channel selection in ***dynamic*** environments where the PUs' evolving behavior cannot be anticipated by the system's SUs, but only in the case where the SUs are equipped with a single antenna and cannot split power across subcarriers.

Extending the above considerations, our goal in this JRA is to derive an adaptive transmit policy for SU rate optimization in dynamically evolving MIMO-OFDM CR networks. In this online optimization framework, the most widely used performance criterion is that of ***regret minimization***, a concept which was first introduced by Hannan [Han57] and which has since given rise to a vigorous literature at the interface of optimization, statistics, game theory, and machine learning - see e.g. [CBL06,SS11] for a comprehensive survey. Specifically, in the language of game theory, the notion of (external) regret compares the agent's cumulative payoff over time to what he would have obtained by constantly playing the same action. Accordingly, the purpose of regret minimization is to devise learning policies that lead to vanishingly small regret against *any* fixed action and *irrespective* of how the agent's environment evolves over time.

In view of the above, we focus in this JRA on ***no-regret*** policies that perform at least as well as the asymptotically best fixed policy in terms of each user's achievable transmission rate – despite the fact that the latter cannot be determined by the network's SUs when they have no means to anticipate the PUs' behavior. In particular, motivated by the no-regret properties of the **exponential weight** (EW) algorithm for problems with discrete action sets [CBL06,Vov90,LW94,ACBG02], we propose in this JRA an **augmented exponential learning** (AXL) approach that can be applied to the continuous regret minimization problem at hand with minimal information requirements.

A key challenge here is that any learning algorithm must respect the problem's semidefiniteness constraints; as such, an important component of our AXL scheme is the

continuous-time technique of **matrix exponential learning** that was recently introduced for ordinary (as opposed to online) rate optimization problems in MIMO multiple access channels (MACs) [MBM12] – and which is closely related to the online mirror descent approach of [SS11] and the matrix regularization techniques of [KSST12].

Of course, since the SUs' optimal transmit profile varies over time, the notions of convergence and/or convergence speed are no longer applicable; instead, the figure of merit is the rate at which the SUs attain a no-regret state. In that respect, AXL guarantees a worst-case average regret of $O(T^{1/2})$ after T epochs, a bound which is well known to be tight [CBL06,SS11]. Additionally, AXL retains its no-regret properties even if the SUs' channel measurements are subject to arbitrarily large observation errors (the imperfect CSI case), thus providing significant performance improvements over more traditional water-filling methods that are sensitive to perfect CSI. As a result, the system's SUs are able to track their individually optimum transmit profile as it evolves over time remarkably well, even under rapidly (and randomly) changing conditions.

4.3.1.2 System Model

In this JRA, we focused on a CR system consisting of a set of wireless MIMO users (primary and secondary alike) that communicate over several non-interfering subcarriers by means of an OFDM scheme [BGP02,LZ06. Focusing on a wireless connection with m transmit antennas and n receive antennas, the received signal on subcarrier *k* will be given by:

$$\mathbf{y}_k = \mathbf{H}_k \mathbf{x}_k + \mathbf{w}_k$$

where $\mathbf{x}_k$ is the transmitted signal, $\mathbf{H}_k$ is the corresponding channel matrix and $\mathbf{w}_k$ is the multi-user interference-plus-noise (MUI) at the intended receiver. Obviously, the covariance $\mathbf{W}_k = \mathbb{E}[\mathbf{w}_k^\dagger \mathbf{w}_k]$ of $\mathbf{w}_k$ above obviously changes over time due to fading, modulations in the PUs' behavior, and more; as a result, employing sophisticated interference cancellation (IC) techniques at the receiver is highly nontrivial, especially with regards to the system's unregulated secondary users. Instead, we work in the single-user decoding (SUD) regime where interference by other users (primary and secondary alike) is treated as additive, colored noise.

In this context, the transmission rate of a user under the signal model \eqref{eq:signal} is given by the familiar expression [Tel99,BGP02]:

$$R(\mathbf{P};t) = \sum_k \log\det(\mathbf{I} + \tilde{\mathbf{H}}_k(t)\mathbf{P}_k\tilde{\mathbf{H}}_k^\dagger(t))$$

where $\tilde{\mathbf{H}}_k = \mathbf{W}_k^{-1/2}\mathbf{H}_k$ is the user's effective channel matrix and $\mathbf{P}_k = \mathbb{E}[\mathbf{x}_k^\dagger \mathbf{x}_k]$ is the user's transmit power matrix, satisfying the constraints:

C1. $\sum_k \mathrm{tr}(\mathbf{P}_k) \leq P$ (constrained total transmit power).

C2. $\mathrm{tr}(\mathbf{P}_k) \leq P_k$ (constrained transmit power per subcarrier).

C3. $\mathbf{P}_k\mathbf{U}_k = 0$ (null shaping constraints).

where U is some tall complex matrix.

Of the constraints above, the first one is a physical constraint on the user's total transmit power, the second imposes a limit on the interference level that can be tolerated on a given subcarrier, and the third one is a ``hard'', spatial version of the second which guarantees that

certain spatial dimensions per subcarrier (the columns of U) are only open to licensed, primary users.

In more detail, the first constraint is equivalent to limiting the maximal average interference that SUs are allowed to incur on the primary transmission while the matrices U of the third one are imposed by the PUs and their columns represent the spatial directions which are forbidden to SU transmission. Such constraints are well-documented in the literature and simply reflect the fact that some carriers or spatial directions per carrier are preferred by the PUs, so stricter constraints are imposed to limit interference by SUs (for a more detailed discussion, see e.g. [LZ06,SP10,WSP11] and references therein).

Obviously, since we are putting no constraints on the behavior of the system's users, the evolution of the effective channel matrices $\mathbf{H}$ over time can be quite arbitrary as well. Formally, we only make the following (minimal) assumptions:

A1. The effective channel matrices $\mathbf{H}$ are bounded throughout the transmission horizon.

A2. The matrices $\mathbf{H}$ change sufficiently slowly relative to the coherence time of the channel so that the standard results of information theory [Tel99] continue to hold.

A3. SUs can obtain possibly imperfect (but otherwise unbiased) estimates for $\mathbf{H}$, e.g. by measuring $\mathbf{H}$ and probing the intended receiver for the MUI covariance matrix $\mathbf{W}$.

In light of the above, and motivated by the ``white-space filling'' paradigm advocated (e.g. by the FCC) as a means to minimize interference by unlicensed users, we focus on the **online rate maximization problem:**

maximize $R(\mathbf{P};t)$
subject to (C1)-(C3)

Of course, since there is no direct causal link between the PUs' behavior and the choices of the SUs, the rate function R evolves arbitrarily over time. This leads to a ``game against nature'' which is played out as follows:

1. At each time slot t=1,2..., the focal user selects an ***action*** (transmit profile) $\mathbf{P}(t)$ satisfying (C1)-(C3).

2. The agent's ***payoff*** (transmission rate) $R(\mathbf{P}(t);t)$ is determined by nature and/or the behavior of other users (via the effective channel matrices $\mathbf{H}(t)$).

3. The agent employs a ***decision rule*** (dynamic transmit policy) to pick a new transmit profile $\mathbf{P}(t+1)$, and the process is repeated until transmission ends.

In this dynamic setting, static solution concepts are no longer applicable, so the most widely used optimization criterion is that of ***regret minimization***, a long-term solution concept which was first introduced by Hannan [Han57] and which has since given rise to an extremely active field of research at the interface of optimization, statistics and theoretical computer science – see e.g. [CBL06,SS11] for a survey. Roughly speaking, the regret compares the payoff obtained by an agent that follows a dynamic policy to the payoff that he would have obtained by constantly choosing the same action over the entire transmission horizon.

More precisely, the ***cumulative regret*** of the dynamic policy **P**(*t*) with respect to a fixed transmit profile **P*** is defined as:

$$\mathrm{Reg}(\mathbf{P}^*;T) = \sum_{t=1}^{T} R(\mathbf{P}^*;t) - R(\mathbf{P}(t);t)$$

i.e. $\mathrm{Reg}(\mathbf{P}^*;t$ measures the cumulative transmission rate difference up to stage T between a benchmark transmit profile **P*** and the dynamic policy **P**(*t*). The user's ***average regret*** then is $\mathrm{Reg}(\mathbf{P}^*;T)/T$ and the goal of regret minimization is to devise a dynamic policy **P**(*t*) that leads to ***no regret***, viz.

$$\limsup \frac{1}{T}\mathrm{Reg}(\mathbf{P}^*;T) \leq 0$$

for all benchmark profiles **P***, and irrespective of the evolution of the objective $R(\boldsymbol{P};t)$ over time. In other words, if we interpret the first term of the user's regret as the long-term average transmission rate of **P***, the no-regret property simply means that, in the long run, the average data rate of the dynamic transmit policy **P**(*t*) is at least as good as that of *any* fixed profile **P***.

Obviously, if the optimum transmit policy which maximizes the online rate maximization problem at hand could be predicted ahead of time at every stage $t=1,2,\dotsc$ in an oracle-like fashion, following it would give negative regret for all time. Therfore, the no-regret requirement is fundamental in the context of online optimization because negative regret is a key indicator of tracking the maximum of the user's rate function as it evolves over time.

In particular, if the channel matrices are drawn at each realization from an *isotropic* distribution [PCL03], spreading power uniformly across carriers and antennas is the optimal choice when nature (including the network's PUs) is actively choosing the worst possible channel realization for the transmitter. A no-regret policy extends this ``min-max'' concept by ensuring that the policy's achieved transmission rate is asymptotically as good as that of any fixed transmit profile, including obviously the uniform one as a special case where nature is actively playing against the transmitter – for instance, as in the case of jamming.

4.3.1.3 Learning algorithm and results

Our proposed learning augmented exponential learning algorithm for the online rate maximization (ORM) problem discussed in the previous section is as follows:

ALGORITHM 1: Augmented Exponential Learning (AXL)

Parameter: $\eta > 0$.
Initialize: t=0; channel scores **Y = 0**.
Repeat
$t \mathrel{-}= t + 1$;
foreach channel k **do**
update transmit power profile
  set $\begin{cases} p_k = \exp(\eta t^{-1/2} y_k) / \sum_i \exp(\eta t^{-1/2} y_i) \\ \mathbf{Q}_k = \exp(\eta t^{-1/2} \mathbf{Y}_k) / \sum_i \exp(\eta t^{-1/2} \mathbf{Y}_i) \end{cases}$
  set $\mathbf{P}_k = p_k \mathbf{Q}_k$
update score matrices
  measure $\mathbf{M}_k = \mathbf{\Pi}_k^{\dagger} \left[\mathbf{I} + \mathbf{\Pi}_k \mathbf{P}_k \mathbf{\Pi}_k^{\dagger} \right]^{-1} \mathbf{\Pi}_k$
  set $\begin{cases} y_k \mathrel{+}= y_k + P \operatorname{tr}[\mathbf{M}_k \mathbf{Q}_k] \\ \mathbf{Y}_k \mathrel{-}= \mathbf{Y}_k + p_k \mathbf{M}_k \end{cases}$
until transmission ends.

From an implementation point of view, AXL has the following desirable properties:

P1. It is ***distributed***: each SU only needs to update his individual transmit policy using local CSI.
P2. It is ***asynchronous***: there is no need for a global update timer to synchronize the system's SUs.
P3. It is ***stateless***: the SUs do not need to know the state of the system (e.g. the network's topology), and/or be aware of each other's actions.
P4. It is ***reinforcing***: the SUs tend to increase their unilateral transmission rates.

One of the main achievements of this JRA is that the AXL algorithm above leads to no regret:

Theorem 1. *The adaptive transmit policy generated by AXL leads to no regret in the online rate maximization problem* (ORM). *In particular, for every fixed transmit profile* **P***, *and independently of how the system's rate function evolves over time, the user's regret is bounded by:*

$$\frac{1}{T} \operatorname{Reg}(\mathbf{P}^*; T) \leq \frac{1}{\sqrt{T}} \left(\frac{\log K + \sum_{k=1}^{K} m_k}{\eta} + 4 P^2 M^2 \eta \right)$$

where m_k is the number of spatial dimensions that are left open to SUs on subcarrier k, P is the user's maximum transmit power, and M is a finite positive constant.

Of course, in practical implementations of AXL, a major challenge occurs if the user does not have perfect CSI with which to run the AXL updates. In particular, since the algorithm's update steps are determined by the user's effective channel matrices, imperfect measurements of the actual channel matrices or of the multi-user interference-plus-noise covariance matrices would invariably interfere with each update cycle.

We model such perturbations as a bounded martingale difference, i.e. as a stochastic process Ξ such that:

A1. Ξ is *bounded* (a.s.).
A2. Ξ is *zero-mean*.

Remarkably, even though the observation noise can become arbitrarily large, we obtain the following robustness result:

Theorem 2. *The AXL algorithm with noisy observations leads to no regret (a.s.).*

4.3.1.4 Numerical simulations

To validate our theoretical predictions for the performance of the AXL algorithm, we conducted extensive numerical simulations from which we illustrate here a selection of the most representative scenarios – though the observations made below remain valid in most typical mobile wireless environments.

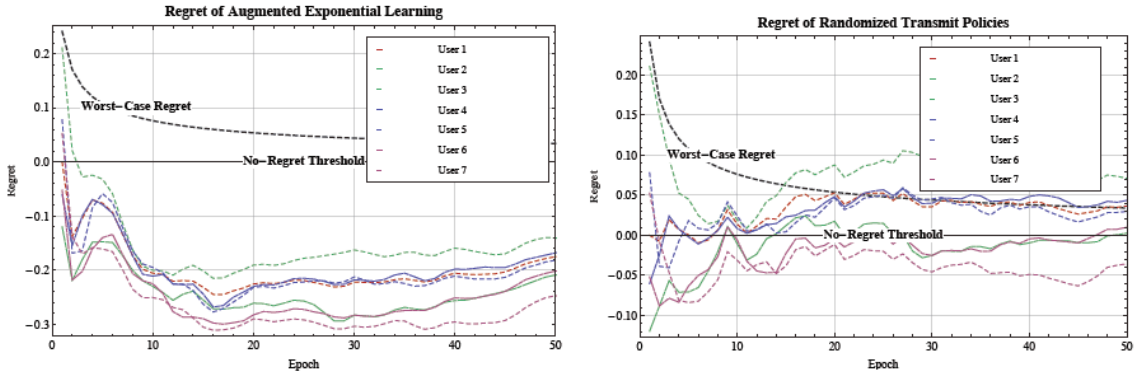

(a) No regret under augmented exponential learning.

(b) Positive regret under randomized power allocation.

Fig. 1. The long-term regret induced by augmented exponential learning and a random sampling transmit policy (Figs 1(a) and 1(b) respectively) for different users (see text for details). In tune with Theorem 1, AXL quickly falls below the no-regret threshold whereas the randomized policy (29) leads to positive regret for several users (in both figures the dashed "worst-case regret" curve represents the regret guarantee (22) of the AXL algorithm).

In Fig. 1, we simulated a network consisting of 10 PUs and 40 SUs, all equipped with 3 transmit/receive antennas, and communicating over K=256 orthogonal subcarriers with a base frequency of 2 GHz. Both the PUs and the SUs were assumed to be mobile with a speed between 3 and 5 km/h (pedestrian movement), and the channel matrices were modeled after the well-known Jakes model for Rayleigh fading [CCGH+07]. For simplicity, we assumed that the PUs were going online and offline following a Poisson process (representing exponential arrivals with exponential call times), while the simulated SUs employed the AXL algorithm with an update epoch of 5 ms. We then calculated the maximum regret induced by the AXL algorithm for every SU with respect to the uniform transmit profile (where power is spread equally across antennas and frequency bands) and all possible combinations of spreading power uniformly across subcarriers while keeping one or two transmit dimensions closed (we plotted the regret for only 7 SUs in order to reduce graphical clutter).

The results of these simulations were plotted in Fig. 1(a): as predicted by Theorem 1, AXL leads to no regret and falls below the no-regret threshold within a few epochs, indicating that its average performance is strictly better than any of the benchmark transmit profiles.

For comparison purposes, we also simulated the same scenario but with the \acp{SU} employing a randomized transmit policy. Even though this dynamic transmit policy is sampling the state space essentially uniforml, Fig. 1(b) shows that several SUs end up having positive regret. We thus see that the no-regret property of AXL is not a spurious

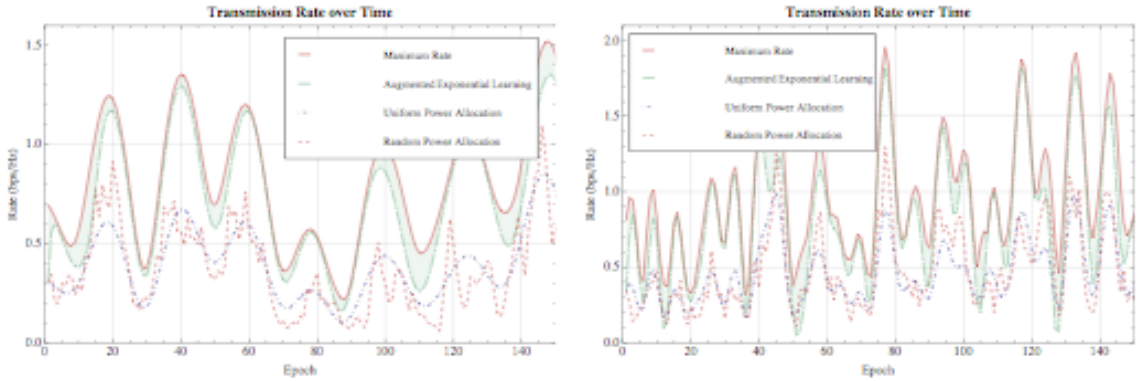

(a) Performance of AXL with average user velocity $v = 5$ km/s. (b) Performance of AXL with average user velocity $v = 15$ km/s.

Fig. 2. Data rates achieved by AXL in a changing environment with different fading velocities: the dynamic transmit policy induced by the AXL algorithm allows users to track their maximum achievable transmission rate remarkably well even under rapidly changing channel conditions.

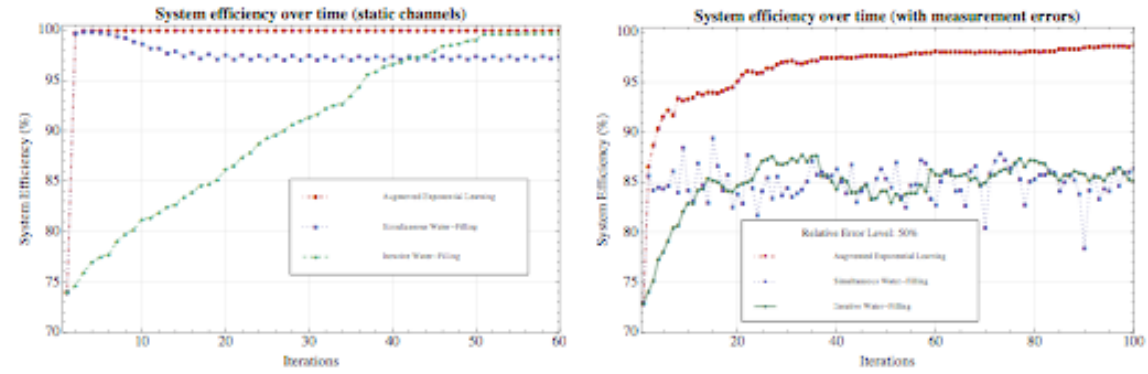

(a) Learning with perfect CSI. (b) Learning with an average relative error level of 50%.

Fig. 3. Convergence and robustness of AXL with imperfect CSI in a MIMO MAC system with 10 PUs and 25 SUs: in contrast to water-filling methods, AXL attains the channel's sum capacity even in the presence of very high measurement errors.

artifact of exploring the problem's state space in a uniform way, but it is inextricably tied to the underlying learning mechanism.

The negative-regret results of Fig. 1 also suggest that the transmission rate achieved by a given SU is close to the user's (evolving) maximum possible rate given the transmit profiles of every other user. To test this hypothesis, we plotted in Fig. 2 the achieved data rate of a SU employing the AXL algorithm along with the user's maximum achievable data rate and the rates achieved by the uniform policy and a randomized policy; to test different fading conditions, we simulated average user velocities of 5 km/h and 15 km/h (Figs. 2a and 2b respectively). We see there that AXL adapts to the changing channel conditions and tracks the user's maximum achievable rate remarkably well, in stark contrast to the uniform and randomized transmit policies.

Finally, to assess the performance of the AXL algorithm with respect to the users' sum rate under SIC and the robustness of AXL under imperfect CSI, we simulated in Fig. 3 a static multi-user MIMO multiple access channel consisting of a wireless base receiver with 5 antennas, 10 PUs and 40 SUs (each with a random number of transmit antennas picked uniformly between 2 and 6). Each user's channel matrix was drawn from a complex Gaussian distribution at the outset of the transmission (but remained static once picked), and we then ran the AXL algorithm. The algorithm's performance over time was then assessed by plotting the normalized efficiency ratio:

$$\mathrm{eff}(t) = \frac{R(t) - R_{\min}}{R_{\max} - R_{\min}}$$

where R(t) is the users' sum rate at the t-th iteration of the algorithm and Rmax, Rmin are the maximum and minimum attainable rates respectively.

For comparison purposes, we also plotted the efficiency ratio achieved by water-filling methods – namely iterative waterfilling (IWF) and simultaneous water-filling (SWF). Remarkably, when the users have perfect CSI, the AXL policy achieves the system's maximum sum rate within 3–4 iterations; by contrast, SWF fails to converge altogether while the convergence time of IWF scales linearly with the number of SUs (Fig. 3(a)). On the other hand, in the presence of imperfect CSI (modeled as zero-mean i.i.d. Gaussian pertrubations to the gradient matrices Mk with relative magnitude of 50%), AXL still achieves the system's sum capacity (albeit at a slower rate) whereas water-filling methods offer no significant advantage over the user's initial transmit profile (cf. Fig. 3(b)) and perform much worse than AXL.

4.3.1.5 References

[1] K. V. Schinasi, "Spectrum management: Better knowledge needed to take advantage of technologies that may improve spectrum efficiency," United States General Accounting Office, Tech. Rep., May 2004.
[2] FCC Spectrum Policy Task Force, "Report of the spectrum efficiency working group," Federal Communications Comission, Tech. Rep., November 2002.
[3] J. Mitola III and G. Q. Maguire Jr., "Cognitive radio: making software radios more personal," IEEE Personal Commun. Mag., vol. 6, no. 4, pp. 13–18, August 1999.
[4] Q. Zhao and B. M. Sadler, "A survey of dynamic spectrum access," IEEE Signal Process. Mag., vol. 24, no. 3, pp. 79–89, May 2007.
[5] S. Haykin, "Cognitive radio: Brain-empowered wireless communications," IEEE J. Sel. Areas Commun., vol. 23, no. 2, pp. 201–220, February 2005.
[6] A. Goldsmith, S. A. Jafar, I. Maric, and S. Srinivasa, "Breaking spectrum gridlock with cognitive radios: An information theoretic perspective," Proc. IEEE, vol. 97, no. 5, pp. 894–914, 2009.
[7] G. J. Foschini and M. J. Gans, "On limits of wireless communications in a fading environment when using multiple antennas," Wireless Personal Communications, vol. 6, pp. 311–335, 1998.
[8] I. E. Telatar, "Capacity of multi-antenna Gaussian channels," Euro- pean Transactions on Telecommunications and Related Technologies, vol. 10, no. 6, pp. 585–596, 1999.
[9] Y. J. A. Zhang and M.-C. A. So, "Optimal spectrum sharing in MIMO cognitive radio networks via semidefinite programming," IEEE J. Sel. Areas Commun., vol. 29, no. 2, pp. 362–373, 2011.
[10] G. Scutari and D. P. Palomar, "MIMO cognitive radio: A game theoretical approach," IEEE Trans. Signal Process., vol. 58, no. 2, pp. 761–780, February 2010.
[11] J. Wang, G. Scutari, and D. P. Palomar, "Robust MIMO cognitive radio via game theory," IEEE Trans. Signal Process., vol. 59, no. 3, pp. 1183–1201, March 2011.
[12] N. Nie and C. Comaniciu, "Adaptive channel allocation spectrum etiquette for cognitive radio networks," in DySPAN '05: Proceedings of the 2005 IEEE Symposium on Dynamic Spectrum Access Networks, 2005, pp. 269–278.
[13] A. Anandkumar, N. Michael, A. K. Tang, and A. Swami, "Distributed algorithms for learning and cognitive medium access with logarithmic regret," IEEE J. Sel. Areas Commun., vol. 29, no. 4, pp. 731–745, April 2011.
[14] H. Li, "Multi-agent Q-learning of channel selection in multi-user cognitive radio systems: A two by two case," in SMC '09: Proceedings of the 2009 International Conference on Systems, Man and Cybernetics, 2009, pp. 1893–1898.
[15] Y. Gai, B. Krishnamachari, and R. Jain, "Learning multiuser channel allocations in cognitive radio networks: A combinatorial multi-armed bandit formulation," in DySPAN '10: Proceedings of the 2010 IEEE Symposium on Dynamic Spectrum Access Networks, 2010.
[16] J. Hannan, "Approximation to Bayes risk in repeated play," in Contri- butions to the Theory of Games, Volume III, ser. Annals of Mathematics Studies, M. Dresher, A. W. Tucker, and P. Wolfe, Eds. Princeton, NJ: Princeton University Press, 1957, vol. 39, pp. 97–139.
[17] N. Cesa-Bianchi and G. Lugosi, Prediction, Learning, and Games. Cambridge University Press, 2006.

[18] S. Shalev-Shwartz, “Online learning and online convex optimization,” Foundations and Trends in Machine Learning, vol. 4, no. 2, pp. 107– 194, 2011.
[19] V. G. Vovk, “Aggregating strategies,” in COLT ’90: Proceedings of the 3rd Workshop on Computational Learning Theory, 1990, pp. 371–383.
[20] N. Littlestone and M. K. Warmuth, “The weighted majority algorithm,” Information and Computation, vol. 108, no. 2, pp. 212–261, 1994.
[21] P. Auer, N. Cesa-Bianchi, and C. Gentile, “Adaptive and self-confident on-line learning algorithms,” Journal of Computer and System Sciences,
vol. 64, no. 1, pp. 48–75, 2002.
[22] P. Mertikopoulos, E. V. Belmega, and A. L. Moustakas, “Matrix exponential learning: Distributed optimization in MIMO systems,” in ISIT ’12: Proceedings of the 2012 IEEE International Symposium on Information Theory, 2012, pp. 3028–3032.
[23] S. M. Kakade, S. Shalev-Shwartz, and A. Tewari, “Regularization techniques for learning with matrices,” The Journal of Machine Learning Research, vol. 13, pp. 1865–1890, 2012.
[24] H. Bo ̈lcskei, D. Gesbert, and A. J. Paulraj, “On the capacity of OFDM-based spatial multiplexing systems,” IEEE Trans. Commun., vol. 50, no. 2, pp. 225–234, February 2002.
[25] K. B. Letaief and Y. J. A. Zhang, “Dynamic multiuser resource allocation and adaptation for wireless systems,” Wireless Communications, IEEE, vol. 13, no. 4, pp. 38–47, August 2006.
[26] J. Huang and Z. Han, Cognitive Radio Networks: Architectures, Protocols, and Standards. Auerbach Publications, CRC Press, 2010, ch. Game theory for spectrum sharing.
[27] C. R. Stevenson, G. Chouinard, Z. Lei, W. Hu, and S. J. Shellhammer, “IEEE 802.22: The first cognitive radio wireless regional area network standard,” IEEE Commun. Mag., vol. 47, no. 1, pp. 130–138, jan 2009.
[28] E. Hazan and C. Seshadri, “Efficient learning algorithms for changing environments,” in ICML ’09: Proceedings of the 26th International Conference on Machine Learning, 2009.
[29] D. P. Palomar, J. M. Cioffi, and M. Lagunas, “Uniform power allocation in MIMO channels: a game-theoretic approach,” IEEE Trans. Inf. Theory, vol. 49, no. 7, p. 1707, July 2003.
[30] H. Robbins, “Some aspects of the sequential design of experiments,” Bulletin of the American Mathematical Society, vol. 58, no. 5, pp. 527–535, 1952.
[31] P. Mertikopoulos, E. V. Belmega, A. L. Moustakas, and S. Lasaulce, “Distributed learning policies for power allocation in multiple access channels,” IEEE J. Sel. Areas Commun., vol. 30, no. 1, pp. 96–106, January 2012.
[32] M. Zinkevich, “Online convex programming and generalized infinites- imal gradient ascent,” in ICML ’03: Proceedings of the 20th Interna- tional Conference on Machine Learning, 2003.
[33] C. D. Cantrell, Modern mathematical methods for physicists and engineers. Cambridge, UK: Cambridge University Press, 2000.
[34] P. Mertikopoulos and E. V. Belmega, “Adaptive spectrum management
in MIMO-OFDM cognitive radio: An exponential learning approach,” in ValueTools ’13: Proceedings of the 7th International Conference on Performance Evaluation Methodologies and Tools, 2013.
[35] J. Kwon and P. Mertikopoulos, “A continuous-time approach to online optimization,” 2014, http://arxiv.org/abs/1401.6956.
[36] F. Alvarez, J. Bolte, and O. Brahic, “Hessian Riemannian gradient flows in convex programming,” SIAM Journal on Control and Optimization, vol. 43, no. 2, pp. 477–501, 2004.
[37] G. Calcev, D. Chizhik, B. Go ̈ransson, S. Howard, H. Huang, A. Ko- giantis, A. F. Molisch, A. L. Moustakas, D. Reed, and H. Xu, “A wideband spatial channel model for system-wide simulations,” IEEE Trans. Veh. Technol., vol. 56, no. 2, p. 389, March 2007.
[38] G. Scutari, D. P. Palomar, and S. Barbarossa, “Simultaneous iterative water-filling for Gaussian frequency-selective interference channels,” in ISIT ’06: Proceedings of the 2006 International Symposium on Information Theory, 2006.
[39] S. Sorin, “Exponential weight algorithm in continuous time,” Mathematical Programming, vol. 116, no. 1, pp. 513–528, 2009.
[40] R. T. Rockafellar, Convex Analysis. Princeton, NJ: Princeton University Press, 1970.
[41] P. Hall and C. C. Heyde, Martingale Limit Theory and Its Application, ser. Probability and Mathematical Statistics. New York: Academic Press, 1980.
[42] K. Azuma, “Weighted sums of certain dependent random variables,” To ̂hoku Mathematical Journal, vol. 19, no. 3, pp. 357–367, 1967.

4.3.2 Adaptive transmit policies for cost-efficient power allocation

To complement our analysis of efficient wireless communications via learning, we aksi examined in this JRA the problem of cost/energy- efficient power allocation in uplink multi-carrier orthogonal frequency-division multiple access (OFDMA) wireless networks. In particular, we focused on a set of wireless users who seek to maximize their transmission rate subject to pricing limitations, and we showed that the resulting non-cooperative game admits a unique equilibrium for almost every realization of the system's channels. We also propose a distributed exponential learning scheme which allows users to converge to the game's equilibrium exponentially fast by using only local (and possibly imperfect) CSI and signal to interference-plus-noise ratio (SINR) measurements.

4.3.2.1 Introduction

Ever since the early development stages of legacy wireless networks, power control has been an essential component of network design and operation, especially in decentralized en- vironments where only local information is available at each mobile terminal [1]. As such, the introduction of fast and distributed power control algorithms (both closed- and open- loop) was one of the main improvements that were brought about in third generation CDMA-based cellular networks, in both single- and multi-carrier settings.

Controlling the transmitted power has two important pur- poses. The first is to minimize the interference of a given node to neighboring receivers, an issue of critical importance in future and emerging wireless network paradigms where cells are deployed at a massive scale – for instance, as in the case of femto-cell networks [2]. Due to their close proximity, neigh- boring users may create significant interference to one another, so care must be taken to choose a power allocation profile that maximizes the users' transmission rate while limiting their overall transmit power – otherwise, the situation could rapidly degenerate to a cascade of power increases.

Second, power control reduces the users' overall transmitted power. Mobile terminals are generally energy-constrained (e.g. due to the limitations of their power source or because of the cost of power consumption), so inefficient power allocation can bring about unnecessary losses in performance. As a result, the problem that arises is to derive distributed power allocation policies that maximize the users' transmission rate in energy- aware scenarios where transmission power also carries a com- mensurate cost. This objective is made more complicated by the fact that wireless users typically have conflicting interests and cannot be assumed to cooperate with each other for their collective benefit (in decentralized environments at least).

In view of the above, non-cooperative game theory has become an important tool to analyze the interactions between mobile users in wireless network scenarios where energy- efficient rate maximization is an issue – see e.g. [3–6] for applications to power control and [7–9] for power allocation problems. In this framework, the primary objective has been to develop policies and algorithms that wireless users can use to optimize their resources (power, bandwidth, etc.), so the main questions that arise are a) whether there exist "equilibrial" power allocation policies which are stable against unilateral deviations; b) whether these (Nash) equilibria are unique (and thus offer some predictive power with regard to the analysis of the system); and c) whether the system's users can reach such a state by means of distributed, adaptive methods that only require local (and readily available) information.

Optimizing power allocation in such a way has been inves- tigated in both single- [4, 5, 10] and multi-carrier scenarios [6, 11, 12]. In particular, the authors of [3, 4, 10] investigated the role of pricing as an effective mechanism to measure the cost of power consumption, thus leading to an energy-efficient formulation where users seek to maximize their transmission rate while keeping their transmit power in check (see also the very recent paper [12] where

the authors consider the problem of maximizing the users' transmission rate per unit of transmitted power subject to minimum rate requirements). Then, to reach an equilibrium state in such a setting, several distributed approaches have been proposed in the existing liter- ature based on reaction functions [4], Gauss-Seidel and Jacobi update algorithms [3] or replicator-based learning [11].

In the context of this JRA, we consider the problem of cost/energy-efficient power allocation in uplink multi-carrier orthogonal frequency-division multiplexing (OFDM) networks, thus fusing and extending the cost-driven treatment of [4] for single-carrier systems with the analysis of [11] for multi-carrier systems in the absence of power consumption considerations. One straightforward scenario where power consumed by the transmitter needs to be priced in some way is related to the modern use of smartphones and other multi-purpose mobile devices. In such devices, the power available for wireless transmission is restricted by the usage of other time-dependent applications of varying priority, so one way to model this scenario is to add a priority-dependent penalty to the available power of the wireless transmission in each user.

To that end, we provide a game-theoretic formulation for the problem of unilateral rate maximization subject to pricing limitations of a general form and we show that the resulting game admits a unique equilibrium for almost every realization of the system's channels. We then propose a distributed exponential learning scheme which converges to equilibrium exponentially fast using only local channel state information (CSI) and signal to interference-plus-noise ratio (SINR) measurements. Importantly, by using powerful tools from stochastic convex programming [13], we are able to show that the algorithm retains its convergence properties even in the presence of imperfect measurements – and irrespective of the magnitude of the observational errors.

4.3.2.2 System model and problem formulation

The network model that we focused on consists of a set of K non-cooperative wireless (single-antenna) transmitters who communicate with a common receiver over a set of M non-interfering subcarriers (typically in the frequency domain if an OFDM scheme is employed). Focusing on the Gaussian SUD MAC regime, each user's achievable transmission rate depends on his individual SINR

$$\mathrm{sinr}_{k\mu} = \frac{g_{k\mu} p_{k\mu}}{\sigma_\mu^2 + \sum_{l=1, l\neq k}^{K} g_{l\mu} p_{l\mu}}$$

where g is the corresponding channel coefficient. Thus, in the SUD regime – where interference by other users is treated as (possibly colored) noise – the maximum information transmission rate (achievable with random Gaussian codes) will be (as before):

$$R_k(p) = \sum_\mu \log\left(1 + \mathrm{sinr}_{k\mu}(p)\right).$$

Given the form of this objective, each user must transmit with maximum possible power in order to maximize his throughput. In practical scenarios however, power consumption carries a commensurate cost, so we will instead consider the energy-aware utility model:

$$u_k(p) = r_k(p) - c_k(p_k)$$

where p_k is total transmit power of user k and c_k is a user-specific cost function measuring the impact of power consumption.

The utility/cost model above admits several interpretations, depending on one's point of view. Perhaps the most straightfor- ward one is that of ck representing the effective monetary cost

of power consumption (whether the cost is paid up front or post- poned to the moment where the battery of the wireless device will need to be recharged). Alternatively, from the viewpoint of energy efficiency, the cost function ck could represent the user's adversity to transmit with higher power when not absolutely necessary. To keep things as general as possible, we will only consider ck as a generic "price" function and assume that it is convex and increasing in pk (in tune with standard economic assumptions).

With all this in mind, unilateral utility maximization leads to a non-cooperative game G ≡ G(K, M, u) for cost-efficient power allocation defined as follows:

1. The set of players of G comprises the set of wireless transmitters K = {1, . . . , K}.
2. Each player's set of actions consists of the corresponding feasible power allocation profiles pk.
3. Each player's utility is given by u_k above.

As we showed during this reporting period, this game admits a single unilaterally stable operation point:

Theorem 3. *The cost-efficient power allocation game G above admits a unique Nash equilibrium for almost every realization of the channel coefficients h.*

4.3.2.3 Distributed learning and convergence analysis

Of course, the fact that the cost-efficient power allocation game G admits a unique equilibrium for almost every channel realization is significant from the point of view of managing the system because it guarantees a unique stable solution. That said, it is far from clear how the system's users could actually reach this equilibrium state, so our goal in this section will be to provide a distributed, adaptive learning mechanism that can be employed by the system's users in order to reach this stable state.

In the absence of power considerations, [11] examined this problem by means of a continuous-time learning scheme based on the replicator dynamics of evolutionary game theory [18] driven by the users' so-called *marginal utility functions*. Unfortunately however, this approach cannot be applied in our case because replicator-driven techniques require the problem's state space to be a product of simplices – which, in our case, would amount to players saturating their total power constraint by default.

To circumvent this difficulty, we propose the following distributed learning algorithm:

ALGORITHM 2: Exponentially-Driven Power Allocation

Parameter: step size γ_n.
Initialize: n=0; scores z = 0.
Repeat
$n \mathrel{+}= n + 1$;
foreach user k **do simultaneously**
set transmit power $p_k = P_k \frac{\exp(z_{k,\mu})}{1+\sum_j \exp(z_{k,j})}$
measure $\mathrm{sinr}_{k,u}$
update marginal utilities $v_{k,\mu} = \frac{1}{p_{k,\mu}} \frac{\mathrm{sinr}_{k,\mu}}{1+\mathrm{sinr}_{k,u}}$
update marginal power cost $v_{k,u} = c_k'(P_k - p_k)$
update scores $z_{k,\mu} \mathrel{+}= z_{k,\mu} + \gamma_n [v_{k,\mu} - v_{k,u}]$

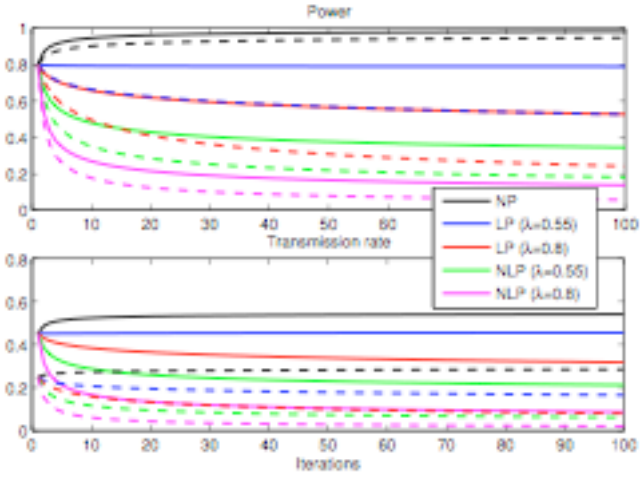

Fig. 1. Total allocated power and transmission rate of User 1 (solid line) and User 2 (dashed line) as a function of different pricing models and values of the pricing parameter λ.

until transmission ends.

One of our main theoretical achievements in this JRA was to show that the above stochastic optimization algorithm converges to the system's equilibrium state:

Theorem 4. *Algorithm 2 run with step size γ_n = 1/n (or any other square-summable but not summable series of step sizes) converges to the system's unique Nash equilibrium, from every initial condition.*

In other words, by using the distributed learning scheme of Algorithm 2, the system's users converge to a unilaterally cost-efficient equilibrium, even though there is no coordination between them - and they only have strictly local information to boot.

4.3.2.4 Numerical Results

To validate the predictions of the previous section for the performance of our exponential learning algorithm in multicarrier wireless systems where power consumption carries a non-negligible cost, we conducted extensive numerical simulations from which we illustrate here a selection of the most representative scenarios. Throughout this section, and unless explicitly stated otherwise, we assume a population of K = 10 users and M = 20 subcarriers, while the channel gain coefficients are drawn randomly from [0, 1]. For simplicity, we also assume symmetric channels and users.

With regards to the users' cost function, we consider three distinct cases: no pricing (NP), linear pricing (LP), and nonlinear pricing (NLP). Specifically:
1) The NP model is defined trivially as c=0.
2) The LP model is definedas c (p)=λp forsome λ>0.
3) The NLP model is defined as c (p) = λ[exp(p/P) − 1].
To develop some intuition, we first provide some general results on the evolution of the cost-aware power allocation game G for K = 2 non-cooperative users that split their transmitting power over M = 4 channels, using only local SINR measurements.

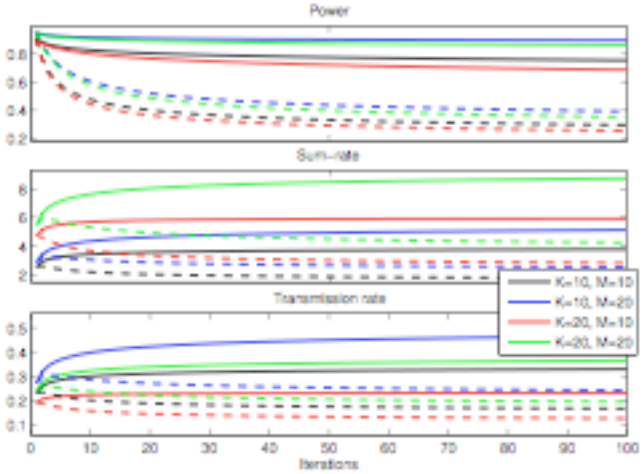

Fig. 2. Evolution of the average allocated power, sum-rate and average transmission rate for the LP (solid line) and NLP (dashed line) models for different network configurations.

Specifically, in Fig. 1, we plotted the total allocated power (3) and achieved transmitted rate (6) for User 1 (solid lines) and User 2 (dashed lines). The figure shows how the users converge to the game's Nash equilibrium by means of the distributed exponential learning scheme XL. As can be seen, User 1 achieves a higher transmission rate than User 2 due to the better channel status experienced by User 1 (which, correspondingly, requires User 1 to spend more power than User 2). Moreover, we also investigate the implication of pricing on game's outcome for different values of the pricing parameter λ. As can be seen, in the NP scenario, each user saturates his total allocated power as predicted by the form of the rate function (6); otherwise, in both the LP and NLP schemes, the cost of power consumption causes users to transmit at lower powers and the exponential learning algorithm (XL) converges to a more cost-efficient power allocation (depending on both the channel quality and the considered pricing model). As expected, the LP scheme allows higher rates than the NLP one, while higher values of the pricing parameter λ force users to allocate less power on each channel – thus reducing their individual transmission rates.

Figure 2 shows how the users' average transmit power, achieved transmission rate and sum-rate evolve at each iteration of the learning algorithm (XL). As expected, the end-state of the algorithm depends quite strongly on the number of users and available channels: as could be expected, best performance is achieved in the uncontested regime where the number of available channels is higher than the number of users trying to access them, i.e. K/M < 1. Fig. 2 also shows how the NLP model affects the power allocation process; in fact, since NLP leads to a sharp increase of the transmission cost for higher powers, it follows that the corresponding loss in transmission rate is not negligible compared to the LP scheme.

In Fig. 3 we plot the sum-rate, average allocated power and its respective cost as a function of different pricing models and values of the pricing parameter λ for different network configurations. The most interesting result is that three distinct regions can be identified: a) For λ below a certain threshold λl, the transmission cost in negligible compared to the contribution of the transmission rate in the utility function, so pricing does not impact the system's performance at equilibrium; b) in the second region, the average allocated power and the sum-rate decrease with λ, thus leading to a nontrivial trade- off between achievable transmission rate and the cost of power consumption; finally, for large λ > λu the transmission cost is so high that it ends up dominating each user's utility function, so users

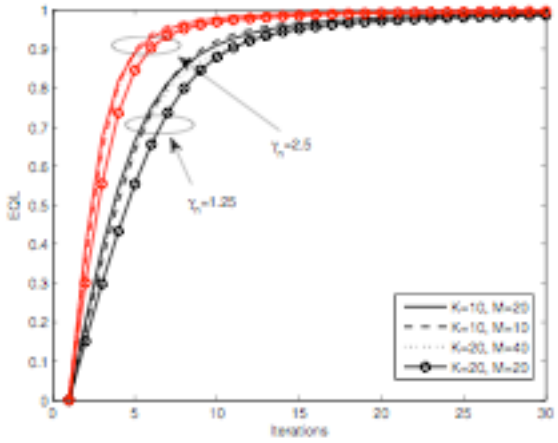

Fig. 5. Evolution of the equilibration rate for the LP model for different values of the step-size γ_n and network configurations.

remain relatively quiet due to the high cost of power consumption. An important result is that the average cost paid by users for each transmission is maximized at λ = λ1. This result could be interesting and useful in all of those scenarios where the receiver of the uplink channel, e.g., the network operator which sells its channels by applying a pricing model, wants to maximize its revenues while maintaining high network performance.2 Fig. 3 also shows that LP performs better than NLP in terms of the users' transmission rate, precisely because users incur a higher cost under the NLP model (so users will allocate less power on each available channel thus decreasing their achievable transmission rates).

We also investigated the impact of different values of the ratio between the number of channels M and the number of users K on the system's overall performance. As shown in Fig. 3, the congested regime K > M leads to worse aggregate throughput values, as expected; in fact, an increase in the number of users reduces the SINR of each user transmitting on the same channel. On the other hand, if K □ M there is a reduction in the multiuser interference, so higher transmission rates can be achieved for all users.

Finally, in Fig. 5 we plot the game's equilibration level (EQL) under the linear pricing model for γn = 1.25, 2.5 and different values of M and K: as expected, the convergence rate with γn = 2.5 is faster compared to the one achieved for γn = 1.25. The most interesting result concerns the scalability of the algorithm: as a matter of fact, the algorithm converges to equilibrium within a number of iterations that is roughly independent of the underly- ing network configuration. To better understand the algorithm's scalability, we plotted in Fig. 6 the number of iterations needed to reach the equilibrium for different network configurations as a function of the step-size parameter. Specifically, we con- sidered K/M = 0.5 and varied M to study the impact of the number of users on the algorithm's convergence rate: Fig. 6 shows that the proposed distributed algorithm scales well with the number of users, especially if higher values of the step-size γn are used in the learning process. More precisely, even for a large number of users, the algorithm converges to the game's equilibrium within a few iterations, and this convergence rate is approximately independent of the exact number of users.

4.3.2.5 References

[1] G. J. Foschini and Z. Miljanic, "A simple distributed autonomous power control algorithm and its convergence," IEEE Trans. Veh. Technol., vol. 42, pp. 641–646, November 1993.

[2] V.Chandrasekhar,J.G.Andrews,andA.Gatherer,"Femtocellnetworks: A survey," IEEE Commun. Mag., vol. 46, no. 9, pp. 59–67, 2008.
[3] G. Scutari, S. Barbarossa, and D. Palomar, "Potential games: A frame- work for vector power control problems with coupled constraints," in Acoustics, Speech and Signal Processing, 2006. ICASSP 2006 Proceed- ings. 2006 IEEE International Conference on, vol. 4, May 2006, pp. IV– IV.
[4] T. Alpcan, T. Bas ̧ar, R. Srikant, and E. Altman, "CDMA uplink power control as a noncooperative game," Wireless Networks, vol. 8, pp. 659– 670, 2002.
[5] C.-W.SungandW.S.Wong,"Anoncooperativepowercontrolgamefor multirate CDMA data networks," IEEE Trans. Wireless Commun., vol. 2, no. 1, pp. 186–194, January 2003.
[6] F. Meshkati, M. Chiang, H. V. Poor, and S. C. Schwartz, "A game- theoretic approach to energy-efficient power control in multicarrier CDMA systems," IEEE J. Sel. Areas Commun., vol. 24, pp. 1115–1129, 2006.
[7] S. T. Chung, S. J. Kim, J. Lee, and J. M. Cioffi, "A game-theoretic approach to power allocation in frequency-selective Gaussian interference channels," in ISIT '03: Proceedings of the 2003 International Symposium on Information Theory, 2003.
[8] G. A. Gupta and S. Toumpis, "Power allocation over parallel Gaussian multiple access and broadcast channels," IEEE Trans. Inf. Theory, vol. 52, no. 7, pp. 3274–3282, 2006.
[9] F. Meshkati, H. V. Poor, and S. C. Schwartz, "Energy-efficient re- source allocation in wireless networks: an overview of game-theoretic approaches," IEEE Signal Process. Mag., vol. Special Issue on Resource- Constrained Signal Processing, Communications and Networking, May 2007.
[10] C.U.SaraydarandD.G.NarayanB.Mandayam,"Efficientpowercontrol via pricing in wireless data networks," IEEE Trans. Commun., vol. 50, no. 2, pp. 291–303, February 2002.
[11] P. Mertikopoulos, E. V. Belmega, A. L. Moustakas, and S. Lasaulce, "Distributed learning policies for power allocation in multiple access channels," IEEE J. Sel. Areas Commun., vol. 30, no. 1, pp. 96–106, January 2012.
[12] G. Bacci, E. V. Belmega, and L. Sanguinetti, "Distributed energy- efficient power optimization in cellular relay networks with minimum rate constraints," in ICASSP '14: Proceedings of the 2014 International Conference on Acoustics, Speech and Signal Processing, to appear.
[13] A. S. Nemirovski, A. Juditsky, G. G. Lan, and A. Shapiro, "Robust stochastic approximation approach to stochastic programming," SIAM Journal on Optimization, vol. 19, no. 4, pp. 1574–1609, 2009.
[14] D. Monderer and L. S. Shapley, "Potential games," Games and Economic Behavior, vol. 14, no. 1, pp. 124 – 143, 1996.
[15] A.Neyman,"Correlatedequilibriumandpotentialgames,"International Journal of Game Theory, vol. 26, pp. 223–227, 1997.
[16] W. H. Sandholm, Population Games and Evolutionary Dynamics, ser. Economic learning and social evolution. Cambridge, MA: MIT Press, 2010.
[17] P. Mertikopoulos, E. V. Belmega, A. L. Moustakas, and S. Lasaulce, "Dynamic power allocation games in parallel multiple access channels," in ValueTools '11: Proceedings of the 5th International Conference on Performance Evaluation Methodologies and Tools, 2011.
[18] P. D. Taylor and L. B. Jonker, "Evolutionary stable strategies and game dynamics," Mathematical Biosciences, vol. 40, no. 1-2, pp. 145–156, 1978.

4.4 Annex D - JRA 1.2.1-5 Clusters organization for multi-hop cooperative communications

4.4.1 Reference Scenario

The WSN under consideration is composed of N sensor nodes, equipped with a single ideal isotropic antenna and randomly distributed over a given area (see Fig. 1). The environmental parameters measured by sensors are sent to N_s sinks through a query-based communication protocol, where sinks periodically send a *query* to the nodes and each node transmits the data to the sink from which it receives the largest received power.

Due to the limited transmit power and constraints in terms of energy consumption, sensor nodes may need to cooperate to reach the final sink with a given reliability. Towards this

goal, sensors are organized in clusters to send data to the relevant sink, with up to N_s clusters of nodes formed at a time, one per sink. We assume that nodes will autonomously decide to act as sources if the measured data is sufficiently different from the one previously sent. Each *source node* takes advantages of a subset of nodes belonging to the same cluster, called *cooperating nodes*, acting as a VAA together with the associated source. Accordingly, denoting with $\mathcal{N}_i$, $i=1,..,N_s$, the set of nodes belonging to the i-th cluster, and with $\mathcal{M}_i$, $i=1,..,N_s$, the set of source nodes in cluster i, we have that $\sum_{i=1}^{N_s}|\mathcal{N}_i|\leq N$ and $\mathcal{M}_i \subseteq \mathcal{N}_i$.

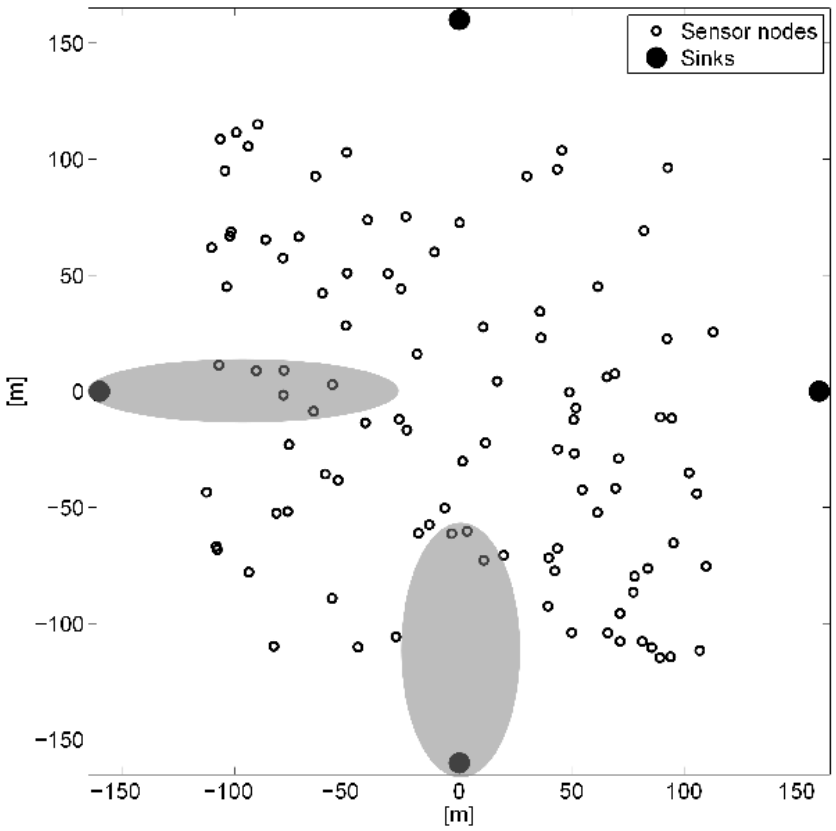

Figure 1: Reference scenario.

The considered node-to-sink channel model can be represented by channel transfer function

$$h_n = \frac{1}{\sqrt{k_0 d^{-\beta} s}} f, n=1,...,N \qquad (4.5.1)$$

where k_0 is the reference pathloss, d is the distance between the transmitter and the receiver, β is the pathloss exponent, s is the log-normally distributed shadowing component and f is the fading component which follows circularly-symmetric complex normal distribution. For the sake of simplicity, the non-cooperative game considers only pathloss component, because shadowing and fading components are less influential, but complicate the formulation of the game.

4.4.2 Game Theoretical Formulation of the VAAs Formation Problem

One of the main objective of this JRA is to derive a noncooperative game model for the WSN described in the previous section, wherein the sensor nodes aim at forming VAAs to maximize their own successful transmission rate. To this end, sensor nodes are coerced to behave as self-interested agents in a social network (SN) in which users can create relationships to share contents or services. More in details, we treat sensors' transmit power as the contents that can be shared among users in an social network (SN), while the relationships established to share those contents model the VAAs structure within the cluster.

Before introducing the strategic game that models the interactions among the nodes, let us introduce the vector $g_m \stackrel{\Delta}{=} \left(g_{m,\mathrm{l}}\right)_{\mathrm{l}\in\mathrm{N},\mathrm{l}\neq m}$, where $g_{m,\mathrm{l}}=1$ if node m wishes to form a VAA with node l, and $g_{m,\mathrm{l}}=0$ otherwise. Analogously to what is proposed in [ZS2012], we assume that cooperation between two sensors can be unilaterally established at the condition that the sensor requesting cooperation will afford the entire *virtual* cost to maintain this relationship. Under this assumption, the cooperation status between nodes m and l is

$$\bar{g}_{m,\ell}=\begin{cases}\max\{g_{m,\ell},g_{\ell,m}\} & m\neq\ell\\ 1 & m=\ell\end{cases} \tag{4.5.2}$$

where nodes m and l are called *neighbors* if $\bar{g}_{m,\mathrm{l}}=1$. Signal to Noise Ratio (SNR) can be expressed by

$$\gamma_m(p,g_m)\stackrel{\Delta}{=}\frac{b_0^2}{\sigma^2}P_{tot,m}(p,g_m), \tag{4.5.3}$$

where b_0^2 is the mean pathloss within a cluster, σ^2 is the noise power and $P_{tot,m}$ is the total power of cooperative transmission defined as

$$P_{tot,m}(p,g_m)\stackrel{\Delta}{=}\sum_{\ell\in\mathcal{L}_m\cup\{m\}}p_\ell \tag{4.5.4}$$

We can now highlight the following.

1) Each node in the WSN is considered as a player of the VAA formation game playing strategy $t_m=(p_m,g_m)$.

2) Each sensor, can form a VAA with the nodes that are only one hop away from it in the connectivity graph (neighbors).

3) The benefit obtained by generic sensor m is a strictly concave and monotonically increasing function of the SNR level γ_m. A convenient choice for the benefit function is

$$v_m(p,g)=\log\left(1+\frac{b_0^2}{\sigma^2}P_{tot,m}(p,g_m)\right), \tag{4.5.5}$$

i.e., the mth VAA's achievable information rate.

4) Since each node should prevent the adoption of a too high transmit power, due to the battery limitation, a linear cost of $\lambda \in \Re^+$ per unit of energy a node produces is introduced.

5) Finally, the bigger the coalitions size, the higher the number of signaling packets, introducing collisions and excessive overheads that may increase waste of energy. Thus, each node is assumed to incur in a VAA formation cost k for each VAA formation request he produces.

The VAA formation game is defined by the tuple $\mathcal{G} \overset{\Delta}{=} \{\mathcal{N}, t_m, u_m\}$, where players are the WSNs in $\mathcal{N}$, the strategy profile of the mth player is $t_m = \left(p_m, g_m\right)$ and its utility function is

$$u_m(t_m, t_{-m}) = v_m(t_m, t_{-m}) - \lambda p_m - k \| g_m \|_1, \tag{4.5.6}$$

where t_{-m} i the vector collecting the strategies played by all the players but the mth. Note that the proposed game is equivalent to the one originally analyzed in [ZS2012] for SNs. The solution concept for this game is the well-known Nash equilibrium (NE), i.e., a strategy profile $t^* = (p^*, g^*)$ such that

$$u_n(t_n^*, t_{-n}^*) \geq u_n(t_n, t_{-n}^*), \quad \forall n \in \mathcal{N}. \tag{4.5.7}$$

According to [ZS2012], when the size of the population is sufficiently high, every nontrivial equilibrium point presents a hierarchical structure with only two possible levels of transmit power, i.e., a high level and a low level. It is worth remarking that equilibria with asymmetric profiles fits with the requirement of having different transmit powers due to the possible heterogeneous levels of energy left available at the sensor nodes. Moreover, at the equilibrium point, a node with low transmit power can only request cooperation to a node presenting a high transmit power [ZS2012], which is suitable for our VAA structure where the sensor nodes with high energy availability shall help the sensors with a poor battery status. Hence, from now on, we will refer to the sensors with low transmit power and high transmit power as *weak nodes* (WNs) and *potential helpers* (PHs), respectively. Unfortunately, all these appealing features are frustrated by the so-called *law of the few* [ZS2012]. According to this, if the user's benefit depends only on the total quantity of acquired contents (i.e. contents are perfectly substitutable), the number of potential helpers will vanish as N tends to infinity. Consequently, the proposed game theoretical model will produce an useless structure for large VAAs.

4.4.2.1 Dixit-Stiglitz Preference Model

A viable solution to this problem is to foster cooperation among nodes via a modified benefit function that models the users' interest in taking advantages from a *variety* of power sources. Hence, instead of assuming the perfect substitutability of the power source, we use the *Dixit-Stiglitz* preference model [DS1977], which enables the possibility of appreciating the variety of the power sources, yielding the concept of *effective power*

$$P_{eff,m}(t_m, t_{-m}) \overset{\Delta}{=} \left(p_m^\rho + \sum_{\ell \in \mathcal{L}_m(\bar{g}_m)} p_\ell^\rho \right)^{1/\rho}, \tag{4.5.8}$$

where $\mathcal{L}_m(\bar{g}_m)$ is the set of neighbors of node m and $\rho \leq 1$ represents the node's appreciation for the variety of power sources. This appreciation increases as $\rho \to 0$, whereas disappears for $\rho = 1$, where (8) is equal to (4) indeed.

Based on the above-mentioned observations, a modified version of the VAA formation game is introduced, with

$$v_m(t_m, t_{-m}) = \log\left(1 + \frac{b_0^2}{\sigma^2} P_{\text{eff},m}(t_m, t_{-m})\right) \tag{4.5.9}$$

being the new players's benefit which replace (5) in (6). We now discuss the properties of the equilibrium points obtained thanks to the Dixit-Stiglitz preference model.

4.4.2.2 Analysis of the Equilibrium Point

The proposed game is a particular case of the IPLF framework investigated in [ZS2012]. Here, it is worth recalling the following two major results.

Existence of the NE [ZS2012, Th.~1]
Pure Nash equilibria of the game always exist and each equilibrium belongs to one of the following types: *i)* a symmetric strategy profile in which each node personally consumes an amount of power $P_{\max} \overset{\Delta}{=} \frac{1}{\lambda} - \frac{\sigma^2}{b_0^2}$, and no one forms any VAA; *ii)* an asymmetric strategy profile in which each node personally consumes an amount of power p_m^* strictly smaller than $P_{\max}$ and forms a VAA with at least one other player. Moreover, at the equilibrium we have

$$P_{\max} = \frac{1}{\lambda} - \frac{\sigma^2}{b_0^2} \leq \left(p_m^* + \sum_{\ell \in \mathcal{L}_m(\bar{g}_m)} p_\ell^*\right). \tag{4.5.10}$$

Hence, if the cost λ is chosen so that $P_{\max}$ respects some minimum performance requirements, the resulting equilibrium point will guarantee those requirements too.

Core-periphery structure of the NE [ZS2012, Th.~2-3]
In an asymmetric equilibrium, when $N = |\mathcal{N}| \to \infty$ and given λ, k, and ρ, we can classify the nodes into two categories: PHs and WNs. PHs transmit with a power P_{ph} and ask for collaboration only to other $N_{\text{p},p}(t^*)$ PHs while WNs transmit with a power P_{wn} and ask for collaboration to $N_{\text{w},p}(t^*)$ PHs. Moreover, the number of PHs $N_{ph}(t^*)$ is such that: *i)* $N_{ph}(t^*) < N_{wn}(t^*)$, where the latter is the number of WNs; *ii*) it grows at the same order as the entire population, i.e.

$$\lim_{N \to \infty} \inf_{t^* \in \Phi_{\mathcal{N}}} \frac{N_{ph}(t^*)}{N} = \eta \tag{4.5.11}$$

where η is a constant and Φ_N is the set of Nash equilibria for a population of size N. As apparent from (11), the law of the few is not valid when the Dixit-Stiglitz model is accounted for, thus making the game theoretical model appealing for a cooperative WSN scenario.

4.4.3 Communication Protocol

Relying on the game theoretical analysis outlined above, this section describes the different steps of the communication protocol required to get the cooperative beamforming transmission. For what concerns the access to the channel, a contention-based protocol, as the Carrier Sense Multiple Access with Collision Avoidance (CSMA/CA) protocol defined by the IEEE 802.15.4 standard, is used for data transmissions, if not otherwise specified.

4.4.4 Cluster Formation

Each sink sends a query, using a power much higher with respect to the maximum power at which nodes may transmit. All nodes triggered by a given sink join its cluster. If more than one query is received by a node, the latter selects the sink from which it receives the highest power. Every node $m \in \mathcal{N}$ sends a short packet, including its battery level e_m, towards the sink. In turn, the sink collects all the battery levels in the vector $\overset{\Delta}{e}=[e_1,\ldots,e_N]^T$, whose elements are sorted in increasing order. Since at this stage lots of nodes will attempt to transmit a packet, a high maximum number of retransmissions is allowed, to avoid packets loss. This step makes each sink aware of the number of nodes belonging to its cluster and of their battery levels. The latter are used as input to compute the VAA formation parameters according to the following procedure.

1) The sink computes the vector of maximum powers at which each sensor may transmit as $\overline{p} = eP_{max}$, where P_{max} is expressed by (10).

2) A minimum number of WNs is selected as $N_{wn} = N/2$.

3) According to the value of N_{wn}, the two levels of power must satisfy the following requirements: $P_{wn} \le \overline{p}(0)$ and $\overline{p}(0) < P_{ph} \le \overline{p}(N_{wn})$.

4) The sink checks if there exists an equilibrium point of the game $\mathcal{G}$ that satisfies the requirements of Step 3 (for the sake of brevity we omit the details of the algorithm). If the equilibrium exists, the sink broadcasts $\overline{p}(0)$, $\overline{p}(N_{wn})$ and P_{ph}, together with the values $N_{w,p}$ and $N_{p,p}$ that guarantee the existence of the equilibrium, and the procedure ends. If the equilibrium does not exist, N_{wn} is increased by 1 and steps 3 and 4 are repeated.

4.4.5 VAA Formation

Once the clusters are established, a subset of the triggered nodes will act as source nodes. For the sake of simplicity we consider the sources to be WN. To form its VAA, each source transmits in broadcast a cooperation request packet. Nodes, sources or not, receiving such a packet, reply with an unicast cooperation reply packet to the source, including the status of its battery, i.e., if it is a WN or a PH. At this point each source selects its cooperating nodes, among those from which the cooperation reply has been received. Since each source knows the optimum number of PHs, N_{ph}, and WNs, N_{wn}, it should cooperate with, in case the number of replies from PH is larger than N_{ph}, or number of replies from WNs is larger than N_{wn}, nodes are selected according to the largest power received. Once the set of cooperating node, $\mathcal{L}_m$, is defined by source m, it sends to such nodes an acknowledge (ACK), to let them know they belongs to its VAA and to provide a time scheduling that will be

used in the VAA to avoid collisions among nodes of the same VAA. Cooperation request and reply are sent using CSMA/CA.

4.4.6 Cooperative Beamforming

Once the VAA formation is done, each source performs CSMA/CA to transmit its data. When the channel is found free, sources broadcast their data so that each node in their VAA has a copy. This transmission is also exploited as a trigger for the next phase in which the cooperating nodes transmit pilots towards their sink using a scheduled time division scheme (each node has an assigned time slot) defined during the VAA formation. These pilot packets are used for channel estimation. Upon the reception of these pilot packets, the sink replies with an ACK packet containing the channel estimation. Immediately after the ACK packet is received by the VAA members, they calculate their transmission weight and the cooperative data transmission occurs.

4.4.7 Numerical results

Numerical results are obtained through simulation and the chosen metrics are SNR and energy consumption of cooperative transmission. $N=100$ sensor nodes are uniformly distributed over $130m\times130m$ observation area, surrounded by $N_S=4$ sinks located $30m$ from the edges. Channel parameters are $k_0=1260$, $\beta=3$, the noise power $\sigma^2=-110dBm$ and the duration of packet transmission $T_{packet}=0.8ms$. Given that all the nodes in a VAA set their transmit weight in a proper way ($w_\ell=e^{-j\arg\{h_\ell\}}$), the overall SNR of the cooperative transmission is defined as $\eta(p,g_m)\overset{\Delta}{=}\frac{1}{\sigma^2}\sum_{\ell\in\mathcal{L}_m\cup\{m\}}p_\ell|h_\ell|^2$, whereas the energy consumption of a cooperative transmission is $E=T_{packet}\sum_{\ell\in\mathcal{L}_m\cup\{m\}}p_\ell$. We compare the case where no cooperation is present with the NE of the game, and the case in which the presented communication protocol is employed. In this way we show both the advantages of cooperative transmission and the extent to which the NE can be achieved in a realistic environment.

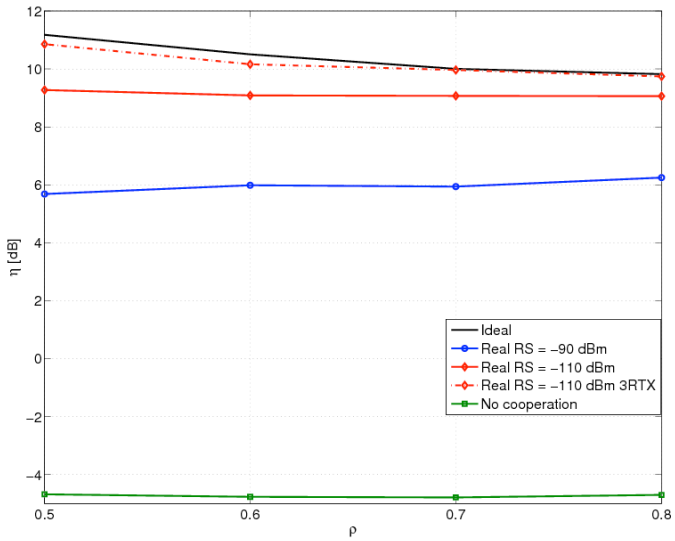

Figure 2: Average SNR of cooperative transmission.

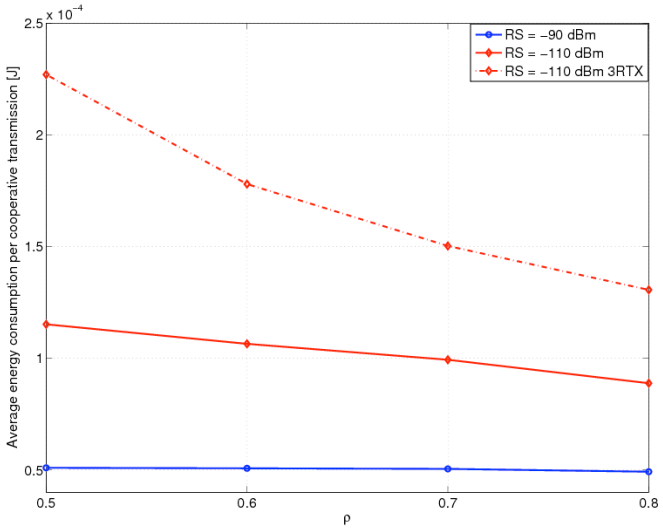

Figure 3: Energy consumed by cooperative transmission.

Fig. 2 shows η as a function of parameter ρ. First, we can observe that the case where there is no cooperation achieves the worst performance by far. This is of course expected, since the transmission power of a source is always lower than the total transmit power of the VAA which includes the source. Looking at the ideal case, represented by the black line, it can be observed that the average SNR decreases with ρ. According to Dixit-Stiglitz model, increasing ρ will decrease the source interest for cooperation, leading to smaller VAAs thus further leading to lower average SNR. The communication protocol is evaluated in different settings. Considering nodes with two levels of receiver sensitivity, we evaluate the impact of connectivity on the performance. On one hand lower receiver sensitivity, RS, means higher number of neighbors, thus higher number of potential cooperating nodes, but, on the other hand, it also increases the collision probability. Observing the results it can be concluded that the former effect is more important as decreasing receiver sensitivity leads to better performance. There are several protocol parameters which can be modified in order to trade off between the generated overhead and the proximity to the ideal case. For example, by setting the maximum number of retransmissions of cooperation request to 3, the protocol achieves almost the same performance as in the ideal case. We can conclude that at cost of certain amount of overhead, the solution of the game can be replicated. Fig. 3 shows the energy consumed by the cooperative transmission as a function of parameter ρ. It can be observed that having higher ρ decreases the energy consumption, since less nodes are involved in the VAA. The curve representing higher receiver sensitivity is practically not affected by ρ, since the number of cooperating nodes is mostly limited by the connectivity. In fact, the curves representing lower receiver sensitivity have steeper slope because the communication protocol is following the game solution.

4.4.8 References

[ZS2012] Y. Zhang, and M. van der Schaar, “Information production and link formation in social computing systems” Selected Areas in Communications, IEEE Journal on, vol. 30, no. 11, pp. 2136–2145, 2012.
[DS1977] A. Dixit and J. Stiglitz, “Monopolistic competition and optimum product diversity,” The American Economic Review, vol. 67, no. 3, pp. 297–308, 1977.

4.5 Annex E - JRA 1.2.2-1 Opportunistic relaying and forwarding

4.5.1 Introduction

Delay Tolerant Networks consist of mobile nodes which occasionally happen to come into each other proximity [1]. The sporadic opportunities of nodes' contacts make support of communications in these networks very challenging and complex and traditional routing solutions proposed for ad hoc scenarios become inappropriate. When considering in particular multicast support in such networks, the traditional criticalities foreseen for ad hoc networks are exacerbated by the need to limit flooding while guaranteeing reliability in data delivery [2].
In the past, the support of unicast data delivery in DTNs has been achieved through the use of replication for information spreading [3], [4]. DTN Multicast instead has been addressed only recently with a focus on the exploitation of sociality to characterize nodes centrality and consequent selection of a subset of nodes as potential packet relays [5], [6], [7].
A relevant problem in these networks is represented by the overwhelming of nodes which can be incurred when the replication overhead becomes excessive. To this purpose adaptive recovery schemes have been proposed [8] which aim at identifying a tradeoff between the need to guarantee reliable data delivery while avoiding data storming. In this paper we address this joint problem in case of multicast DTNs. To this purpose we propose to exploit intrinsic sociality among users to improve data delivery and tune the adaptive recovery scheme. Moreover, in order to increase the chances to have successful packets exchange among nodes, network coding is employed in our setting. We provide a theoretical model of the multicast data dissemination and adaptive infection recovery, while taking into account both the use of network coding and users sociality. Our analysis shows that sociality can turn into an advantage for multicast data dissemination in DTNs and can be associated with adaptive infection recovery to avoid excessive dissemination overhead.

In this work we focus on multicasting in DTN. In particular we try to increase the chance that information can be delivered to the destination also in these challenging scenarios, while decreasing the overhead of replication or mobility information dissemination as discussed above, and taking into account the intuition that social relationships among users can help to achieve the above targets.

4.5.2 System model

4.5.2.1 Interest-casting

In [10] it was observed from real traces that individuals characterized by similar interests tend to meet more often and spend more time together. This implies that similarity of interests is a clue of sociality and trend of nodes to create a group. Accordingly in the following we model sociality using similarity of interests as proposed in [10].
In our system we consider that each user is characterized by her *interest profile* that identifies her interests (as an example the interest could be related to a topic, e.g. cinema, type of music, or to the fact that the user belongs to a specific social community e.g. twitter group, Facebook group, residential community, etc...) in a Z-dimensional unit cube (that is the interest space) where Z is the overall number of interests into the network [10]. The interest profile of the user will consist of a *Z*-dimensional vector where each element of the array is a number in the interval [0, 1] that characterizes the degree of interest of a user in one of the Z possible elements of the interest space. We assume that users characterized by having the same non empty fields in the interest profile$_1$ form a group.
In order to quantify how close the interests of two different users Λ and Φ are, i.e. their *homophily*, the cosine similarity metric can be employed. More specifically, this metric is defined as follows:
Given two G-dimensional arrays Λ and Φ, the cosine similarity metric Θ(Λ, Φ) is defined as:

$$\Theta(A,\Phi) \quad cos(\angle A\Phi) \quad \frac{A\Phi^t}{|A|\,|\Phi|} \quad (1)$$

where $|\cdot|$ denotes the norm of the array and the apex t denotes the transpose array.
Observe that higher values of the cosine similarity metric imply that the angle formed by the two arrays is low which means that the two arrays tend to be identical. On the contrary, low values of the metric imply that the two arrays are significantly different, i.e. low degree of homophily is met.
Each node into the network can be both a source and a forwarder of messages. Accordingly it maintains in a buffer the packets which should be relayed to the destinations. Each packet is characterized by a header which includes a *packet relevance profile* ν. The packet relevance profile is usually set by the source node upon issuing the packet into the network.
When two nodes happen to be in each other coverage range, they exchange their interest profile and the list of the relevance profiles of the packets stored in their buffers. Then a cosine similarity metric is estimated between the interest profile of each node involved in the meeting procedure, e.g. node Φ, and the relevance profiles of the packets stored by other nodes, e.g. ν. For each estimation of this metric, a comparison with a threshold α (called the *relaying threshold*) is performed; if the value of the cosine similarity metric is larger than α, the node will be interested in the content and the content relaying procedure will take place. Otherwise, the content relaying will not be executed. More in detail,

$$\begin{cases} if\ cos\angle(IP(\Phi),\nu) > \alpha & packet\ is\ relayed \\ if\ cos\angle(IP(\Phi),\nu) \leq \alpha & packet\ is\ not\ relayed \end{cases} \quad (2)$$

The choice of the threshold α is relevant to characterize how aggressive the relaying procedure can be.
More specifically, upon decreasing α, the delivery delay can be reduced because the strategy becomes more epidemic and aggressive. On the contrary, upon increasing α, the routing procedure becomes more conservative and in the extreme case only few nodes will be able to receive the resource, i.e. the packet.

4.5.2.2 Traffic model

We study a network consisting of G groups of users. Each group i = {1, 2, . . . G} consists of $N_i + 1$ wireless mobile nodes where there is one source and a set of N_i candidate relay nodes moving within a constrained area according to a random mobility model. Multicast communication is considered from the source node to a set of destinations in each group, D^i, where $D^i \leq N_i$, $\forall i = \{1, 2, . . . G\}$. We also assume that, once obtained the needed packet, destinations can also forward the packet to each other. This approach is referred to as destination cooperative multicast (DCM) to distinguish it from the case where destinations do not cooperate to the dissemination procedure.
Two nodes can communicate only when they come within the transmission range of each other, which represents a communication opportunity to forward packets to each other. Also due to the low node density, the interference among nodes is ignored [11], [12]. Without loss of generality, it is assumed that when two nodes meet, the transmission opportunity is only sufficient to completely transmit one data packet per node. This assumption is justified by choosing the proper packet length (maximum packet length allowed by the rendezvous time) and allowing only one packet transmission per flow per node during the nodes rendezvous [13]. It is straightforward to extend this to the general case where an arbitrary number of packets can be delivered when the opportunity arises.
We consider that nodes have infinite buffer size. Also, it is assumed that the time between two consecutive transmission opportunities when nodes meet follows an exponential distribution as widely adopted in the literature, e.g., [13], [8], [9], [14].
Also, use of this exponential distribution has the advantage of enabling theoretical analysis by using continuous Markov models.

4.5.3 Polymorphic Epidemic Routing

We consider a set of destinations $D = \sum_{i=1}^{G} D^i$ that request a common message f from the multicast source. In general it is known that in conventional multicast/ broadcast networks, network coding improves the performance of the network [15]. For this reason, we include network coding in our DTN model and extend the study to the network behavior in multicast scenarios.

Let us consider the case where the multicast source splits the message in two packets a and b (f = a, b). Then, the source infects the network with both packets a and b, and their combination c = a + b where ''+'' stands for XOR operation on binary data stream. Similarly to what happens for disease spreading, infection with two different packets is referred to as polymorphic infection and DNA combination of these packets into a new packet c is referred to as the mutation. In the following we will use equivalently the term agent to denote both the node that stores a packet or the packet itself. Agent c will transmit a useful packet if it meets either user b (since c+b = a) or user a (since c+a = b). A user is infected with f when it has received a and b (f = a, b). The infection process is illustrated in detail in Table I, where a matrix structure is reported. More specifically for each possible packet owned by node i and node j, the element of the matrix represents the new pair of packets owned by the two nodes after meeting, respectively. As an example if Node i owns packet a and meets Node j who has packet b, by exchanging their packets it will follow that Node i obtains packet b and Node j has packet a.

To model Polymorphic Epidemic Routing the following notation is used. We denote as $A_i(t)$, $B_i(t)$, $C_i(t)$ and $F_i(t)$ the number of users in group i infected by agents a, b, c and f, respectively at time t. We denote as $I_i(t) = A_i(t) + B_i(t) + C_i(t) + F_i(t)$ the overall number of infected users in group i and as $I(t) = \sum_{i=1}^{G} I_i(t)$ the overall number of infected users in the network. We model the infection rate for users a, b, c and f by using ODEs as a fluid limit of the Markov model [8].

In order to take sociality into account and see how this impacts on the overall dissemination perfor- mance, the model of the polymorphic epidemic routing incorporates also the fact that users are grouped and can be interested into a content (i.e. a packet) or not. To this purpose we use an interest probability IP_{ij} that we assume characterizes users of group i when they come into contact with users of group j. Hence, the fluid model of the polymorphic infection can be represented through a system of equations as follows:

$$\begin{cases} X_i'(t) = [N^i - I_i(t)] \sum_{j=1}^{G} \left[X_j(t)\lambda_{ij} IP_{ij} + \frac{1}{3} F_j(t)\lambda_{ij} IP_{ij}\right] - X_i(t) \sum_{j=1}^{G} \left[\lambda_{ij} IP_{ij} (I_j(t) - X_j(t))\right] \\ X_i(t) \in \{A_1(t), \dots A_G(t), B_1(t), \dots B_G(t), C_1(t), \dots C_G(t)\} \\ F_i'(t) = A_i(t) \sum_{j=1}^{G} \left[\lambda_{ij} IP_{ij} (B_j(t) + C_j(t))\right] + B_i(t) \sum_{j=1}^{G} \left[\lambda_{ij} IP_{ij} (A_j(t) + C_j(t))\right] + \\ + C_i(t) \sum_{j=1}^{G} \left[\lambda_{ij} IP_{ij} (B_j(t) + A_j(t))\right] + F_i(t) \sum_{j=1}^{G} \lambda_{ij} IP_{ij} \left[I_j(t) - F_j(t)\right] \end{cases} \quad (3)$$

In the set of eqs. in (3) we observe that the increment of $X_i(t)$ for the different groups, denoted as $X_i'(t)$ depends on the contribution coming from all the possible inter-contacts among groups. Accordingly we distinguish an inter-contact rate which depends on the considered groups. More specifically we denote λ_{ij} as the rate characterizing the inter-contact time exponential distribution for groups i and j, where i can be also equal to j if users belong to the same group. We are assuming that the inter-contact rate matrix is symmetric, i.e. $\lambda_{ji} = \lambda_{ij}$. Also, according to what has been discussed in [16], inter-contact rates among users have been proved to be larger for users belonging to the same group and lower for users belonging to different groups. Accordingly, we have $\lambda_{ii} \geq \lambda_{ij}$, $\forall$ i, j . In the set of eqs. in (3) the increment of $X_i(t)$ for the different groups takes into account that, for each pair of groups that interact, the rate at which $X_i(t)$ increases is positively impacted by the rate at which a node infected by packet x in any group meets a node not infected by any packet in group i, plus the rate that a node infected by f meets a non infected node which will occur randomly, in the average with probability 1/3 when f chooses one of the three infection options: packet a,b or c. The second term represents the event of losing packet x (negative increment) which happens when it becomes f after meeting a node in any group infected by any other packet except x and performing recombination. Similarly, an increment in $F_i(t)$ in eq. (3), is

obtained by considering contributions of nodes in the different groups and assuming that, if a node of a generic group carrying packet a meets a node carrying packet b in any group, they can exchange packets and after the exchange each of the two can reconstruct packet f. Analogously, the reconstruction of f will happen when a node having packet a meets a node having packet b or c, and viceversa. Similarly if f meets a, b or c, one extra f will be created, which is included in the last term $F_i'(t)$. These equations can be solved with initial conditions $A_i(0) = B_i(0) = C_i(0) = 1$ and $F_i(0) = 0$ $\forall i \in \{1, \ldots G\}$ where we have indicated as $\mathbf{X}(0)$ the matrix of the initial values for the groups, i.e. $\mathbf{X}(0) = [\mathbf{X}_1(0); \ldots \mathbf{X}_G(0)]$ and $\mathbf{X}_i(0) = [A_i(0)\ B_i(0)\ C_i(0)\ F_i(0)]$. In this section, we first extend the most common recovery schemes [17] applied so far to unicast routing to the multicast case combined with Polymorphic Epidemic Routing. Later on, we present possible adaptive recovery schemes to additionally tune the recovery procedure.

4.5.4 Recovery schemes

Once a node delivers a packet to the destination, it should delete the copy from its buffer both to save storage space, and to prevent the node from infecting other nodes. This process is called infection recovery process. The packet is deleted for efficient buffer and bandwidth utilization. On the other hand, a node retains packet delivered information in the form of an anti-packet that prevents it from accepting another copy of the same packet. Reference [17] refers to this scheme as immune scheme. With immune scheme, a node stores a packet copy in the buffer until it meets the destination, often long after the first copy of the packet is delivered. An alternative and more aggressive approach to delete obsolete copies is to propagate the anti-packets among the nodes. The anti-packet can be propagated (transmitted) only to infected nodes (immune TX scheme), or also to susceptible nodes (vaccine scheme). The conventional infection recovery process starts as soon as the packet reaches the first destination which, in the case of multicast session, may reduce the chances that the rest of the destinations receive the message. So, in a multicast application there is a need to delay the initialization of this recovery process in order to allow more efficient delivery of the information to all intended destinations.

4.5.4.1 Recovery schemes with interest-casting applied to multicast

Similar to our earlier analysis, we can derive ODE models of the infection and recovery process as the limit of Markov models [8]. In general, by modifying eq. (3) to include the recovery process, the infection rates for user $x \in \{a, b, c\}$, and f are:

$$\begin{cases} X_i'(t) = [N^i - I_i(t) - R_i(t)] \sum_{j=1}^{G} \lambda_{ij} IP_{ij} \left[X_j(t) + \frac{1}{3} F_j(t)\right] - X_i(t) \sum_{j=1}^{G} [\lambda_{ij} IP_{ij} (I_j(t) - X_j(t))] - R_i'^{x}(t) \\ X_i(t) \in \{A_1(t), \ldots A_G(t), B_1(t), \ldots B_G(t), C_1(t), \ldots C_G(t)\} \\ F_i'(t) = A_i(t) \sum_{j=1}^{G} [\lambda_{ij} IP_{ij} (B_j(t) + C_j(t))] + B_i(t) \sum_{j=1}^{G} [\lambda_{ij} IP_{ij} (A_j(t) + C_j(t))] + \\ + C_i(t) \sum_{j=1}^{G} [\lambda_{ij} IP_{ij} (B_j(t) + A_j(t))] + F_i(t) \sum_{j=1}^{G} \lambda_{ij} IP_{ij} [I_j(t) - F_j(t)] - R_i'^{f}(t) \end{cases} \quad (4)$$

In the above set of equations, the recovery process has been characterized through the introduction of terms $R'_x(t)$ and $R'_f(t)$ which are the recovery rates for users $x \in \{a,b,c\}$ and f, in the generic group i, respectively. In the following, we derive the expressions for the number of recovered nodes for all three schemes extended to our multicast system when use of polymorphic epidemic routing is assumed. It is obvious that, also in this case, we are assuming that a single packet can be delivered at a time. Moreover, in order for the destination to be infected by packet f, it should be already infected by a or b or c.

1) ***Immune***: In immune scheme, as illustrated in Table II, the infected node is recovered when it meets any destination. So, the recovery rates $R'_x(t)$ and $R'_f(t)$ are obtained as follows:

$$\begin{cases} R_i'^x(t) = X_i(t)\sum_{j=1}^{G} IP_{ij}\lambda_{ij}D^j \\ R_i'^f(t) = F_i(t)\sum_{j=1}^{G} IP_{ij}\lambda_{ij}(D_j^a + D_j^b + D_j^c + D_j^f) \\ R_i(t) = R_i^a(t) + R_i^b(t) + R_i^c(t) + R_i^f(t)\ \forall i \in \{1,\dots G\} \end{cases} \quad (5)$$

In the above equations, we observe that the recovery rate increases when a destination in group i meets any node of any group who is infected by x; similarly the recovery rate for packet f increases when any node in group i infected by f meets any destination in any group already infected by packet a, b, c or f . From now on, the latter terms will be identified as $D_j^a(t)$, $D_j^b(t)$, $D_j^c(t)$ and $D_j^f(t)$. In case of the destinations cooperating and forwarding the packet to other destinations, the rate of the destinations infected by x ∈ {a, b, c} is modeled as:

$$\begin{cases} D_i'^x(t) = [D^i - D_i^a(t) - D_i^b(t) - D_i^c(t) - D_i^f(t)]\cdot \\ \cdot\sum_{j=1}^{G} IP_{ij}\lambda_{ij}[X_j(t) + \frac{1}{3}F_j(t) + D_j^x(t) + \frac{1}{3}D_j^f(t)] - IP_{ij}D_i^x(t)\cdot \\ \cdot\sum_{j=1}^{G}\lambda_{ij}[I_j(t) - X_j(t) + D_j^a(t) + D_j^b(t) + D_j^c(t) + D_j^f(t) - D_j^x(t)] \end{cases} \quad (6)$$

We observe that the rate of destinations infected for group i increases when one destination not infected by anyone meets a node of any group infected by x or f (with probability 1/3) or a destination already infected by x or f (again with probability 1/3). Instead, the infection rate decreases when a destination infected by x meets any node infected by a packet other than x or a destination in any group infected by any packet except for x. The same reasoning applies for the infection rate $D_j^f(t)$ which can be written in compact form as:

$$\begin{cases} D_i'^f(t) = [F_i(t) + D_i^f(t)]\sum_{j=1}^{G} IP_{ij}\lambda_{ij}\cdot\sum_{x\in\{a,b,c\}} D_j^x(t) + \sum_{x\in\{a,b,c\}} IP_{ij}[X_j(t) + D_j^x(t)]\cdot \\ \cdot\sum_{j=1}^{G}\lambda_{ij}\sum_{y\in\bar{x}} D_j^y(t) \end{cases} \quad (7)$$

Also in case of $D_j^f(t)$ we observe that the infection rate for packet f in group i increases when a node in group i, either storing f or being one of the destinations storing f, meets any other destination of any other group j storing a, b or c. Also the rate increases when a node in group i either storing x or being one of the destinations in i storing x meets any other destination in any other group storing the complementary packet of x.

2) ***Immune TX***: In this scheme, the anti-packet can be transmitted to the infected nodes. So, a new recovered node is obtained when an infected node meets a node that has been recovered or the destination. The infection rates for agent x ∈ {a, b, c} and f are defined as in eq. (4) and the recovery rates are obtained as

$$\begin{cases} R_i'^x(t) = X_i(t)\sum_{j=1}^{G}\lambda_{ij}IP_{ij}D^j + X_i(t)\sum_{j=1}^{G} IP_{ij}\lambda_{ij}R_j^x(t) + X_i(t)\sum_{j=1}^{G} IP_{ij}\lambda_{ij}R_j^f(t) \\ R_j'^f(t) = F_i(t)\sum_{j=1}^{G} IP_{ij}\lambda_{ij}[D_j^a(t) + D_j^b(t) + D_j^c(t) + D_j^f(t) + R_j^f(t)] \\ R_i(t) = R_i^a(t) + R_i^b(t) + R_i^c(t) + R_i^f(t) \end{cases} \quad (8)$$

In case of the immune TX mechanism, differently from the immune scheme, also a node of group i that has been recovered from f , can recover a node infected by x ∈ {a, b, c}. This is because, once the packet f (which intrinsically includes a, b and c) has been received, there is no need to transmit more packets.

3) ***Vaccine***: In this scheme, differently from the immune and immune TX approaches, the uninfected users can also be vaccinated when they are susceptible of receiving the packet. We vaccinate the users of a generic group i that have neither been infected nor recovered, when they meet a recovered node or a destination that has been infected by that packet. The infection rates for users a, b, c and f are defined as in eq. (4). The recovery rates are now obtained as:

$$\begin{cases} R_i'^x(t) = X_i(t)\sum_{j=1}^{G} IP_{ij}\lambda_{ij}D^j + X_i(t)\sum_{j=1}^{G} IP_{ij}\lambda_{ij}R_j^x(t) + X_i(t)\sum_{j=1}^{G} IP_{ij}\lambda_{ij}R_j^f(t) + \\ +[N^i - I_i(t) - R_i^x(t)]\sum_{j=1}^{G} IP_{ij}[D_j^x(t) + R_j^x(t)] \\ R_j'^f(t) = F_i(t)\sum_{j=1}^{G} IP_{ij}\lambda_{ij}[D_j^a(t) + D_j^b(t) + D_j^c(t) + D_j^f(t) + R_j^f(t)] + [N^i - I_i(t) - R_i(t)]IP_{ij}\cdot \\ \cdot\sum_{j=1}^{G}[D_j^f(t) + R_j^f(t)] \\ R_i(t) = R_i^a(t) + R_i^b(t) + R_i^c(t) + R_i^f(t) \end{cases} \quad (9)$$

As compared to the case of immune TX scheme, here we are also accounting for the fact that a node in a generic group i, not infected or recovered, is also vaccinated if it meets either a destination in a generic group j infected by x or a x recovered node. Also in case of f, the recovery rate is impacted by a similar term.

4.5.4.2 Adaptive recovery

Unfortunately the recovery schemes start deleting packets as soon as the first destination is reached, thus slowing down the packet infection procedure and avoiding all the multicast destinations to receive packet copies [17]. In order to cope with this limitation, an adaptive procedure is proposed. To this purpose in the following, we will illustrate two procedures which can be employed to achieve adaptability, although implying different cost in terms of overhead and signaling into the network. Observe that, as a consequence of this adaptive recovery schemes, equations discussed before should be modified by replacing the meeting rate $\lambda_{ij}(t)$ for nodes in groups i and j, respectively, with $\lambda'_{ij}(t) = \lambda_{ij}(t)p_r(t)|_{ij}$ in the three models, immune, immune TX and vaccine.
In the following the recovery probability $p_r(t)|_{i,j}$ will be elaborated for the different adaptive recovery schemes.

1) ***Adaptive soft recovery scheme***: Let us denote as $p_r(t)|_{i,j}$ the recovery probability at time t. More specifically, when a node of group i meets a destination of group j, the destination will send the anti- packet to the node with probability $p_r(t)|_{i,j}$. In the recovery schemes illustrated so far this probability was always equal to one. The aim of the adaptive recovery schemes is to modify $p_r(t)|_{i,j}$ based on the number of destinations in such a way that the packets are removed slowly while the infection process is still ongoing or the recovery is delayed until the majority of the destinations have received the packets. In general, in case of numerous multicast destinations, the initialization of the recovery process can be postponed longer. In this way, the recovery probability is adjusted to the amount of multicast traffic. To this purpose, in the following we consider a time dependent probability of packet recovery

$$p_r(t)|_{ij} = 1 - e^{-(\frac{\lambda_{ij}N}{D})t} \quad (10)$$

where $D = \sum_{i=1}^{G} D^i$ and D^i is the number of destinations in group i. Observe that in eq. (10) the decay parameter is proportional to the inter-contact rate among pairs of nodes belonging to groups i and j, respectively, and to the overall number of nodes into the network, $N = \sum_{i=1}^{G}(N_i + 1)$. Moreover, the packet dependent probability is inversely proportional to the number of destinations. This is because we expect that sociality of nodes has an impact on network dissemination performance and consequently nodes of group i cooperate to the dissemination also to nodes of group j. Similarly, when the number of network nodes is large, an increase in the recovery probability should be searched to avoid network overloading. Please observe that the approach proposed so far for data recovery exploits only parameters whose values can be assumed known by network nodes through a simple signaling management.

2) ***Adaptive global timeout recovery scheme***: As an alternative to the above scheme, the recovery can be delayed for certain time T_D^f. This is evaluated as the time that is needed

to deliver the packets to all destinations (delivery delay). The adaptive global timeout recovery scheme extends the model denoted as just–TTL recovery scheme introduced in [17]. We aim at extending this model to the Polymorphic Epidemic Routing for Multicast in DTN scenarios. According to the just – T T L recovery scheme, a node upon receiving a packet, starts a timer which duration is distributed according to an exponential distribution with rate μ. When the timer expires, the packet is removed from the queue and an anti-packet is stored to avoid future infections by the same packet. The node recovers from the infection of packet x when the associated timer expires. Accordingly, anti-packets are not explicitly transmitted. The infection rates for users a, b, c and f are defined as in eq. (4), where the number of packets recovered is obtained as:

$$\begin{cases} R_i^{tx}(t) = \mu(X_i(t) - 1) \\ R_i^{tf}(t) = \mu(F_i(t) - 1) \\ R_i(t) = R_i^a(t) + R_i^b(t) + R_i^c(t) + R_i^f(t) \end{cases} \tag{11}$$

The proposed scheme, differently from the adaptive soft recovery, requires that a notification procedure is implemented so that, when the last destination receives the packet f, it can update the source about this and then, the recovery process can start with probability

$$p_r(t)|_{ij} = \begin{cases} 1 & t \geq T_D^f \\ 0 & t < T_D^f \end{cases} \tag{12}$$

Note that this adaptive global timeout recovery scheme can result more costly than the previous one in terms of additional signaling overhead needed in case of distributed network management. Alternative centralized solutions could be also considered. However this adaptive recovery scheme represents a benchmark in our analysis in the sense that it assumes perfect knowledge of the system.

4.5.5 Performance

We estimated the performance in terms of *packet delivery delay* T_D^f that is the time from the moment when packets a,b and c are generated at the source to the time when f = a,b is received by all destinations. Another delay metric that quantifies the efficiency of the recovery scheme is the *average lifetime* L^f defined as the time from when packet a, b and c are generated at the source and when all copies of the packets are removed.

Other relevant metrics considered are the number of times a packet is copied during the average network lifetime and the number of times a packet is copied until it is delivered. The former is denoted as G_{L^f}, the latter $G_{T_D^f}$. The number of times a packet is copied until it is delivered depends, similarly to the previous case, on the average delivery delay for multicast.

We analyze the performance obtained by the proposed multicast polymorphic epidemic routing scheme when considering also the network coding approach and a recovery methodology. The social aspects are modeled by considering that users are organized in groups and inter-contact time distributions of users depend on their belonging to groups. More specifically, users belonging to groups are characterized by interests into contents that are thus disseminated according to a corresponding probability of acceptance. Two settings are considered:

- **Setting 1**: Two groups, same number of destinations per group, same number of nodes per group, probability of interest into contents equal to one, inter-contact time distribution for users of the same group characterized by a rate equal to $\lambda = 4 \cdot 10^{-3}$ and no contacts among users belonging to different groups. This is the case of the so called LABEL

forwarding scheme [16] where only nodes belonging to the same community cooperate in data dissemination.

- **Setting 2**: Two groups, same number of destinations per group, same number of nodes per group, probability of interest into contents equal to one, inter-contact time distribution for users of the same group characterized by a rate equal to $\lambda = 4 \cdot 10^{-3}$ and inter-contact time distribution for users of different groups characterized by a rate equal to $\lambda_{IG} = 8.3 \cdot 10^{-4}$ as proposed in [16]. In this case we assume that contacts among nodes of different groups are possible.
- The numerical estimation will be aimed at evaluating the impact of sociality on the multicast dissemination and recovery schemes.

In Figure 1 we show the average delay $E\{ T_D^f \}$ and the lifetime L^f in the three cases of Immune, Immune TX and Vaccine recovery. We observe that the Immune recovery is a slow mechanism. Indeed, the average lifetime is larger than the delivery delay to reach all destinations. For the immune TX recovery, note that the effect of the more aggressive recovery is such that the inversion happens when the number of destinations is high, i.e. around 70 destinations. In the vaccine case, the recovery and the dissemination procedure are aggressive and, thus, when the number of destinations is larger than 30, the delivery delay is slower than the average packet lifetime. This witnesses the inefficiency of the recovery procedure which, in case of immune TX and vaccine schemes can be too fast and does not allow all destinations to get packets before the recovery is terminated. Also observe that in general the delivery delay achieves lower values in the Immune case, increases in the ImmuneTX case and achieves the largest values in the Vaccine case. This is because the recovery slows down the delivery mechanism, thus increasing the overall delivery delay. When the probability $p_r(t)I_{i,j}$ is no longer unitary but varies according to the exponential law in eq. (10) as shown in Figure 3 observe that the recovery is slowed down because the packet recovery probability is almost zero and slowly increases. Observe that, as a consequence, the average lifetime of the packet is always at the maximum tolerable value (in our simulations this has been set to 100 s; afterwards packets will be discarded.). In case of the timeout mechanism used for the recovery, i.e. $p_r(t)I_{i,j}$ as in eq. (12 the recovery is too late and the delivery delay is always lower than the average lifetime. Also immune and immune TX exhibit the same performance when considering the adaptive timeout recovery scheme.
Observe however that the improvement which can be achieved in terms of lower delivery delay and higher lifetime which allows not to stop the dissemination procedure before all destinations have obtained the packet, is payed in terms of larger overhead in packet copies as shown in Figures 2, 4 and 5. In Figure 2 we show the average number of times a packet is copied in its entire lifetime and until the delivery delay. Observe that, for the three recovery schemes, the curves are basically the same for the delivery delay and for the lifetime. When considering different recovery probabilities we note that the remarkable difference in the delivery delay and lifetime, due to the very slow recovery, causes a significant difference in the number of copies produced. The difference is initially negligible for the immune case when $p_r(t)I_{i,j}$ varies as in eq. (10); then the difference becomes remarkable even in case of immune TX and vaccine recovery when eq. (12) holds. Observe that the curve in case of vaccine recovery exhibits a different behavior as compared to the other curves. In fact, upon increasing the number of destinations, the number of packet copies initially decreases. Then it again increases. This is due to the vaccine action; indeed when a limited number of destinations is considered, the vaccine approach is sufficient to limit the overhead of packet copies. When instead many destinations should be reached, more overhead is met and the vaccine action is not able to limit the packet storm.

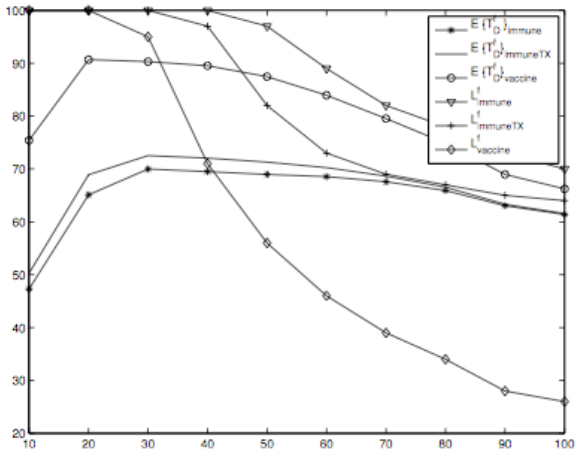

Fig. 1. Setting 1: Average delivery delay and lifetime vs. D when $p_r(t) = 1$.

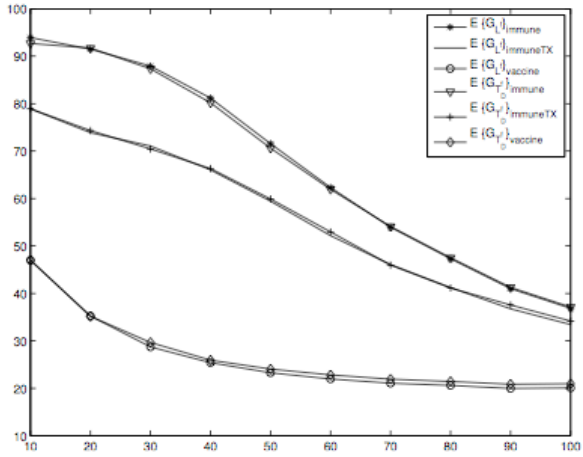

Fig. 2. Setting 1: Average number of copies vs. D when $p_r(t) = 1$.

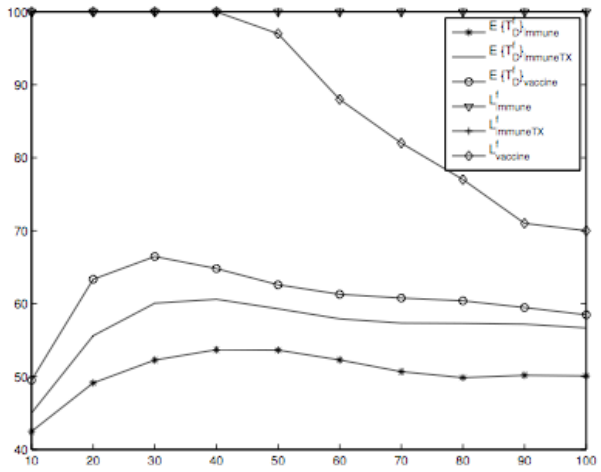

Fig. 3. Setting 1: Average delivery delay and lifetime vs. D when $p_r(t)$ as in eq. (10).

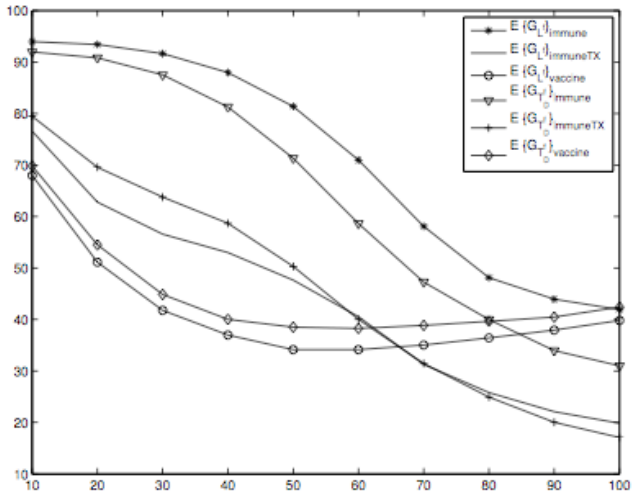

Fig. 4. Setting 1: Average number of copies vs. D when $p_r(t)$ as in eq. (10).

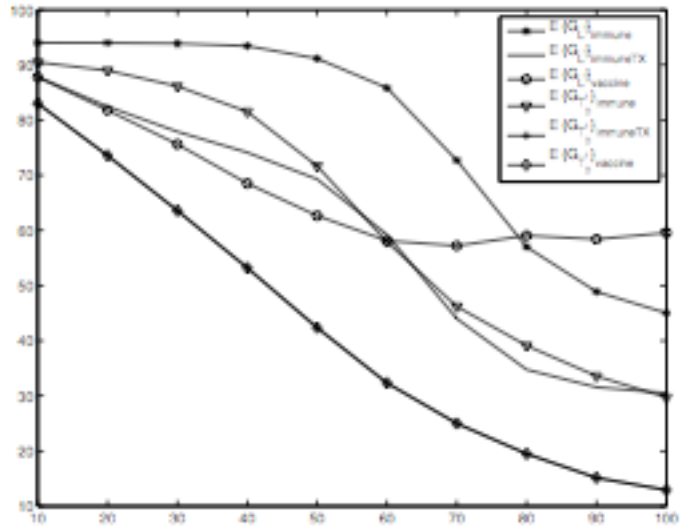

Fig. 5: Setting 1: Average number of copies vs. D when $p_r(t)$ as in eq. (12).

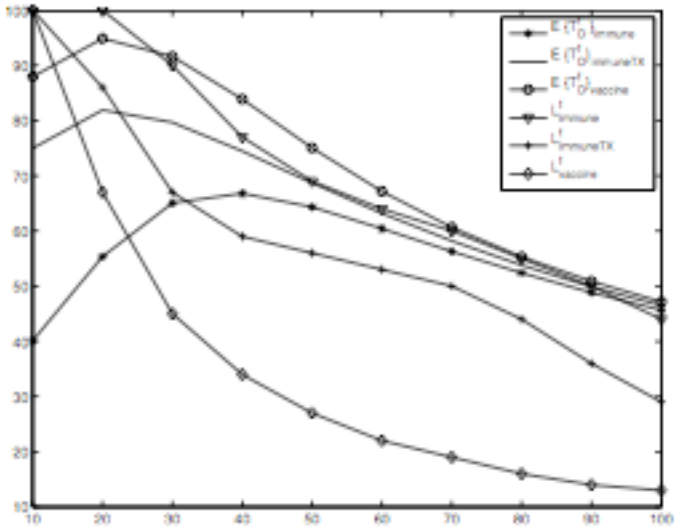

Fig. 6: Setting 2: Average delivery delay and lifetime vs. D when $p_r(t)=1$.

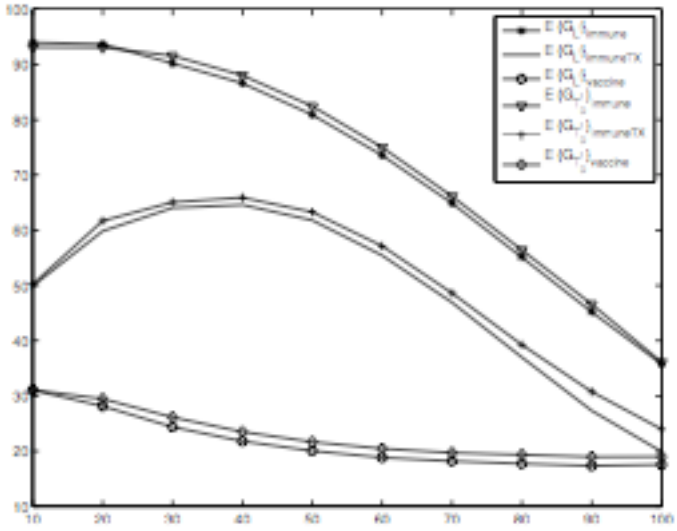

Fig. 7: Setting 2: Average number of copies vs. D when $p_r(t)=1$.

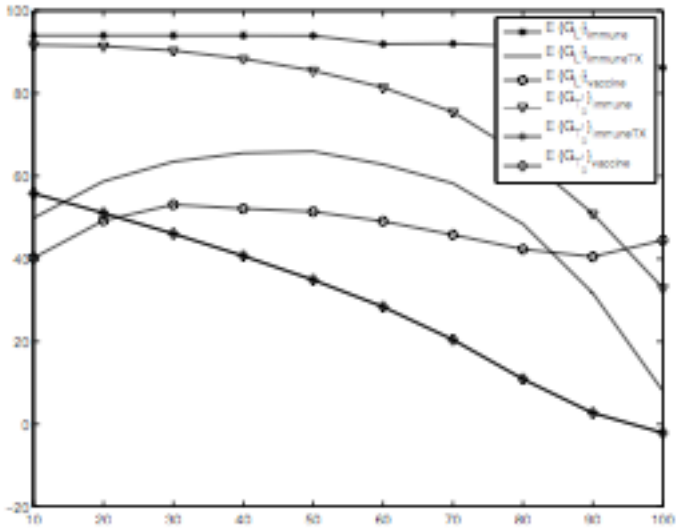

Fig. 8: Setting 2: Average number of copies vs. D when $p_r(t)$ as in eq. (12).

In setting 2 we have considered inter-contact time distributions for users belonging to different groups. In particular we have assumed the values proposed in [16]. In this case the rate of inter-contacts among nodes belonging to different groups has been increased so as to make it comparable with the case of intra-group contacts. Observe that, as compared to Setting 1, in Figure 6 it is evident that the average delivery delay and the lifetime can be reduced. This is because the impact of inter-group contacts is proficuous in the view of information dissemination. This effect is particularly relevant in case of the slower recovery schemes such as the Immune. Observe that in this case a maximum reduction of about 20% is obtained. In case of immune TX and vaccine schemes the impact of sociality is such that when few destinations are considered the immune TX approach performs worse than the immune scheme. Then, upon increasing the number of destinations, the immune and immune TX schemes perform similarly.

Concerning the average number of packet copies circulating in the network, please note that again a reduction is achieved. This is more relevant for the immune TX and vaccine schemes because the more aggressive recovery schemes are positively impacted by the social relationships which allow nodes of different groups to cooperate in data delivery. A relevant aspect to be considered is associated to number of copies in case the ImmuneTX recovery is obtained as shown in Figures 7 and 8. In fact observe that the numerous inter-group contacts allow to increase the number of packet copies when there are not too many destinations (i.e. less than about 40). This is because the anti-packet propagation mechanism is still not sufficient to stop message replication. Instead when the number of destinations increases, the anti-packet approach is able to counteract the message replication storm and the average number of copies decreases. This problem is not met in case of both the immune and vaccine recovery. The reason is because, on the one hand the immune approach does not use anti-packets and thus only when the destination is met the node is immunized. The vaccine approach instead is very aggressive itself and, thus, coupled with sociality which increases the inter-contacts among nodes, leads to a proliferation of immunized nodes and less packet copies around the network. Also note that when $p_r(t)l_{i,j}$ is not equal to 1, vaccine and immune TX schemes exhibit analogous performance in terms of $E\{T_D'\}$. This is because sociality balances the difference in the aggressiveness of the recovery scheme.

4.5.6 References

[1] M. Khabbaz, C.M. Assi, W. F. Fawaz, Disruption-Tolerant Networking: A Comprehensive Survey on Recent Developments and Persisting Challenges. IEEE Communications Surveys & Tutorials, vol. 14, no. 2, pp. 607-640, February 2012.
[2] Y. Wang, X. Li, J. Wu, Multicasting in Delay Tolerant Networks: Delegation Forwarding. IEEE Globecom. December 2010.
[3] A. Balasubramanian, B.N. Levine, A. Venkataramani, Replication routing in DTNs: a resource allocation approach.
IEEE/ACM Transactions on Networking. Vol. 18, No. 2. pp. 596-609. April 2010.
[4] A. Vahdat, D. Becker, Epidemic routing for partially-connected ad hoc networks, Technical Report, Duke University, 2000.
[5] W. Zhao, M. Ammar, and E. Zegura, Multicasting in delay tolerant networks: semantic models and routing algorithms, ACM SIGCOMM Workshop on delay tolerant networking, August 2005.
[6] U. Lee, S. Oh, K. Lee, and M. Gerla, Scalable multicast routing in delay tolerant networks, IEEE ICNP, October 2008. [7] W. Gao, et al., Multicasting in delay tolerant networks: A social network perspective, ACM MobiHoc, May 2009.
[8] X. Zhang, G. Neglia, J. Kurose, and D. Towsley, Performance Modeling of Epidemic Routing, Elsevier Computer Networks, Vol. 51, pp. 2867-2891, December 2006.
[9] W. Gao, Q. Li, B. Zhao and G. Cao Multicasting in Delay Tolerant Networks: A Social Network Perspective. ACM
MobiHoc. May 2009.
[10] A. Mei, G. Morabito, J. Stefa, P. Santi. Social-Aware Stateless Forwarding in Pocket Switched Networks. IEEE Infocom Miniconference. April 2011.
[11] K. Sohrabi, J. Gao, V. Ailawadhi, and G.J. Pottie. Protocols for self- organization of a wireless sensor network. IEEE
Personal Communications. Vol. 7, No. 5, pp. 16-27. October 2000.
[12]C.Guo,L.C.Zhong,andJ.M.Rabaey.LowPowerDistributedMACforAdHocSensorRadioNetworks.IEEEGlobeCom. November 2001.
[13] Y. Lin, B. Li, B. Liang, Stochastic analysis of network coding in epidemic routing, IEEE Journal on Selected Areas in Commun., Vol. 26, No. 5 , pp.794-808, June 2008.
[14] H. Zhu, L. Fu, G. Xue, Y. Zhu, M. Li and L. M. Ni. Recognizing Exponential Inter-Contact Time in VANETs. IEEE Infocom Miniconference. April 2010.
[15] R. Ahlswede, et al., Network Information Flow, IEEE Transactions on Information Theory, Vol. 46, No. 4, pp. 1204-1216, July 2000.
[16] A.Mtibaa, A. Chaintreau, J. LeBrun, E. Oliver, A.-K. Pietilainen, C. Diot. Are You Moved by Your Social Network Application? IEEE/IFIP WONS August 2008.
[17] Z. J. Haas and T. Small, A new networking model for biological applications of ad hoc sensor networks, IEEE/ACM Transactions on Networking, vol. 14, no. 1, pp. 27-40, February 2006.

4.6 Annex F - JRA 1.2.2-2 Game theoretic approach to timing channel communication

4.6.1 Introduction

A timing channel is a logical communication channel in which information is encoded in timing between events. Thanks to their interesting features, timing channels has been proposed in the wireless domain as a promising technique to support energy efficient [1] [2], communications as well as low rate, secure and resilient communications [3][4].
In our research activities, we mainly focused on the resilience of timing channels to jamming attacks performed by malicious users [5][6]. As jamming is energy consuming and, in most scenarios, it is battery powered, we consider reactive jamming as the jammer begins the transmission of its jamming signal as soon as it detects an ongoing transmission activity on the monitored channel.
As the interfering signal only disrupts the transmitted packet, the timing information can properly be decoded by the receiver, hence, timing channels are more immune from reactive jamming attacks then other traditional transmission schemes.
In this JRA we study the interactions between a jammer and a node under attack, i.e., the target node, by means of a game theoretical framework. We investigate the ordinary Nash game in which the two adversaries act simultaneously. To this purpose, we study the Nash Equilibria (NEs) of the game aiming at showing their existence, uniqueness and convergence features.

4.6.2 Proposed Game Model

Let us consider the scenario we have proposed in [7] where two wireless nodes, a transmitter and a receiver, want to communicate, while a reactive jammer aims at disrupting their communication. Let us refer to the malicious node as the jammer, J , and the transmitting node under attack as the target node, T.
Upon detecting a possible transmission activity performed by T , J starts emitting a jamming signal after an activation time, T_{AJ}, As shown in Fig. **Errore. L'origine riferimento non è stata trovata.Errore. L'origine riferimento non è stata trovata.**. The duration of the jamming signal, Y_j, that disrupts the transmission of the j-th packet can be modelled as a continuous random variable with mean value y.
When the target node realizes that a jamming attack is ongoing, it exploits a timing channel where the information is encoded in the duration of the interval between the instant when the jammer J terminates the emission of the jamming signal and the beginning of the transmission of a next packet.

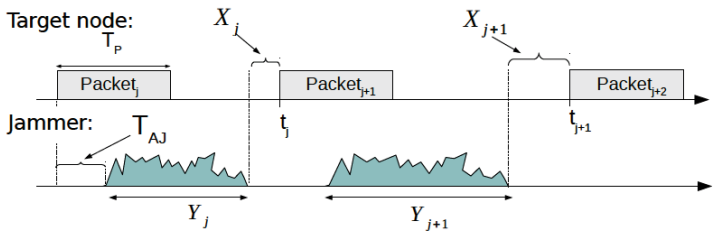

Figure 1 Interactions between the jammer and the target node.

The j-th silence period duration, X_j, can be modelled as a continuous random variable uniformly distributed in the range [0, x] .
Thus, we consider the jamming game, defined by a 3-tuple G = (N,S,U) , where N is the player set, S is the strategy set, and U is the utility set. In our model, N is composed by the T

and J , while the strategy set is S=S_T X S_J , where S_T and S_J are the set of strategies of T and J, respectively.
In our model we assume that the jammer is energy-constrained, hence, its choice of y comes from the trade-off between the reduction of the amount of information that T can transmit and the energy consumption related to the jamming attack. On the other hand, the target node has to properly set the value of x to maximize the achievable capacity C(x;y) of the timing channel, while minimizing the energy consumption.
Therefore, the utility set of the game is defined as U = (U_T ; U_J), where U_T and U_J are the utility functions of T and J, respectively, which are defined as follows [7]:

$$\begin{cases} \mathcal{U}_T(x,y) &= +C(x,y) - c_{T^*} \cdot T_P \cdot P_T \\ \mathcal{U}_J(x,y) &= -C(x,y) - c_T \cdot y \cdot P \end{cases} \quad (1)$$

where P_T and P_J are the transmission power of the target node and the jammer, respectively, T_P is the duration of a transmitted packet in seconds, c_T* and c_T are positive transmission costs expressed in [bit/(s J)] which in the following will be referred to as weight parameters. Finally, the capacity C(x;y) can be calculated as follows [1]:

$$C(x,y) = \frac{\log_2(x/\Delta)}{T_{AJ} + y + x/2} \quad (2)$$

where Δ is the precision of the clocks.

4.6.3 Nash Equilibrium

Now we solve the game and we find the *Nash Equilibrium* points (NEs), in which both players achieve their highest utility given the strategy profile of the opponent. More in detail, we will provide sketch of proofs of the existence, uniqueness and convergence to the Nash Equilibrium under best response dynamics.

4.6.3.1 NE existence and uniqueness

One possible way to study the NE and its properties is to look at the *best response functions* (BRs). A best response function is a function that maximizes the utility function of a player, given the opponents' strategy profile. Let $b_T(y)$ be the BR of the target node and $b_J(x)$ the BR of the jammer. In our model, we can analytically derive such functions which can be written as follows:

$$b_T(y) = \Delta e^{\psi(y)+1} \quad (3)$$

$$b_J(x) = \begin{cases} \chi(x), & \text{if } \chi(x) \geqslant 0 \\ 0, & \text{if } \chi(x) < 0 \end{cases} \quad (4)$$

where

$$\psi(y) = W\left(\frac{2[T_{AJ}+y]}{e\Delta}\right) \qquad \chi(x) = \sqrt{\frac{\log(\frac{x}{\Delta})}{\eta}} - T_{AJ} - \frac{x}{2} \quad (5)$$

In order to prove the existence and uniqueness of the NE we have to show that the intersection between the BRs of both players admits only one intersection point.
In other words, it is sufficient to find one pair (x*; y*) ∈ S such that (b_T (y*); b_J (x*)) = (x*; y*). Some easy algebras shows that the game admits a unique equilibrium.

Figure 2 shows how the unique intersection between the best response functions, i.e., the unique NE, varies as a function of the weighting parameter of the jammer. We assume $c_{T1} < c_{T2}$. As expected, for higher values of c_T the jammer incurs in higher transmission costs and chooses a lower value of y which results in lower values of the strategy x of the target node.

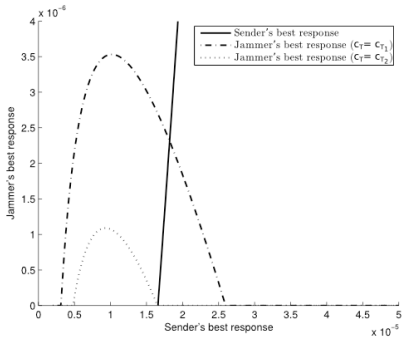

Figure 2 Intersection points between the best response functions as a function of c_T.

4.6.3.2 NE convergence

An important issue in game theory consists in providing distributed algorithms to allow each player in individually reaching the NE.
One of the possible way to do this, is to exploit some well-known iterative algorithms already present in the literature. In our model we consider the Best Response Dynamics (BRDs) algorithm in which each player updates its strategy iteratively according to their BR. More in detail, each player updates its own strategy as follows:

$$\begin{cases} x^{(i)} = b_T(y^{(i-1)}) \\ y^{(i)} = b_J(x^{(i-1)}) \end{cases} \tag{6}$$

It has been proved that BRD has useful properties as it allows fast convergence to the NE.
In our model it is possible to prove that such dynamic converges to the NE. In fact, as the *Diagonal Strict Concavity* (DSC) property holds, it follows that the convergence to the NE is guaranteed.

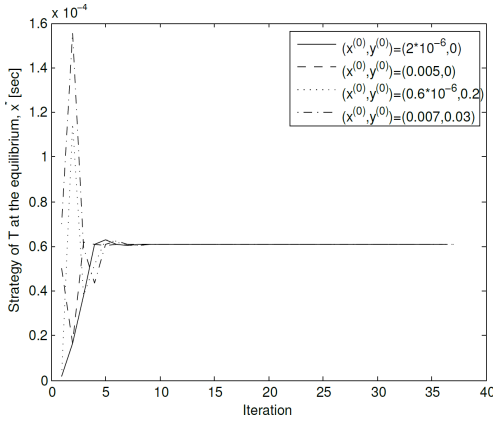

Figure 3 Evolution of the strategy of T, x.

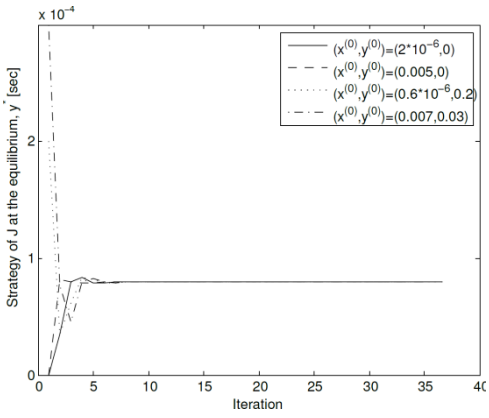

Figure 4 Evolution of the strategy of J, y.

In Figure 3 and Figure **4** we show how the BRD converges to the unique NE for different starting points. Note that in any case the convergence is reached in few iterations.

4.6.4 References

[1] G. Morabito, "Exploiting the timing channel to increase energy efficiency in wireless networks," Selected Areas in Communications, IEEE Journal on, vol. 29, no. 8, pp. 1711–1720, 2011.
[2] L. Galluccio, G. Morabito, and S. Palazzo, "TC-Aloha: A novel access scheme for wireless networks with transmit-only nodes," Wireless Communications, IEEE Transactions on, vol. 12, no. 8, pp. 3696–3709, August 2013.
[3] W. Xu, W. Trappe, and Y. Zhang, "Anti-jamming timing channels for wireless networks," in Proceedings of the first ACM conference on Wireless network security. ACM, 2008, pp. 203–213.
[4] S. D'Oro, L. Galluccio, G. Morabito, and S. Palazzo, "Efficiency analysis of jamming-based countermeasures against malicious timing channel in tactical communications," in Communications (ICC), 2013 IEEE International Conference on. IEEE, 2013, pp. 4020–4024.
[5] W. Xu, K. Ma, W. Trappe, and Y. Zhang, "Jamming sensor networks: attack and defense strategies," Network, IEEE, vol. 20, no. 3, pp. 41–47, 2006.
[6] R. Saranyadevi, M. Shobana, and D. Prabakar, "A survey on preventing jamming attacks in wireless communication," International Journal of Computer Applications, vol. 57, no. 23, pp. 1–3, November 2012, published by Foundation of Computer Science, New York, USA.
[7] S. D'Oro, L. Galluccio, G. Morabito, S. Palazzo, L. Chen, F. Martignon, "Defeating jamming with the power of silence: a game-theoretic analysis" submitted to the IEEE for possible publication.

4.7 Annex G - JRA 1.2.3-1 Multiple source detection, localization, and transmit power estimation in lognormal fading environment

4.7.1 Introduction

Transmitter localization via sensor networks is an important topic for many wireless applications. In particular, radio-source localization comprises an important component in upcoming cognitive radio networks [1]. Endowed with the capability to sense and record radioactivity in the surrounding environment, cognitive radios then can efficiently plan, decide upon and then execute the respective actions [2],[3]. Benefits can result for operators and regulators alike; the first to improve network operation, the second to detect and locate malicious and non-licensed spectrum users. Non-cooperative communication systems would also benefit from this theory.
A standard practice is to exploit the Received Signal Strength (RSS) at the various sensors in order to detect and locate a radio source. Techniques based on RSS are the most popular because of their simplicity and direct applicability of commercial off-the-shelf radio hardware. The downside of the RSS statistic is its unreliability in ground propagation, fading, etc., because the relationship between a given RSS measurement and the respective source-sensor distance is not the classic power law anymore but, rather, a complicated probabilistic one.
It is known that this unreliability can be reduced by the fact that modern networks has access to large databases of past localized measurements, or a sensor network that builds such database. This is due to the spatial correlation of the main factor off unreliability, the shadow fading. Many models that describe the spatial correlation of the shadow fading have been proposed in the literature [4]. Experimental campaigns have also been used to measure it [5][6], and various techniques have been proposed in the literature that utilize it [7]. The analysis of the performance of RSS localization methods in such environments has been proposed [8], but never to explicitly model the utilization of past measurements.
In this work, we focus on analyzing the performance of RSS based localization, for first time in a correlated log-normal environment. The main goal is to answer the following questions: a) what is the density of the real-time measurement network for a target localization performance? b) how much is this density reduced when utilizing high density-past measurements? c) How these two densities (real time and past measurements) are related

given a propagation environment parameterization? These conclusions will be based on a rather simple analytic model for the propagation environment. So, the last and most important question is: how close are those conclusions to the true performance encountered in practice?
This is hard to answer, since any experimental setup represents just one realization of the random performance of a specific setup. As long as the theoretical model is close to the real one, you expect at least the general conclusions to be in agreement with experimental results. There exists though, a lot of work in the literature which show a qualitative agreement on the potential gains [8] when exploiting spatial correlation. In order to have also a quantitative one, a large number of experimental campaigns is needed. We add our contribution to this collective effort by one more experimental campaign in an indoor environment and using the OpenAirInterface (OAI) [9] platform. Based on the collected measurements, various options for modeling the spatial correlation were assessed.
The paper is organized as follows: In section II the propagation model is presented for the correlated log-normal propagation environment. The statistics of the received energy when having also access to past stored measurements are given, needed for the derivation of the CRLB. In section III the CRLB is derived, needed for the semi-analytic performance assessment which follows on section IV. For the performance assessment, two scenarios were chosen, representing indoor and outdoor cases. Based on those results valuable conclusions are drawn regarding the potential gains when having past measurements. Finally, in section V, we present real performance results using the OpenAirInterface platform in an indoor environment.

4.7.2 Propagation Model

Weather passive or active localization is under consideration, RSS measurements are assumed to be taken either from a set of known position sensors, or from the radio receiver under consideration. Without loss of generality, the scenario under consideration involves sensors of known positions and one active transmitter within an area of interest.
The localization problem (including power estimation), using RSS measurements can be briefly described as the process in which the input is RSS measurements from different sensors of known location in a certain area and the output is estimates of the location, the power and implicitly the amount of emitters existing in the specified area. In our problem we have only one active emitter within the area of interest (the number of emitters is known), and we have at max three unknown parameters to estimate: two Cartesian coordinates and the Power (x, y, P).
To estimate any emitter parameter (location or power) first the propagation model should be defined. The log-normal propagation model is adopted, more suitable for outdoor measurements, which has the following form:

$$R_i = P^{tx} - L_0 - 10\alpha \log(d_i/d_0) + n_i^s + n_i^f \quad (1)$$

where R_i is the power measured by i-*th* sensor coming from the source, $d_i = \|x_i - s\|$ is the distance between them (x_i is the coordinates of i-*th* sensor and s is the coordinates of source), P^{tx} is the emitting power, d_0 is a reference distance and L_0 is the power loss in that distance, α is the path loss exponent constant, n_i^f is the noise due to fast fading, modeled as zero-mean Gaussian (in the linear domain). We try to eliminate the fast fading by taking measures around the correct location and calculating the average. This maybe seems unpractical for an application point of view, but the same effect could be accomplished by moving the sensors instead of the sources. Thus, assuming that the error due to fast fading is averaged out, only the shadow fading (n_i^s) remains (shadow fading is assumed to be the same within the small averaging area). It is assumed to follow a lognormal distribution, i.e. Gaussian in the log domain with zero mean and variance of σ_s^2.

4.7.3 Typical RSS Model in lognormal fading

The typical model does not assume past measurements (pilots), and the sensors are considered way far from one another, such that the spatial correlation does not affect their measurements.

If we set $m_i(\theta) = P^{tx} - L_0 - 10a\log(d_i/d_0)$, in the general case $\theta = [P^{tx}, L_0, d_0, a, x, y]$ are the unknown parameters which we want to estimate, and i indicates the sensor number, so

$$R_i = m_i(\theta) + n_i \tag{2}$$

So the R_i follows Gaussian distribution

$$P_i(R_i|\theta) = \frac{1}{\sigma_i\sqrt{2\pi}} e^{-\frac{(R_i - m_i(\theta))^2}{2\sigma_i^2}} \tag{3}$$

And since no spatial correlation among the sensors is assumed, the PDF of the measurements is given by

$$P(\mathbf{R}|\theta) = \prod_{i=1}^{N} P_i(R_i|\theta) \tag{4}$$

where $\boldsymbol{R} = [R_1, \ldots, R_N]$.

4.7.3.1 RSS Model in lognormal fading with past measurements

The same propagation model applies us before. Additionally we denote the r.v of the real-time measurement of the i-*th* sensor from a source at a location t as $R_i^{[t]}$ and as $\boldsymbol{R}_i^{[p]}$ the r.v's modeling the stored pilot measurements.

The joint PDF for all power measurements are assumed to be joint Gaussian., i.e.

$$\begin{bmatrix} R_i^{[t]} \\ \mathbf{R}_i^{[p]} \end{bmatrix} \sim \mathcal{N}\left(\begin{bmatrix} \mu_i^{[t]} \\ \boldsymbol{\mu}_i^{[p]} \end{bmatrix}, \begin{bmatrix} \sigma_i^{[t]} & \mathbf{C}_i^{[t\times p]} \\ \mathbf{C}_i^{[p\times t]} & \mathbf{C}_i^{[p]} \end{bmatrix} \right) \tag{5}$$

where

$$\begin{aligned} \mu_i^{[t]} &= P_T - 10a\log_{10}\left(d_i^{[t]}\right) \\ \boldsymbol{\mu}_i^{[p]} &= P_T \mathbf{1}_M - 10a\log_{10}\left(\mathbf{d}_i^{[p]}\right) \\ \sigma_i^{[t]} &= \sigma^2 \end{aligned} \tag{6}$$

$$\mathbf{C}_i^{[p]} = \sigma^2 \begin{bmatrix} \rho_i^{[p_1]} & \cdots & \rho_i^{[p_1\times p_M]} \\ \vdots & \ddots & \vdots \\ \rho_i^{[p_M\times p_1]} & \cdots & \rho_i^{[p_M]} \end{bmatrix} \tag{7}$$

and

$$\mathbf{C}_i^{[p\times t]} = \mathbf{C}_i^{[t\times p]^T} = \sigma^2 \begin{bmatrix} \rho_i^{[p_1\times t]} \\ \vdots \\ \rho_i^{[p_K\times t]} \end{bmatrix} \tag{8}$$

where $P_T = P^{tx} - L_0 + 10a\log(d_0)$ is a simplification parameter assuming the pilots and the unknown source have the same transmitting Power, $d_i^{[t]}$ is the unknown distance between the transmitter and the i-*th* sensor, $\mathbf{d}_i^{[p]}$ is $Mx1$ vector with the known distances between the i-*th* sensor and the positions of the pilot measurements (totally we have M pilot positions). Also, $\rho_i^{[p_k\times p_l]} = e^{-a_c d^{[p]}}$ is the correlation factor and $d^{[p]}$ is the distance between p_i and p_j pilot transmitters. Where the correlation constant is depicted as a_c. The de-correlation distance is defined as $d_c = 1/a_c$. We have also assumed that the standard deviation is equal for all sensors, i.e. $\sigma_i^{[p]} = \sigma$. Respectively $\rho_i^{[p_k\times t]}$ is the correlation factor between the p_k pilot and the unknown transmitter.

Given the above, the conditional PDF of $R_i^{[t]}$ given $\boldsymbol{R}_i^{[p]} = r_i^{[p]}$ ($r_i^{[p]}$ are the values of the pilot measurements) is also Gaussian $N(\mu_i^{[t|p]}, \sigma_i^{[t|p]^2})$ with mean and variance given by

$$\mu_i^{[t|p]} = \mathrm{E}\left\{R_i^{[t]} | \mathbf{R}_i^{[p]} = \mathbf{r}_i^{[p]}\right\} = \mu_i^{[t]} - \mathbf{C}_i^{[p\times 1]^{\mathrm{T}}} \mathbf{C}_i^{[p]^{-1}} \left(\boldsymbol{\mu}_i^{[p]} - \mathbf{r}_i^{[p]}\right) \tag{9}$$

and

$$\sigma_i^{[t|p]^2} = \sigma^2 - \mathbf{C}_i^{[p\times 1]^{\mathrm{T}}} \mathbf{C}_i^{[p]^{-1}} \mathbf{C}_i^{[p\times 1]} \tag{10}$$

So we have $\boldsymbol{R}^{[t]} \sim N\left(\boldsymbol{\mu}(\boldsymbol{\theta}), \boldsymbol{C}_s(\boldsymbol{\theta})\right)$, where

$$\boldsymbol{\mu}(\boldsymbol{\theta}) = \left[\mu_1^{[t|p]}, \mu_2^{[t|p]}, \ldots, \mu_N^{[t|p]}\right] \tag{11}$$

is the $N\times 1$ mean vector and

$$\mathbf{C}_s(\boldsymbol{\theta}) = \begin{bmatrix} \sigma_1^{[t|p]^2} & \cdots & 0 \\ \vdots & \ddots & \vdots \\ 0 & \cdots & \sigma_N^{[t|p]^2} \end{bmatrix} \tag{12}$$

is the $N\times N$ covariance matrix between the sensors, which we have already calculated. Both of them depends by $\boldsymbol{\theta}$. So, the PDF of the received power is expressed as:

$$\mathrm{P}\left(\mathbf{R}^{[t]}; \boldsymbol{\theta}\right) = \frac{1}{(2\pi)^{\frac{N}{2}} det\left[\mathbf{C}_s(\boldsymbol{\theta})\right]^{\frac{1}{2}}} exp\left[-\frac{1}{2}\left(\mathbf{R}^{[t]} - \mu(\boldsymbol{\theta})\right)^{\mathrm{T}} \mathbf{C}_s^{-1}(\boldsymbol{\theta})\left(\mathbf{R}^{[t]} - \boldsymbol{\mu}(\boldsymbol{\theta})\right)\right] \tag{13}$$

4.7.4 Cramer-Rao Lower Bound

The Fisher information matrix for the case of Gaussian r.vs is equal to [10]:

$$[J(\boldsymbol{\theta})]_{kl} = \frac{1}{2} tr\left(\mathbf{C}_s^{-1}(\boldsymbol{\theta}) \frac{\partial \mathbf{C}_s(\boldsymbol{\theta})}{\partial \theta_k} \mathbf{C}_s^{-1}(\boldsymbol{\theta}) \frac{\partial \mathbf{C}_s(\boldsymbol{\theta})}{\partial \theta_l}\right) + \frac{\partial \mu(\boldsymbol{\theta})^{\mathrm{T}}}{\partial \theta_k} \mathbf{C}_s^{-1}(\boldsymbol{\theta}) \frac{\partial \boldsymbol{\mu}(\boldsymbol{\theta})}{\partial \theta_l} \tag{14}$$

where $tr(\,)$ is the trace of the matrix. All we need is to calculate the Partial derivatives for the computation of (14):

$$\frac{\partial \mathbf{C}_s(\boldsymbol{\theta})}{\partial \theta_k} = \begin{bmatrix} \frac{\partial \sigma_1^{[t|p]^2}}{\partial \theta_k} & \cdots & 0 \\ \vdots & \ddots & \vdots \\ 0 & \cdots & \frac{\partial \sigma_N^{[t|p]^2}}{\partial \theta_k} \end{bmatrix} \tag{15}$$

where

$$\frac{\partial \sigma_i^{[t|p]^2}}{\partial \theta_k} = -2\sigma_i^{[t|p]} \left[\frac{\partial \mathbf{C}_i^{[p\times 1]^{\mathrm{T}}}}{\partial \theta_k} \mathbf{C}_i^{[p]^{-1}} \mathbf{C}_i^{[p\times 1]} + \mathbf{C}_i^{[p\times 1]^{\mathrm{T}}} \mathbf{C}_i^{[p]^{-1}} \frac{\partial \mathbf{C}_i^{[p\times 1]}}{\partial \theta_k}\right] \tag{16}$$

also

$$\frac{\partial C_i^{[p\times t]}}{\partial \theta_k} = -a_c e^{-a_c d_i^{[p\times t]}} \frac{\partial d_i^{[p\times t]}}{\partial \theta_x} \quad (17)$$

For $\theta_k = x^{[t]}$, (same for $y^{[t]}$)

$$\frac{\partial C_i^{[p\times t]}}{\partial x^{[t]}} = \frac{a_c (x^{[p]} - x^{[t]})}{d_i^{[p_i\times t]}} \rho_i^{[p_i\times t]} \quad (18)$$

For the derivatives of the mean value we have

$$\frac{\partial \mu(\boldsymbol{\theta})}{\partial \theta_k} = -10a \frac{\partial \log_{10}\left(d_i^{[t]}\right)}{\partial \theta_k} - \frac{\partial C_i^{[p\times t]^T}}{\partial \theta_k} C_i^{[p]^{-1}} \left(P_T 1_M - 10a \log_{10}\left(\mathbf{d}_i^{[p]}\right) - \mathbf{r}_i^{[p]}\right) \quad (19)$$

Having made all the necessary derivations we are able to compute the CRLB (inverse of the Fisher) for a given sensor and pilot network. In order to assess the performance of a random network deployment with random past measurements we need to average out all randomness. This is what we do at the next section.

4.7.5 Performance Assesment

At the previous section we derived the CRLB of the localization error given a specific measurement network setup, for the stored (pilots) as well as the real time RSS measurements. In order to assess the performance of a random deployment network, a semi-analytic approach will be followed, where the positions of the real-time measurements as well as stored measurements are averaged out. This process will be described at the following two subsections, where at the first, no pilot measurements will be consider, averaging only the sensor positions, and at the second, the pilot positions will be used.

4.7.5.1 Performance without pilot measurments

For the random real-time measurement network we will assume 2D Gaussian distribution with mean a square grid of points based on a given density, and variance relative to that density. What we are trying to model is the results of a practical sensor deployment having a target density. In all simulations we will assume that the transmitter lies at the center of this deployment, and the sensors capable of measuring its power are determined by a coverage area, a circle around the transmitter. The radius of this coverage area is determined by the received power sensitivity of the measurement network, the transmit power of the source, and the propagation characteristics (path-loss exponent).

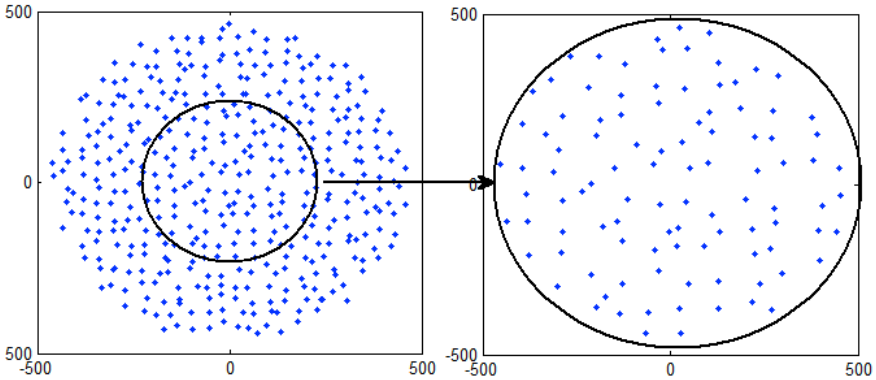

Figure 5: Active sensors example for two different densities.

As an example, in Figure 5 the positions of a random deployment are depicted for two different densities. The simulation process always begins with a very dense realization and gradually we expand the distances of the sensors until the point where less than three sensors are within the coverage area. The performance is measured for each step, and averaged over different realizations.

Two different propagation scenarios will be examined, one called 'Indoor' and the other 'Outdoor', using respectively a parameterization that tries to reflect such scenarios, i.e. small coverage, de-correlation distance, large path-loss exponent for the indoor scenario and the opposite for the outdoor. The exact values used for those two scenarios are depicted in table I.

TABLE I: Parameterization of the propagation scenarios

Parameters	**Scenarios**	
	Indoor	***Outdoor***
Path loss	2	3
Shadow Fading	16	8
Correlation coefficient (de-corellation distance, d_c)	2 (0.5m)	0.1 (10m)
Range (coverage)	33dB(~3000m^2)	80dB(0.6km^2)

The semi-analytic performance assessment of those scenarios is conducted by the following way. For a given density of deployment network random realizations of such networks are produced and based on the coverage, the active sensors are selected. Based on those sensors, the CRLB is computed, and averaged over a large number of network realizations. The results for the indoor scenario for different levels of shadow fading variance are depicted in Figure 6.

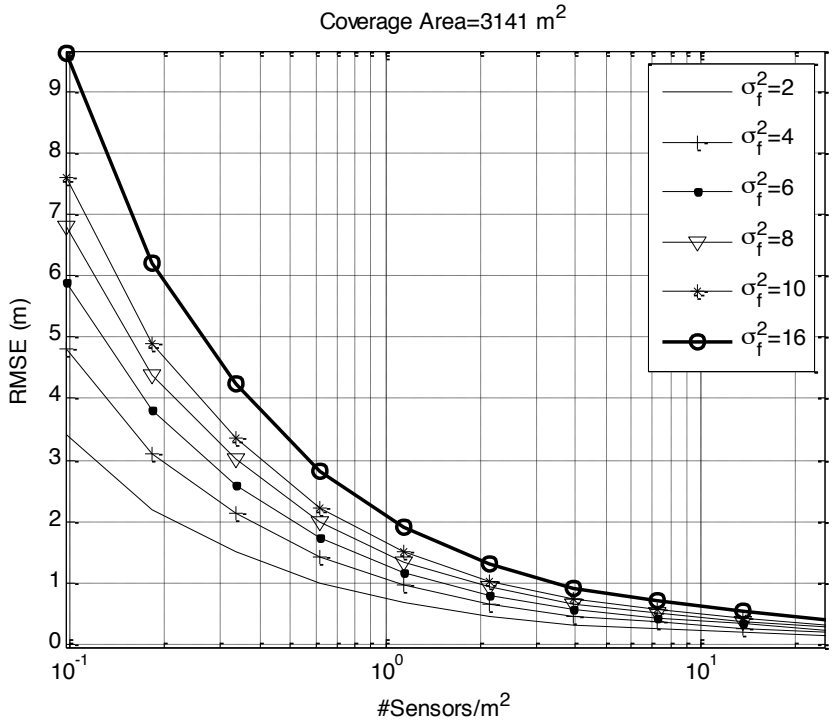

Figure 6: Indoor scenario for different shadow fading values

Shadow fading levels from 2 to 16 are used. The error is kept below 2 meters in most cases for a density of 1 sensor per square meter, which is considered very dense. For the case of 1 sensor per 10m^2, which is again a rather dense network error is above 9m for the case of 16dB shadow fading, a value that has been measured experimentally by our group in several

measurement campaigns [11]. The coverage area of this example is 33meters, so a 9m error for a high density network is consider very high, since it is larger than the de-correlation distance. We want a performance to be within this range for CR applications, since our primary goal is the estimation of the radio field..
For the outdoor scenario, the respective assessment is depicted in Figure 7. The coverage radius in this scenario is 464 meters. Assuming a correlation distance of 10m, the error for the case of 8db shadow fading is around 70m for a rather high density network of 1 sensor per $100m^2$. It is clear from the performance results depicted so far that the RSS based localization for CR applications requires very high density sensor networks, if no past measurements are utilized.

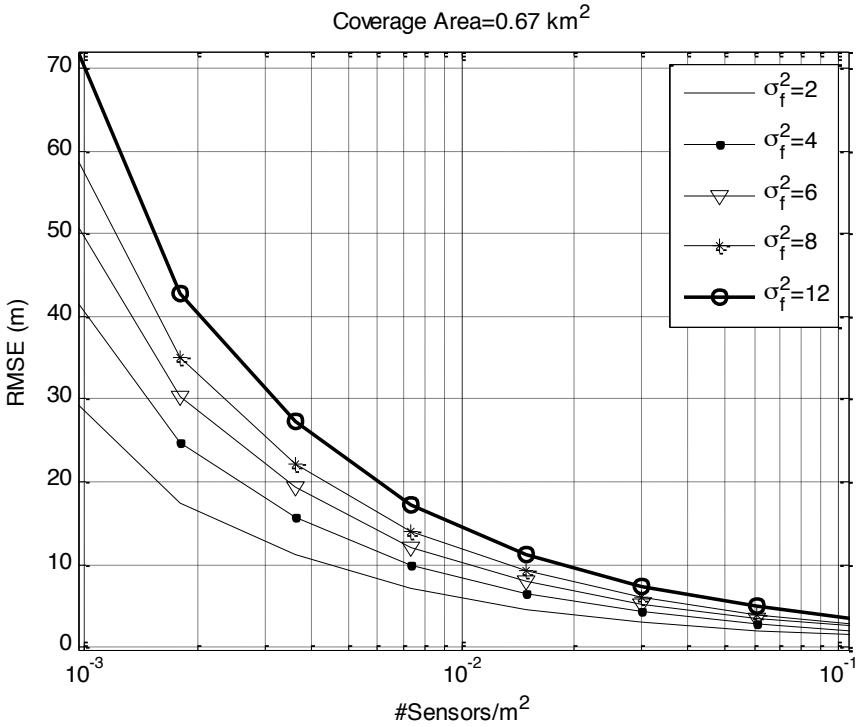

Figure 7: Outdoor scenario for different shadow fading values

4.7.5.2 Performance using stored measurements

This is the most important part of our contribution, since we will see how much the past measurements can reduce the error and/or the density of the needed measurement network. The process is the same as in the previous section, but here we also have to average out the random positions of the past measurements. There are many spatial models that are used for the positions of radios leading to different performances. Here we take a very simple approach the results of which can then be used to assess the performance of any model. We assume that n_p is the number of past measurements found in a distance d_p from the source. The de-correlation distance will be used as the unit of measure. The angle of the pilot positions w.r.t the source will be random and thus be averaged out by simulation. The underline pilot density assumed by this method is not easily defined. As a measure of it, we define it to be equal to $n_p/(\pi d_p^2)$. This can be used to bound the performance of any statistical pilot distribution, by computing for example the outage of finding a circular area of radius d_p that does not contain n_p pilots. When $n_p = 1$ this simple modeling approach can be viewed as lower-bound performance using measurements with arbitrary placement but guaranteed equal or greater density than $1/(\pi d_p^2)$. The lower-bound is due to the fact that the pilot is placed always at the maximum distance from the source with a given density, and that other pilots further away from d_p are not taken under consideration. We believe that this is

also the case for $n_p > 1$ but the proof of this is out of the scope of this paper. Two different values of n_p are adequate to assess the expected performance improvement. Starting from the 'indoor' scenario, the performance curves for the case of $n_p = 1,2$ are depicted for various distances (or densities). For the case of distance equal to $0d_c$ the performance is equal as the one without pilots, for both cases. For the case of $4d_c$ the performance gain is 1.4-fold when $n_p = 1$ and 3.6-fold when $n_p = 2$. For the case of $2d_c$ the gain is 2-fold for $n_p = 1$ and 50-fold for the case of $n_p = 2$. As we can see, the expected theoretical gain is huge; enough to enable practical use of RSS based localization for CR applications, as long as a dense measurement database of past measurements is available.

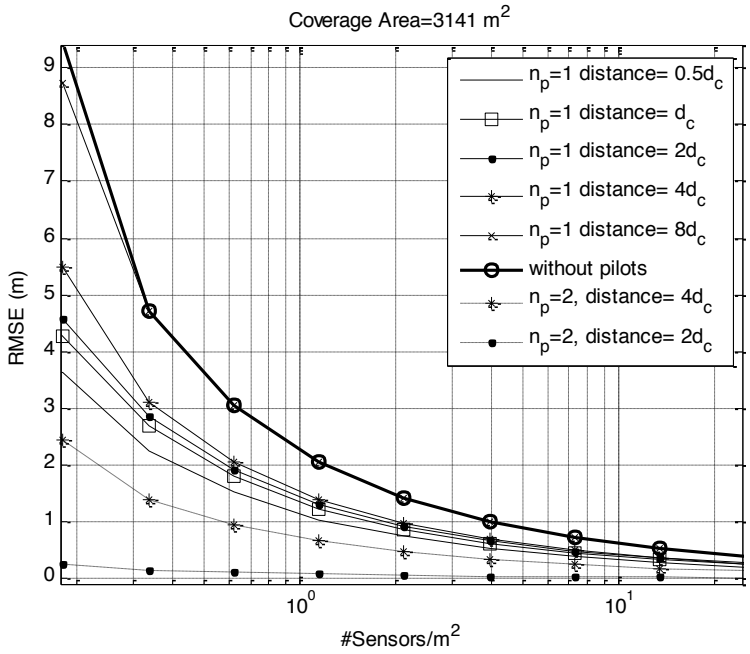

Figure 8: Outdoor scenario for various pilot placement cases and shadow fading equal to 16dB

The performance for the 'outdoor' scenario is also depicted in Figure 9.

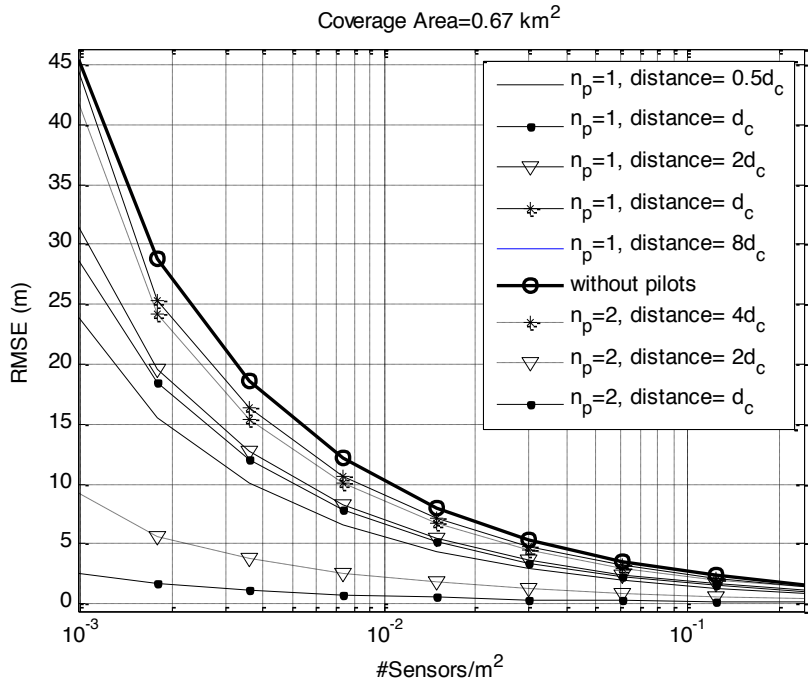

Figure 9: Outdoor scenario for various pilot placement cases and shadow fading equal to 8dB

Equivalent performance enhancement is displayed. When the distance equals $4d_c$ both pilot schemes perform near the case without pilots. Significant performance gain (2-fold) is depicted in case of $n_p = 1$ in close range, i.e. when $0.5d_c$. In case of $n_p = 2$ a 4-fold and a 20-fold for distances $2d_c$ and d_c respectively.

What we can see is that in theory, the potential of performance enhancement is large when having access to stored measurements with density at the order of the de-correlation distance. What the theory does not say, is the method of getting such performance. The CRLB characterizes the performance of the Maximum Likelihood estimator, which is a non-convex optimization problem.

4.7.6 References

[1] J. Mitola, “Cognitive Radio An Integrated Agent Architecture for Software Defined Radio,” Royal Institute of Technology (KTH), 2000.

[2] F. J. Casadevall Palacio, R. Agustí Comes, J. Pérez Romero, M. López Benítez, S. Grimoud, B. Sayrac, I. Dagres, A. Polydoros, J. Riihijärvi, J. N. Nasreddine, P. Mähönen, L. Gavrilovska, V. Atanasovski, and J. Van de Beek, “Radio environmental maps: information models and reference model. Document number D4.1,” 10-May-2012. [Online]. Available: http://www.recercat.net/handle/2072/184976. [Accessed: 22-Aug-2013].

[3] D. Denkovski, V. Rakovic, M. Pavloski, K. Chomu, V. Atanasovski, and L. Gavrilovska, “Integration of heterogeneous spectrum sensing devices towards accurate REM construction,” in 2012 IEEE Wireless Communications and Networking Conference (WCNC), 2012, pp. 798–802.

[4] Gudmundson, M., "Correlation model for shadow fading in mobile radio systems," *Electronics Letters* , vol.27, no.23, pp.2145,2146, 7 Nov. 1991

[5] Nam-Ryul Jeon; Kyung-Hoe Kim; Jung-Hwan Choi; Seong-Cheol Kim, "A Spatial Correlation Model for Shadow Fading in Indoor Multipath Propagation," *Vehicular Technology Conference Fall (VTC 2010-Fall), 2010 IEEE 72nd* , vol., no., pp.1,6, 6-9 Sept. 2010

[6] Oestges, Claude; Czink, Nicolai; Bandemer, Bernd; Castiglione, Paolo; Kaltenberger, Florian; Paulraj, Arogyaswami "Experimental characterization and modeling of outdoor-to-indoor and indoor-to-indoor distributed channels",IEEE Transactions on Vehicular Technology, Vol.59, N°5, June 2010

[7] Bshara, M.; Orguner, U.; Gustafsson, F.; Van Biesen, L., "Fingerprinting Localization in Wireless Networks Based on Received-Signal-Strength Measurements: A Case Study on WiMAX Networks," *Vehicular Technology, IEEE Transactions on* , vol.59, no.1, pp.283,294, Jan. 2010

[8] Maja STELLA, Mladen RUSSO, Dinko BEGUŠIĆ, "RF Localization in Indoor Environment," RADIOENGINEERING, Vol. 21, no. 2, pp.557-567, June 2012

[9] OpenAir Interface, http://www.openairinterface.org/
[10] S. Kay, Fundamentals of Statistical Signal Processing, Volume I: Estimation Theory, Prentice Hall, 1993.
[11] Dagres, I.; Polydoros, A.; Denkovski, D.; Angjelicinoski, M.; Atanasovski, V.; Gavrilovska, L., "Algorithms and bounds for energy-based multi-source localization in log-normal fading," Globecom Workshops (GC Wkshps), 2012 IEEE , vol., no., pp.410,415, 3-7 Dec. 2012

4.8 Annex H - JRA 1.2.3-3 Source detection in the presence of interference and noise

For technical details see:

[1] http://ieeexplore.ieee.org/xpls/abs_all.jsp?arnumber=6850352&tag=1

4.9 Annex I - JRA 1.2.3-4 Hybrid Spectrum Sensing Architecture for Cognitive Radio: Overcoming Noise Uncertainty

For technical details see:

[1] http://ieeexplore.ieee.org/xpls/abs_all.jsp?arnumber=6849724

4.10 Annex I - JRA 1.2.3-5 on energy-efficient data collection and estimation in wireless sensor networks

For technical details see:

[1] http://ieeexplore.ieee.org/xpls/abs_all.jsp?arnumber=6854843&tag=1

Comments and suggestions for the improvement of this document are most welcome and should be sent to:

project_office@newcom-project.eu

---

http://www.newcom-project.eu